Stable isotope data ($\delta^{13}C$, $\delta^{15}N$) for anadromous, coastal, and offshore marine fishes of the Canadian Beaufort Sea and Frobisher Bay from 2011-2020, with supporting modelled ocean data

Lauren E. Dares, Ashley Ehrman, Jasmine Brewster, Laurissa Christie, Karen Dunmall, Colin Gallagher, Kevin Hedges, Kimberly Howland, Ellen V. Lea, Christopher Lewis, Yazhou Liu, Tracey Loewen, Zhenxia Long, Lisa Loseto, Andrew Majewski, Darcy McNicholl, Dana Neumann, Will Perrie, Dayanne Raffoul, Cole Wolbaum, Minghong Zhang, Andrea Niemi

Fisheries and Oceans Canada
Freshwater Institute
501 University Crescent
Winnipeg. MB
R3T 2N6

2025

Canadian Data Report of
Fisheries and Aquatic Sciences 1463

Fisheries and Oceans Canada | Pêches et Océans Canada

Canada

Canadian Data Report of Fisheries and Aquatic Sciences

Data reports provide a medium for filing and archiving data compilations where little or no analysis is included. Such compilations commonly will have been prepared in support of other journal publications or reports. The subject matter of the series reflects the broad interests and policies of Fisheries and Oceans Canada, namely, fisheries management, technology and development, ocean sciences, and aquatic environments relevant to Canada.

The correct citation appears above the abstract of each report. Each report is abstracted in the data base *Aquatic Sciences and Fisheries Abstracts*.

Data reports are produced regionally but are numbered nationally. Requests for individual reports will be filled by the issuing establishment listed on the front cover and title page.

Numbers 1-25 in this series were issued as Fisheries and Marine Service Data Records. Numbers 26-160 were issued as Department of Fisheries and Environment, Fisheries and Marine Service Data Reports. The current series name was changed with report number 161.

Rapport statistique canadien des sciences halieutiques et aquatiques

Les rapports statistiques servent de base à la compilation des données de classement et d'archives pour lesquelles il y a peu ou point d'analyse. Cette compilation aura d'ordinaire été préparée pour appuyer d'autres publications ou rapports. Les sujets des rapports statistiques reflètent la vaste gamme des intérêts et politiques de Pêches et Océans Canada, notamment la gestion des pêches, la technologie et le développement, les sciences océaniques et l'environnement aquatique, au Canada.

Le titre exact figure au haut du résumé de chaque rapport. Les rapports à l'industrie sont résumés dans la base de données *Résumés des sciences aquatiques et halieutiques*.

Les rapports statistiques sont produits à l'échelon régional, mais numérotés à l'échelon national. Les demandes de rapports seront satisfaites par l'établissement d'origine dont le nom figure sur la couverture et la page du titre.

Les numéros 1 à 25 de cette série ont été publiés à titre de Records statistiques, Service des pêches et de la mer. Les numéros 26-160 ont été publiés à titre de Rapports statistiques du Service des pêches et de la mer, ministère des Pêches et de l'Environnement. Le nom de la série a été modifié à partir du numéro 161.

Canadian Data Report of
Fisheries and Aquatic Sciences 1463

2025

Stable isotope data ($\delta^{13}C$, $\delta^{15}N$) for anadromous, coastal, and offshore marine fishes of the Canadian Beaufort Sea and Frobisher Bay from 2011-2020, with supporting modelled ocean data

by

Lauren E. Dares[1], Ashley Ehrman[1], Jasmine Brewster[2], Laurissa Christie[1], Karen Dunmall[1], Colin Gallagher[1], Kevin Hedges[1], Kimberly Howland[1], Ellen V. Lea[2], Christopher Lewis[3], Yazhou Liu[4], Tracey Loewen[1], Zhenxia Long[4], Lisa Loseto[1], Andrew Majewski[1], Darcy McNicholl[1], Dana Neumann[1], Will Perrie[4], Dayanne Raffoul[1], Cole Wolbaum[1], Minghong Zhang[4], Andrea Niemi[1]

[1]Fisheries and Oceans Canada
Freshwater Institute
501 University Crescent
Winnipeg, MB, R3T 2N6

[2]Fisheries and Oceans Canada
8 Arctic Road
PO Box 1871
Inuvik, NT, X0E 0T0

[3]Fisheries and Oceans Canada
630 Queen Elizabeth Way
Iqaluit, NU, X0A 3H0

[4]Fisheries and Oceans Canada
Bedford Institute of Oceanography
1 Challenger Drive
Dartmouth, NS, B2Y 4A2

Cat. Fs97-13/1463E-PDF ISBN 978-0-660-79513-3 ISSN 1488-5395

Correct citation for this publication:

Dares, L.E., Ehrman, A., Brewster, J., Christie, L., Dunmall, K., Gallagher, C., Hedges, K., Howland, K., Lea, E.V., Lewis, C., Liu, Y., Loewen, T., Long, Z., Loseto, L., Majewski, A., McNicholl, D., Neumann, D., Perrie, W., Raffoul, D., Wolbaum, C., Zhang, M., and Niemi, A. 2025. Stable isotope data ($\delta^{13}C$, $\delta^{15}N$) for anadromous, coastal, and offshore marine fishes of the Canadian Beaufort Sea and Frobisher Bay from 2011-2020, with supporting modelled ocean data. Can. Data Rep. Fish. Aquat. Sci. 1463: x + 66 p.

Contents

List of Figures

List of Tables

Abstract

Dares, L.E., Ehrman, A., Brewster, J., Christie, L., Dunmall, K., Gallagher, C., Hedges, K., Howland, K., Lea, E.V., Lewis, C., Liu, Y., Loewen, T., Long, Z., Loseto, L., Majewski, A., McNicholl, D., Neumann, D., Perrie, W., Raffoul, D., Wolbaum, C., Zhang, M., and Niemi, A. 2025. Stable isotope data ($\delta^{13}C$, $\delta^{15}N$) for anadromous, coastal, and offshore marine fishes of the Canadian Beaufort Sea and Frobisher Bay from 2011-2020, with supporting modelled ocean data. Can. Data Rep. Fish. Aquat. Sci. 1463: x + 66 p.

This data report provides multi-year and multi-location mean-standardized carbon and nitrogen isotope data for 16 species of anadromous, coastal, and offshore marine fishes in the Canadian Arctic from 2011-2020. Mean-standardized values represent the annual deviation from the long-term mean of $\delta^{13}C$ and $\delta^{15}N$ for each of 12 study areas delineating fish habitats in the Beaufort Sea and Amundsen Gulf system in the western Canadian Arctic, and Frobisher Bay in the eastern Canadian Arctic. Coupled ice-ocean model outputs identified as potential drivers of fish resource use are summarized weekly and for periods relating to ice cover (ice break-up, open water, freeze-up, and ice-covered) for each fish habitat area and across depths related to stratified water mass layers. These datasets provide key indicators of fish diet and habitat use and potential environmental drivers in the Canadian Arctic.

Résumé

Dares, L.E., Ehrman, A., Brewster, J., Christie, L., Dunmall, K., Gallagher, C., Hedges, K., Howland, K., Lea, E.V., Lewis, C., Liu, Y., Loewen, T., Long, Z., Loseto, L., Majewski, A., McNicholl, D., Neumann, D., Perrie, W., Raffoul, D., Wolbaum, C., Zhang, M., and Niemi, A. 2025. Stable isotope data ($\delta^{13}C$, $\delta^{15}N$) for anadromous, coastal, and offshore marine fishes of the Canadian Beaufort Sea and Frobisher Bay from 2011-2020, with supporting modelled ocean data. Can. Data Rep. Fish. Aquat. Sci. 1463: x + 66 p.

Ce rapport fournit des données standardisées d’isotopes de carbone et d'azote, sur plusieurs années et plusieurs sites, pour 16 espèces de poissons anadromes, côtiers et marins hauturiers de l'Arctique canadien entre 2011 et 2020. Les valeurs moyennes normalisées représentent l'écart annuel par rapport à la moyenne à long terme des isotopes $\delta^{13}C$ et $\delta^{15}N$ pour chacune des 12 zones d'étude délimitant les habitats des poissons dans le système de la mer de Beaufort et du golfe d'Amundsen, dans l'ouest de l'Arctique canadien, et dans la baie de Frobisher, dans l'est de l'Arctique canadien. Les résultats du modèle couplé glace-océan identifiés comme forçages potentiels de l'utilisation des ressources halieutiques sont résumés par semaine et pour les périodes liées au couvert de glace (dégel, eau libre, gel et couvert de glace) pour chaque zone d'habitat des poissons et à toutes les profondeurs liées aux couches stratifiées de la masse d'eau. Ces ensembles de données fournissent des indicateurs clés du régime alimentaire et de l'utilisation de l'habitat des poissons, ainsi que des forçages environnementaux potentiels dans l'Arctique canadien.

Acknowledgements

The data presented in this report represent a significant collaborative effort by staff of several Fisheries and Oceans Canada ocean modelling and field programs and local Indigenous partners. We thank the Fisheries Joint Management Committee, Inuvialuit Game Council, Aklavik Hunters and Trappers Committee, Herschel Island-Qikiqtaruk Territorial Park Rangers, Olokhaktomiut Hunters and Trappers Committee, Paulatuk Hunters and Trappers Committee, and Amaruq Hunter and Trappers Association for their valuable feedback and support of the various field programs that contributed to these datasets. Thanks to the captains and crews of the *F/V Frosti* and *R/V Nuliajuk* over the years for their support in offshore fish sampling, and the many DFO staff, community members, and monitors who have contributed to coastal and offshore field work and sample collection. We are grateful for the assistance of Krystal Woodard, Caitlin Allison, Judy Li, Mia Grabovac, Alyssa Goertz, and Sarah Rauf in selection and preparation of fish samples at the Freshwater Institute (Winnipeg) for laboratory analysis, and Mark Ouellette for BREA and CBS-MEA cruise data QA/QC.

The Beaufort Regional Environmental Assessment (Crown-Indigenous Relations and Northern Affairs Canada), Regional Strategic Environmental Assessment (Crown-Indigenous Relations and Northern Affairs Canada), Environmental Studies Research Fund (Natural Resources Canada), Program of Energy Research and Development (Natural Resources Canada), ArcticNet, and various internal Fisheries and Oceans Canada sources, notably the Marine Conservation Targets program, provided funding for BREA and CBS-MEA. Fish sampling in Frobisher Bay was conducted under the auspices of DFO's Coastal Environmental Baseline Program. Compilation of fish isotope data and downscaled ice-ocean model outputs was made possible thanks to DFO Competitive Science Research Fund (CSRF) support awarded to A. Ehrman and A. Niemi.

1.0 Introduction

The Arctic has experienced warming due to climate change faster than other parts of the world in recent decades, affecting physical processes like sea ice formation and phenology (Galley et al. 2016; Stammerjohn et al. 2012; Steele et al. 2015; Trischenko et al. 2022). Ocean models have been used to fill observational gaps in the investigation of large-scale physical processes across the Canadian Arctic, identify historical trends, and project future changes under varying climate change scenarios (Steiner et al. 2015). Changes to the physical environment over varying timescales covered by ocean models can affect Arctic marine ecosystems through bottom-up processes that cause shifts in timing and level of primary productivity and prey availability that can affect energy transfer through food webs (e.g., Grebmeier et al. 2006). Shifts in prey availability and timing can affect important fish species like Arctic cod (*Boreogadus saida*), which are keystone species in the transfer of energy from lower to upper trophic levels in offshore marine habitats as prey items for marine mammals and seabirds (Bouchard et al. 2017; Herbig et al. 2023; Welch et al. 1992). In coastal areas, fish species including Arctic char (*Salvelinus alpinus*) and Dolly Varden (*S. malma*) are important for subsistence and cultural use.

Changes in fish resource and habitat use can be investigated using stable isotopes, which can help differentiate between pelagic and benthic resource pathways and trophic levels. $\delta^{13}C$ differentiates basal resource use due to differing carbon isotope signatures in terrestrial and marine primary producers and benthic and pelagic sources (Fischer 1991; Peterson and Fry 1987), distinguishing species among broad habitat domains (e.g., coastal vs. offshore habitats) and feeding ecology (benthic vs. pelagic zones) within a region. $\delta^{15}N$ can be used as an indicator of trophic dynamics due to the fractionation of the lighter and heavier isotope in consumers relative to their diet (De Niro and Epstein 1981; Post 2002), and can reflect trophic position of individuals and the population (Layman et al. 2007).

This report summarizes two datasets compiled as part of Competitive Science Research Fund (CSRF) project 21-CC-03-14, linking sea-ice and physical ocean conditions to changes in resource use of anadromous, coastal, and marine fishes in the Canadian Arctic. First, $\delta^{13}C$ and $\delta^{15}N$ stable isotope data are summarized for 16 anadromous, coastal, and offshore marine fish species sampled in the Beaufort Sea and Amundsen Gulf areas of the western Canadian Arctic, and Frobisher Bay in the eastern Canadian Arctic. Second, environmental variables relevant to fish resource use derived from a coupled ice-ocean model are summarized weekly and by ice period (i.e., ice covered, break-up, open water, and freeze-up periods) for fish habitat areas in these regions.

2.0 Methods

2.1 Ecosystem Context

Coupled ice-ocean model outputs and Arctic fish isotopic signatures from two regions of the Canadian Arctic (Fig. 1) are described. In the western Canadian Arctic, the Beaufort Sea is defined by a broad continental shelf that extends approximately 120 km offshore, with the Amundsen Gulf system located to the east. Water mass structure comprises four vertically stacked layers (described in detail by Lansard et al. 2012; McLaughlin et al. 1996): 1) the surface mixed layer extends to ~50 m depth, characterized by low salinity due to its formation by ice melt, riverine freshwater inputs, and wind mixing; 2) the Pacific layer originates from the Pacific Ocean and displays variable salinity, extending from ~50-200 m deep; 3) a warmer, saltier layer of Atlantic-origin water extending from approximately 300-750 m depth; and 4) a layer of very cold, very saline Arctic Deep Water at depths deeper than 750 m. The transition between the Pacific and Atlantic layers (200-300 m depth) is characterized by a thermohalocline where temperature and salinity rapidly increases with depth (McLaughlin et al., 1996), which is included as a separate layer in this report.

In the eastern Canadian Arctic, Frobisher Bay is a large (~265 km) fjord located on the southeastern coast of Baffin Island (Fig. 1). The most inland end reaches maximum depths of 350 m (Deering et al. 2018),

and experiences extreme tidal amplitudes ranging from 7 to 11 m (Canadian Hydrographic Service 2024) which thoroughly mix surface waters (Lovrity 1984). Coastal areas are influenced by freshwater input from several rivers, however offshore water mass stratification and circulation is not well characterized.

Datasets described in this report are divided into a total of 14 sub-areas to differentiate environmental conditions in coastal areas and embayments from offshore areas, and delineate foraging habitat for anadromous fish in the marine environment (Fig. 1). Due to its small size relative to the western Canadian Arctic region, Frobisher Bay is considered a single area, and inshore and offshore habitats are not differentiated since only data from fish classified as using offshore marine habitats are included here.

In the western Canadian Arctic, coastal areas are outlined according to the distribution of coastal and freshwater-influenced habitats in Darnley Bay and on the Mackenzie Shelf (< 20 m depth; McNicholl et al. 2020). The offshore Beaufort Sea area includes the Mackenzie Shelf and slope (> 20 m depth), the western shelf of Banks Island, and deep areas in central Amundsen Gulf. Distinct environmental conditions in embayments of the Amundsen Gulf system (i.e., Franklin Bay, Darnley Bay, Minto Inlet, Prince Albert Sound, Prince of Wales Strait, and Dolphin and Union Strait) relative to the offshore sub-areas delineate each as an embayment sub-area (Fig. 1; Galley et al. 2023). Additional sub-areas for Dolly Varden (*S. malma*) foraging habitat on the Mackenzie Shelf (between 139.39°W, west of Herschel Island and 132.89°W, east of Tuktoyaktuk, within 150 km of shore; (Gallagher et al. 2021), and Arctic char (*S. alpinus*) foraging habitat (Minto Inlet and Prince Albert Sound, and areas along the coast of Ulukhaktok; Hollins et al. 2022; Lea et al. 2022; Fig. 1) are also included. Arctic char typically forage within ~1.5 km of shore in the Ulukhaktok region (Moore et al. 2016); however a buffer of 15 km along the coastline is

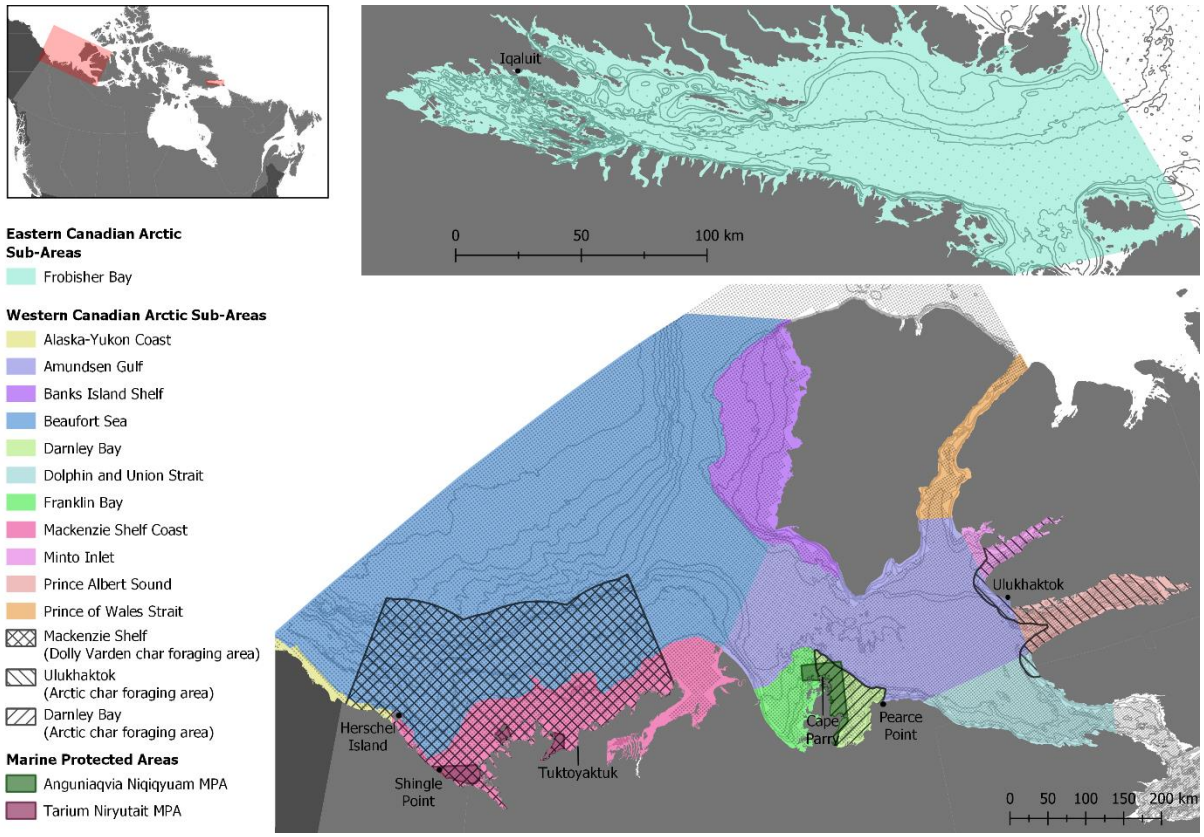

Figure 1 – Study regions in the eastern and western Canadian Arctic. Transparent grid centrepoints on each map indicate resolution and extent of coupled ice-ocean model data summarized for each area. Bathymetry lines within the study area are derived from GEBCO contours, and indicate 25 to 2,500 m depths.

used to ensure some environmental grids in this area are represented in the environmental data summaries. Arctic char caught in Darnley Bay typically forage in the shallow waters of the bay, occasionally occurring in deeper waters (Harwood and Babaluk 2014; McNicholl et al. 2020), such that the Darnley Bay sub-area between Cape Parry and Pearce Point is also identified as an Arctic char sub-area.

2.2 Fish Sample Collection

Fish data included in this report are from samples collected by five field programs focusing on coastal, anadromous and offshore fish species from various locations across the western Canadian Arctic, and Frobisher Bay.

2.2.1 Arctic Char and Dolly Varden Monitoring

Arctic char and Dolly Varden monitoring programs partner with experienced harvesters to annually collect fisheries data and sample Arctic char at Darnley Bay and Ulukhaktok, NT, and Dolly Varden at Herschel Island and Shingle Point, YK (Fig. 1). Anadromous (sea-run) char were harvested by local fishers using gill nets or occasionally fishing rods in summer months (June-September) from 2011-2020, and biological samples (e.g., dorsal muscle tissue for stable isotope analysis) collected with harvester permission by local monitors or staff of Fisheries and Oceans Canada (DFO) (Gallagher et al. 2017; Gallagher et al. 2013; Lea et al. 2022).

2.2.2 Arctic Coastal Ecosystem Study (ACES)

The Arctic Coastal Ecosystem Study (ACES) is conducted cooperatively by DFO and the Aklavik Hunters and Trappers Committee to monitor ecosystem health in the Tarium Niryutait Marine Protected Area (TNMPA; Fig. 1). Key fish species were caught in the coastal (< 20 m depth) habitat along Tapqap harvesting camp (Shingle Point, YK) by gill and seine net during summer (July). Fish species collected from 2011-2020 by the ACES program and included in this report include Arctic cisco (*Coregonus autumnalis*), broad whitefish (*C. nasus*), Arctic flounder (*Liopsetta glacialis*), starry flounder (*Platichthys stallatus*), and saffron cod (*Eleginus gracilis*).

2.2.3 Arctic Coast Monitoring Program

The Arctic Coast monitoring program is a community-based monitoring program developed in partnership with the Paulatuk Hunters and Trappers Committee (PHTC) to monitor ecosystem health in Darnley Bay, NT and the Anguniaqvia Niqiqyuam Marine Protected Area (ANMPA; Fig. 1). Fish were sampled with a variety of gear types between June-September from 2014-2020, and this report contains the same five coastal fish species sampled by the ACES program (Arctic cisco, broad whitefish, Arctic flounder, starry flounder, saffron cod), with the addition of capelin (*Mallotus villosus*) also sampled in Darnley Bay and the ANMPA (Christie et al. 2025; McNicholl et al. 2024).

2.2.4 Beaufort Regional Ecosystem Assessment Marine Fishes Project (BREA-MFP)/Canadian Beaufort Sea Ecosystem Assessment (CBS-MEA)

Offshore marine fish (20 to 1250 m depth) were collected as part of the Beaufort Regional Environmental Assessment Marine Fishes Project (BREA-MFP; 2012-2014) and the Canadian Beaufort Sea Marine Ecosystem Assessment (CBS-MEA; 2017-2019). Fish were sampled aboard the *F/V Frosti* during the open water period in the Beaufort Sea and Amundsen Gulf region (July-September; Fig. 1) using a modified Atlantic Western IIA otter trawl with a mesh cod-end and intermediate liner (Majewski et al. 2016). Eight species are included in this data report: Arctic alligatorfish (*Aspidophoroides olrikii*), Arctic cod (*Boreogadus saida*), gelatinous seasnail (*Liparis fabricii*), Greenland halibut (*Reinhardtius hippoglossoides*), longeared eelpout (*Lycodes seminudus*), ribbed sculpin (*Triglops pingelii*), spatulate sculpin (*Icelus spatula*), and twohorn sculpin (*I. bicornis*).

2.2.5 Iqaluit Coastal Ecosystem Baseline Program (ICEBP)

In Frobisher Bay in the eastern Canadian Arctic (Fig. 1), sampling was conducted as part of the Iqaluit Coastal Environmental Baseline Study (ICEBP) delivered through the coordination and partnership of

local (e.g., Iqaluit (Amaruq) Hunters and Trappers Association) and DFO partners. In coastal areas, fish were collected from August to October of 2018-2020 at depths from 8 to 59 m with a benthic sled. Offshore sampling from 220 to 470 m was conducted from September to October of 2019 onboard the *R/V Nuliajuk* using a Campelen 1200 research trawl. Although sampling occurred in coastal areas of inner Frobisher Bay, only offshore marine species including Arctic cod, Greenland halibut, spatulate sculpin, and twohorn sculpin were included in this data report.

2.3 Stable Isotope Analysis

Muscle tissue collected from all samples for stable isotope analysis was freeze-dried (Labconco FreeZone 18 freeze-drier) or oven-dried at 50°C, ground to a fine homogenate using a mortar and pestle, and analyzed for stable C and N isotopic composition. Samples were analyzed by a Delta Plus (Thermo-Finnigan) and a Thermo Advantage V Plus (Thermo Scientific) continuous flow isotope mass spectrometer at the Environmental Isotopes Laboratory (Waterloo, Canada) and Fisheries and Oceans Canada Biotracers Laboratory (Winnipeg, Canada), respectively, coupled with a 4010 Elemental Analyzer (Costech instruments). Data comparability between labs had been previously verified (Rosenberg et al. 2015). Stable isotope ratios were expressed in standard delta (δ) notation in parts per thousand (‰) as the ratio of heavy to light isotope relative to the international standards Vienna Pee Dee Belemnite for C and atmospheric N_2 for N (Craig 1957; Mariotti 1983). Working laboratory standards for animal tissues included two standards of $(NH_4)_2SO_4$ for $\delta^{15}N$ and cellulose for $\delta^{13}C$ at the Environmental Isotopes Laboratory, and two standards of glutamic acid (USGS 40 and 41) as well as an in-house fish tissue standard at the Biotracers Laboratory. All working laboratory standards were cross calibrated to the international standard materials mentioned above. Analytical error for $\delta^{15}N$ and $\delta^{13}C$ did not exceed 0.3 and 0.2 ‰ per run, respectively, based on repeated measurements of laboratory standard material, comprising no less than 20% of each run. Repeatability based on duplicate measurements of sample material was 0.20‰ and 0.23‰ for $\delta^{13}C$ and $\delta^{15}N$, respectively.

High C:N ratios (>3.5; Skinner et al. 2016) indicated high lipid content of some Arctic alligatorfish, Arctic char, Dolly Varden, Greenland halibut, and ribbed sculpin samples. Lipids were extracted from these samples following the protocol described in Choy et al. (2016), and the extracted samples were re-analyzed for $\delta^{13}C$ and $\delta^{15}N$ as described above. Lipid correction followed the methods outlined in Logan et al. (2008), where differences in mean changes in C and N isotopes ($\delta^{13}C' - \delta^{13}C$ and $\delta^{15}N' - \delta^{15}N$) between lipid-extracted ($\delta^{13}C'$ and $\delta^{15}N'$) and untreated ($\delta^{13}C$ and $\delta^{15}N$) samples were tested using paired t-tests with Holm-Bonferroni corrections to account for multiple comparisons across species. The relationship between the isotope differences and log-transformed C:N ratio tested was using robust regression in the robustbase package in R (Maechler et al. 2022), and model significance determined using f-tests comparing each regression against null models, again applying Holm-Bonferroni corrections. Significant lipid-correction regression models relating differences in $\delta^{13}C$ pre- and post-extraction to C:N were applied to all samples of Greenland halibut, Arctic char, and Dolly Varden (Table A1).

Individual fish $\delta^{15}N$ values were adjusted to the mean weight of the sample population following Logan et al. (2008) using the slope of the relationship between $\delta^{15}N$ and mass (g) for each fish taxa to account for ontogenetic dietary variation (Romanuk et al. 2011). Where missing, mass was estimated using species-specific linear regressions with $\log_{10}$ fork length (3.6% of Arctic cod samples, 2% of Greenland halibut samples caught in the western Canadian Arctic). Further adjustments to fish $\delta^{15}N$ were made using the slope of the relationship between $\delta^{15}N$ and sampling depth to standardize values to the mean depth at which each species was sampled due to baseline $\delta^{15}N$ values being higher in high-latitude, deep water benthic habitats relative to shallower waters as a result of preferential remineralization of the lighter isotope, ^{14}N, by bacteria in the water column (Sigman and Casciotti, 2001). Regression results and standardized masses and water depths to which each species was corrected can be found in Table A2.

To reduce the impact of differing isotopic baselines among fish habitat sub-areas, fish isotope values were rescaled by mean-standardizing for each species and sub-area by subtracting the mean isotope value for each species in each area across the study period, then dividing by the standard deviation. Means of these mean-standardized isotope values were calculated by species for each sub-area (Table A3).

2.4 Coupled Ice-Ocean Model Data

Ocean and sea ice variables were summarized weekly for each habitat area from 2010-2021 from outputs of a NEMO-LIM2 coupled ice-ocean model (Madec et al. 2017). The downscaled model outputs comprised daily temporal resolution and were downscaled to a 1/12^{o} spatial grid (see Long et al. 2024) for the Beaufort Sea and Davis Strait to enable resolution of coastal habitats in the western and eastern Canadian Arctic. Downscaled model output variables are defined in Table 1 and comprised three dimensional variables with 50 z-vertical levels including potential temperature, potential salinity, sea water velocity. Two-dimensional variables included surface downward stress, sea ice concentration, sea ice thickness, and snow thickness. Vector addition was used to calculate the total magnitude of variables with directional components (sea water velocity and surface downward stress).

Table 1 – Sea ice and ocean variables derived from a NEMO-LIM2 coupled ice-ocean model. Three-dimensional variables have a depth component and were summarized for approximate water mass depths.

Variable	Symbol	Unit	Dimensions	Definition
Potential temperature	votemper	C	3D	Mean potential temperature calculated for each water mass in each area.
Potential salinity	vosaline	ppt	3D	Mean potential salinity calculated for each water mass in each area.
Sea water velocity (magnitude)	crtxyz	m/s	3D	Combined sea water velocity (magnitude); calculated by vector addition of horizontal and vertical components of sea water velocity.
Surface downward stress (magnitude)	uvtau	Pa	2D	Total magnitude of stress exerted on the ocean surface, due to ice movement or wind when ice was not present; calculated by vector addition of directional components of surface downward stress.
Sea ice concentration	siconc		2D	Mean proportion of each area covered by sea ice.
Sea ice thickness	sithic	m	2D	Mean sea ice thickness across each area.
Snow thickness	snow	m	2D	Mean thickness of snow atop sea ice across each area.
Break-up start date	bu_start	Day of year		First day of the year where mean sea ice concentration on each day of the previous two weeks was less than the winter (Jan-Feb) mean (per Walsh et al., 2022).
Break-up end date	bu_end	Day of year		Last day of the year when the previous two weeks' mean sea ice concentration was less than the mean summer (Aug-Sept) sea ice concentration (per Walsh et al., 2022).
Break-up period duration	bu_duration	Days		Number of days from ice break-up start to ice-break up end, defined by Walsh et al. (2022).
Open water season duration	ow_duration	Days		Number of days from ice break-up end (Walsh et al. 2022) to date fish was sampled.
Freeze-up start	fu_start	Day of year		The first day of the latter half of the year when the daily mean sea ice concentration increased to more than one standard deviation above the summer mean sea ice concentration.
Freeze-up end	fu_end	Day of year		First day after freeze-up start when the daily sea ice concentration during the previous two weeks exceeds the winter (Jan-Feb) mean sea ice concentration.

Sea ice concentration was used to derive days of the year corresponding to ice break-up start, break-up end, freeze-up start, and freeze-up end according to the definitions of these dates defined by Walsh et al. (2022). Briefly, weekly or bi-weekly means of sea ice concentration for each area were compared with thresholds based on summer (Aug-Sept) and winter (Jan-Feb) mean sea ice concentration. Break-up start was defined as the first day of the year where mean sea ice concentration on each day of the previous two weeks was less than the winter (Jan-Feb) mean; break-up end was the last day of the year when the previous two weeks' mean sea ice concentration was less than the mean summer (Aug-Sept) sea ice concentration. Freeze-up start occurred on the first day of the latter half of the year when the daily mean sea ice concentration increased to more than one standard deviation above the summer mean sea ice concentration; and freeze-up end was defined as the first day after freeze-up start when the daily sea ice concentration during the previous two weeks exceeds the winter (Jan-Feb) mean sea ice concentration. Durations of break-up and freeze-up periods were calculated by subtracting end date from start date for each period. Ice-covered period duration was calculated by subtracting break-up start date from freeze-up end date, and open water period duration was calculated by subtracting freeze-up start date from break-up end date.

Weekly summaries of two-dimensional (sea ice concentration, snow thickness, surface downward stress) variables were calculated for each fish habitat sub-area. Three-dimensional variables (potential temperature, potential salinity) were also divided by depth roughly corresponding to the surface (< 60 m), Pacific (60-200 m), and Atlantic (600-900 m) and Arctic (> 900 m) water layers of the highly stratified and well-studied western Canadian Arctic study area. Water mass structure in Frobisher Bay is less well-studied compared with the Beaufort Sea, so NEMO variables from Frobisher Bay were only summarized for the surface layer (< 60 m).

Seasonal summaries were prepared by classifying each week into break-up, open-water, freeze-up, and ice-covered periods based on break-up and freeze-up start and end dates in each year. Combined means and standard deviations were calculated based on the number of days in each week falling into each period. As with the weekly summaries described above, two-dimensional variables are presented for each fish habitat sub-area, and three-dimensional variables are also summarized by depths approximating water masses in the western Canadian Arctic and only the surface layer for Frobisher Bay.

3.0 Results and Discussion

The stable isotope data presented identifies spatial, interannual, and inter-species variability in fish isotope ratios between 2011-2020 from the western and eastern Canadian Arctic. Catches from year-to-year were variable, especially of offshore marine fish due to the large habitat areas, as well as sea ice conditions that may have interfered with repeated sampling in multiple years. Fish isotope data are presented for each year and location for which they were available. Consistent sampling of stable isotopic baseline organisms (e.g., Calanus sp., bivalves) were not available for comparison versus stable isotope values of fish for the entire study period and in all habitat areas, so we used mean-standardized values representing the deviation in each year from the long-term mean isotope ratio for each area.

There were no obvious long-term trends in either mean-standardized $\delta^{13}C$ or $\delta^{15}N$ for any species or study areas. Some individual samples exceeded two standard deviations from the long-term mean, and although there was year-to-year variability across species, only median values $\delta^{15}N$ of Arctic flounder sampled along the Mackenzie Shelf coast in 2019 and $\delta^{13}C$ of Arctic cod sampled in Frobisher Bay in 2020 differed considerably from the long-term mean (> 2 s.d.), though few individuals of each species were sampled in those years (n = 4, and n = 5, respectively).

Among the years with smaller interannual variability, (< 2 s.d.), anadromous Arctic char sampled in Darnley Bay exhibited above- and below-average $\delta^{13}C$ and $\delta^{15}N$, respectively, in 2016, while Arctic char sampled in Ulukhaktok deviated from the long-term mean of $\delta^{13}C$ in 2015 and 2017 (Fig. 2). Anadromous

Dolly Varden sampled on the Mackenzie Shelf similarly showed above-average $\delta^{13}C$ in 2016 and below-average $\delta^{15}N$ in 2016 and 2017 (Fig. 3).

Stable isotope data for coastal fish sampled along the Mackenzie Shelf Coast in the TNMPA were consistently available for all years from 2011-2020, while sampling in Darnley Bay in the ANMPA began in 2015 (Figs. 4-8). $\delta^{15}N$ of Arctic flounder sampled in the TNMPA was highest in 2019, the only year where it exceeded the long-term average by more than two standard deviations (Fig. 4). Median annual $\delta^{13}C$ of saffron cod sampled in the TNMPA was slightly lower than the long-term meane in 2016, while $\delta^{15}N$ gradually increased to a peak in 2014 decreased to the lowest value in 2017, and returned to values near the long-term mean from 2018-2020 (Fig. 6). $\delta^{13}C$ of Arctic cisco sampled in the TNMPA in 2019 and 2020 was higher than the long-term mean, while $\delta^{15}N$ of fish sampled in Darnley Bay was lower than average in 2020 (Fig. 8).

Arctic cod is the most abundant forage fish in the Arctic (e.g., Benoit et al. 2008; Geoffroy et al. 2016), and were sampled in the Mackenzie Shelf, Amundsen Gulf, and Dolphin and Union Strait areas in five of the six years (2012-2014 and 2017-2019) within the study period that offshore trawl surveys were conducted in the western Canadian Arctic, and all years (2018-2020) that sampling was conducted in Frobisher Bay (Fig. 9). Arctic cod $\delta^{13}C$ was higher than the long-term average for Amundsen Gulf, Dolphin and Union Strait, and Minto Inlet in 2017, as well as Amundsen Gulf for 2018, and was more than two standard deviations from the long-term mean in Frobisher Bay in 2020. $\delta^{15}N$ for Arctic cod did not deviate significantly from the long-term means in any study areas (Fig. 9). Capelin, the other forage fish species included in this report, were all sampled in Darnley Bay in 2014 and 2017-2019 and also exhibited higher than average $\delta^{13}C$ in 2017 (Fig. 10).

Mean-standardized $\delta^{13}C$ and $\delta^{15}N$ of other offshore marine fish generally did not deviate significantly from the long term mean except where sample sizes were very small ($n < 5$; Figs. 11-17; also see Appendix 1). Exceptions included lower than average $\delta^{13}C$ and higher than average $\delta^{15}N$ in Arctic alligatorfish sampled in the Beaufort Sea in 2014 ($n = 7$; Fig. 11), higher than average ribbed sculpin $\delta^{13}C$ and $\delta^{15}N$ in the Beaufort Sea in 2014 ($n = 5$; Fig. 15), and higher than average spatulate sculpin $\delta^{13}C$ and $\delta^{15}N$ in Frobisher Bay in 2020 ($n = 10$; Fig. 16).

Modelled ice and ocean variables relevant to fish habitat use and diet are summarized for each week from 2010-2021 for each habitat area in Figures 18-25, and for each period (break-up, open water, freeze-up, ice-covered) in Figures 26-31. Note that the final ice-covered period summary for each area (ice 2020) contains data from the end of the freeze-up period in late 2020 to the beginning of the ice break-up period in early 2021, accounting for the difference in years between the two temporal resolutions. Variables with depth components, including potential temperature (Fig. 23; Fig. 30), potential salinity (Fig. 24; Fig. 31), and sea water velocity (Fig. 25; Fig. 32), are also summarized by water mass, which display variable conditions. The largest amplitude of variability across all depth-integrated environmental variables occurs in the surface water layer, gradually decreasing with depth. Seasonal, interannual, and spatial variability is also evident across modelled ocean and ice data, reflecting variable habitat conditions for coastal and anadromous fishes, as well as offshore pelagic and benthic fish species.

Mean-standardized stable isotope dataset summaries and weekly ice-ocean model data for the habitat areas described in this report will be available on the Open Government Portal (www.open.canada.ca) by searching keywords including “fish”, “resource use”, “isotope”, “ice-ocean model”, “Canadian Beaufort Sea” and “Frobisher Bay”. Raw isotope data and daily coupled ice-ocean model outputs from the 1/12° nested NEMO-LIM2 model covering the Beaufort Sea and Davis Strait can be requested from the respective program leads (see Appendix 4).

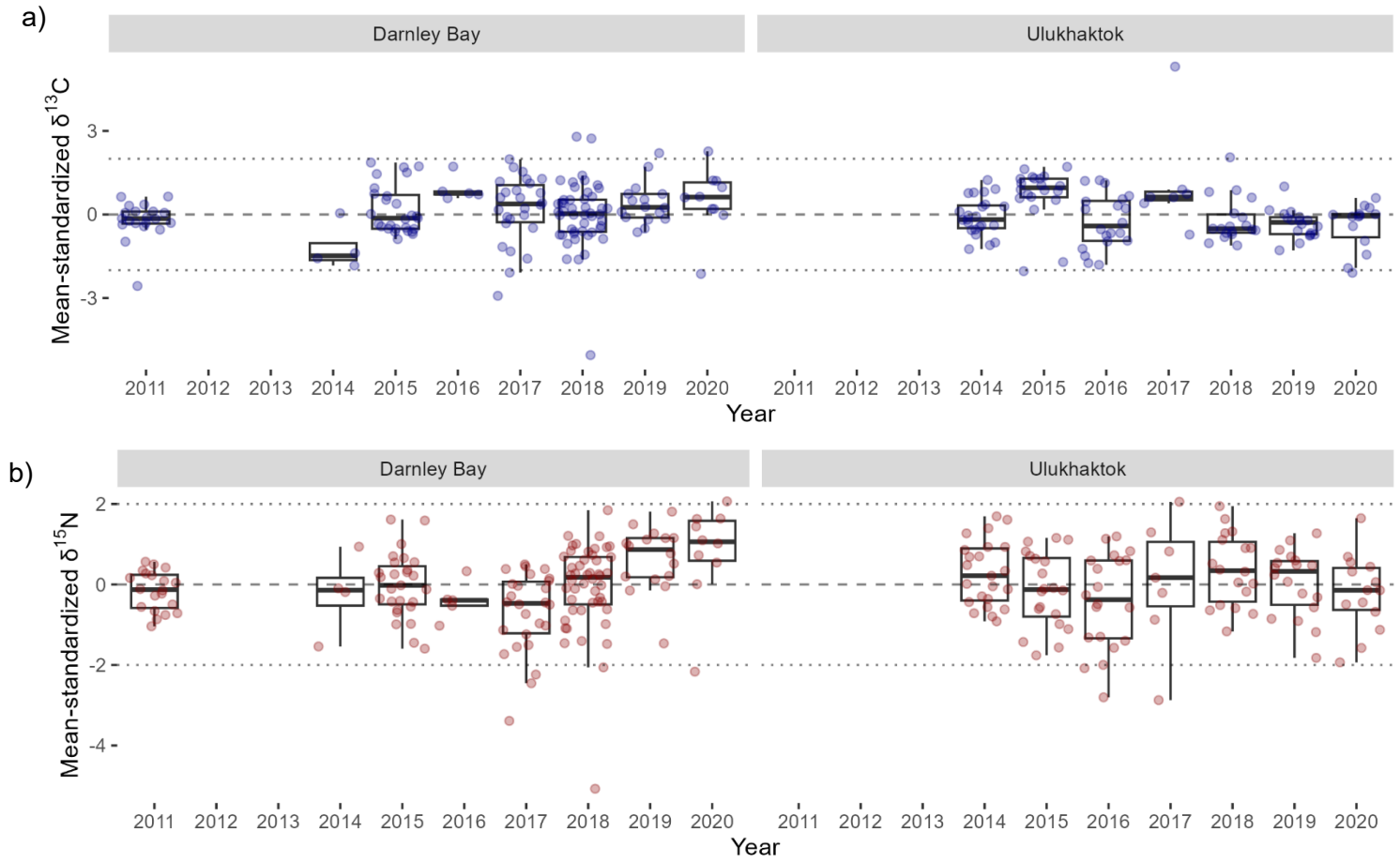

Figure 2 – Arctic char (*Salvelinus alpinus*) spatial and temporal variability in mean-standardized $\delta^{13}C$ (a) and $\delta^{15}N$ (b) isotope ratios from 2011 to 2020. Points represent individual samples, dashed lines indicate no difference from the mean isotope ratio across the entire study period for each area, and dotted lines indicate two standard deviations from the long-term mean.

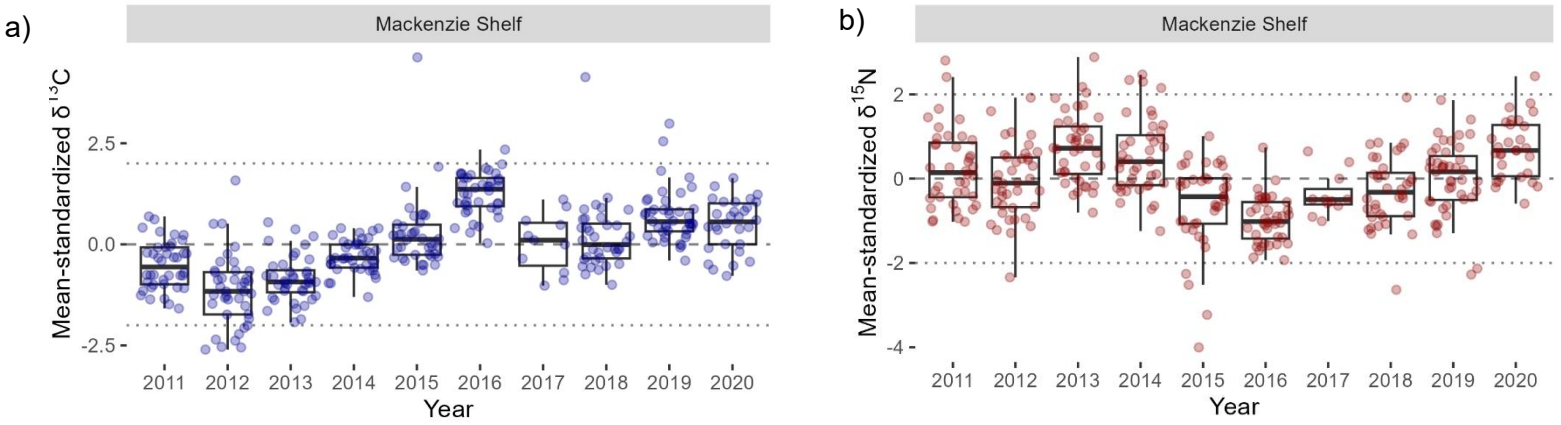

Figure 3 – Dolly Varden (*Salvelinus malma*) temporal variability in mean-standardized $\delta^{13}C$ (a) and $\delta^{15}N$ (b) isotope ratios from 2011 to 2020. Points represent individual samples, dashed lines indicate no difference from the mean isotope ratio across the entire study period for each area, and dotted lines indicate two standard deviations from the long-term mean

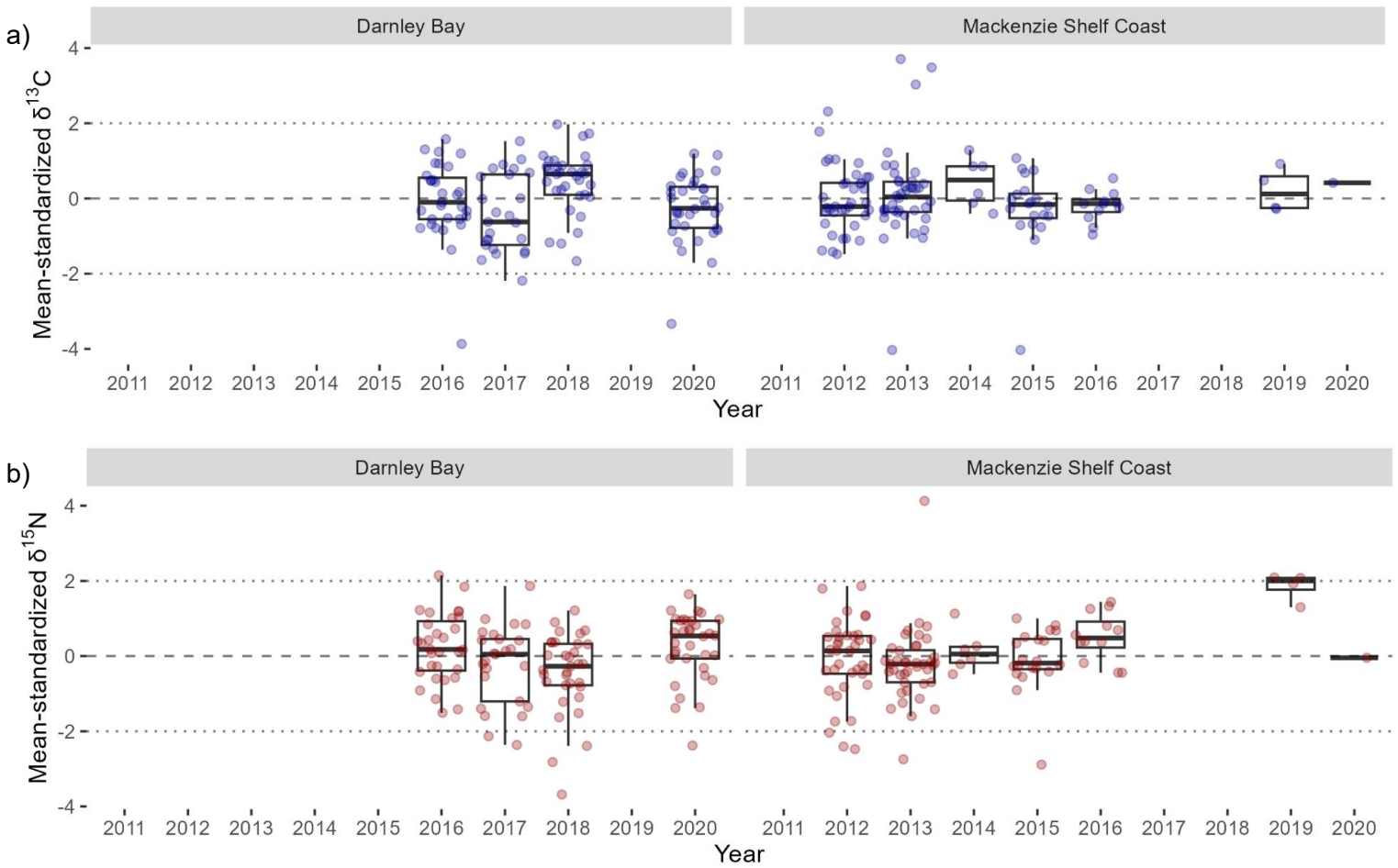

Figure 4 – Arctic flounder (*Liopsetta glacialis*) spatial and temporal variability in mean-standardized $\delta^{13}C$ (a) and $\delta^{15}N$ (b) isotope ratios from 2011 to 2020. Points represent individual samples, dashed lines indicate no difference from the mean isotope ratio across the entire study period for each area, and dotted lines indicate two standard deviations from the long-term mean

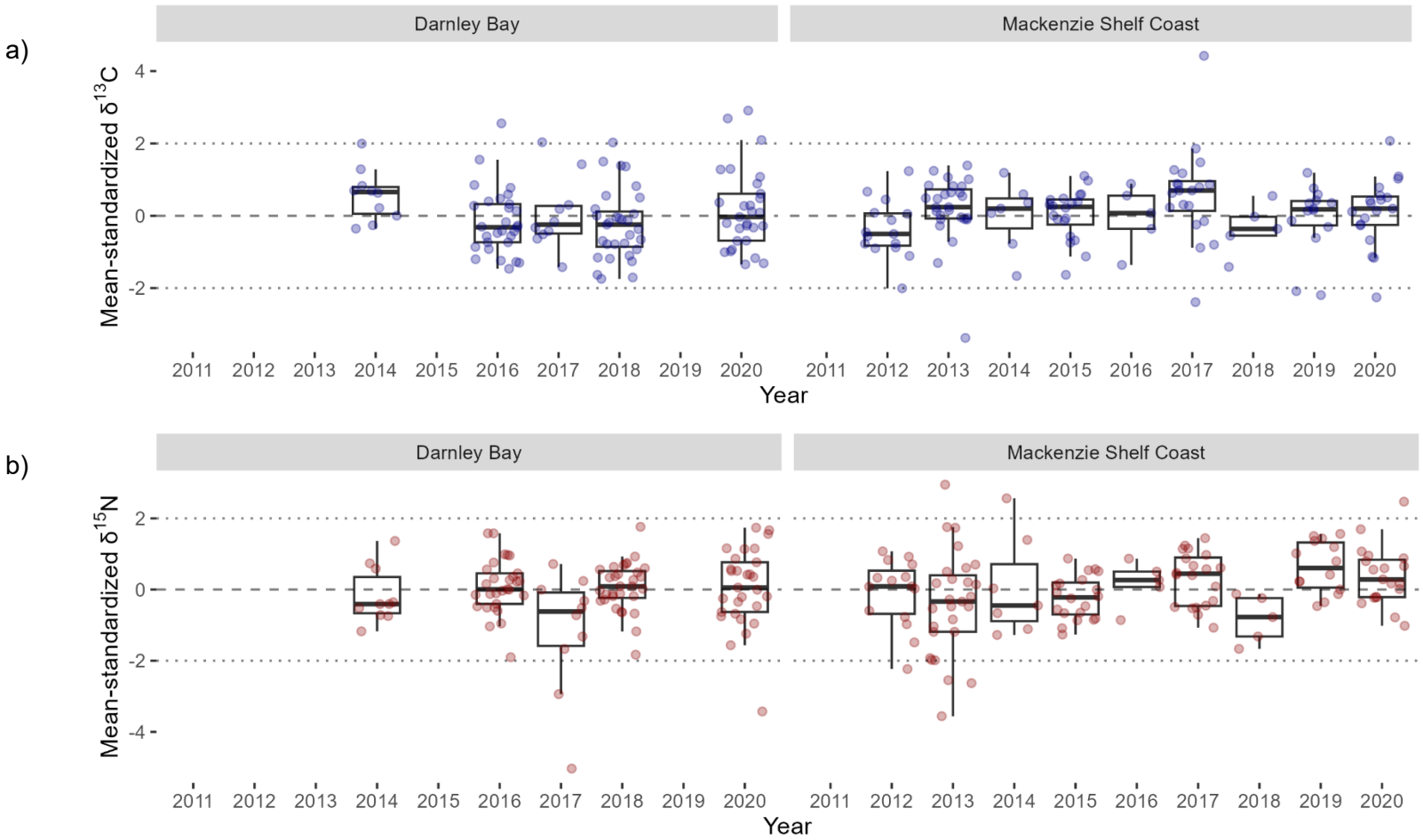

Figure 5 – Starry flounder (*Platichthys stellatus*) spatial and temporal variability in mean-standardized $\delta^{13}C$ (a) and $\delta^{15}N$ (b) isotope ratios from 2011 to 2020. Points represent individual samples, dashed lines indicate no difference from the mean isotope ratio across the entire study period for each area, and dotted lines indicate two standard deviations from the long-term mean

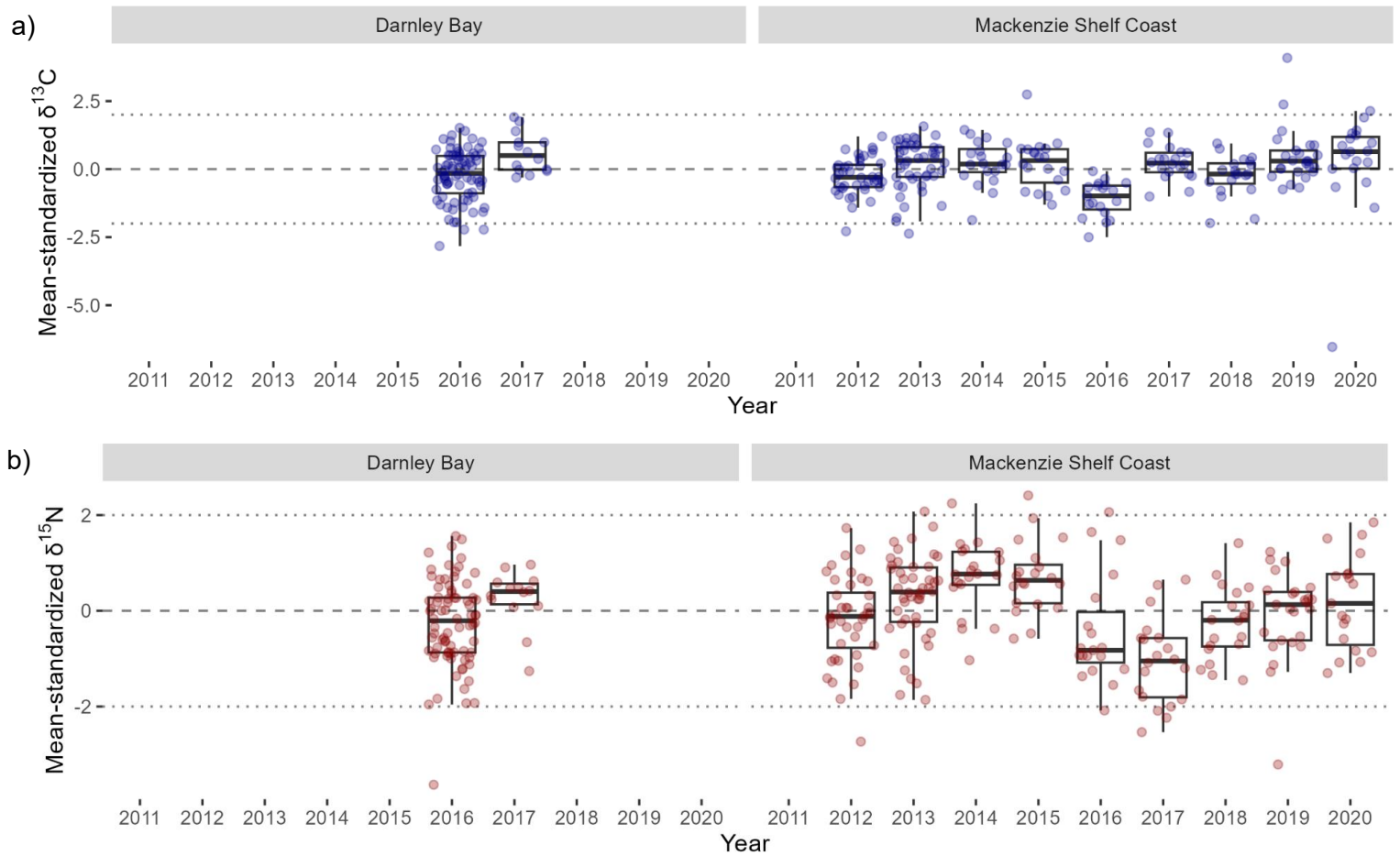

Figure 6 – Saffron cod (*Eleginus gracilis*) spatial and temporal variability in mean-standardized $\delta^{13}C$ (a) and $\delta^{15}N$ (b) isotope ratios from 2011 to 2020. Points represent individual samples, dashed lines indicate no difference from the mean isotope ratio across the entire study period for each area, and dotted lines indicate two standard deviations from the long-term mean

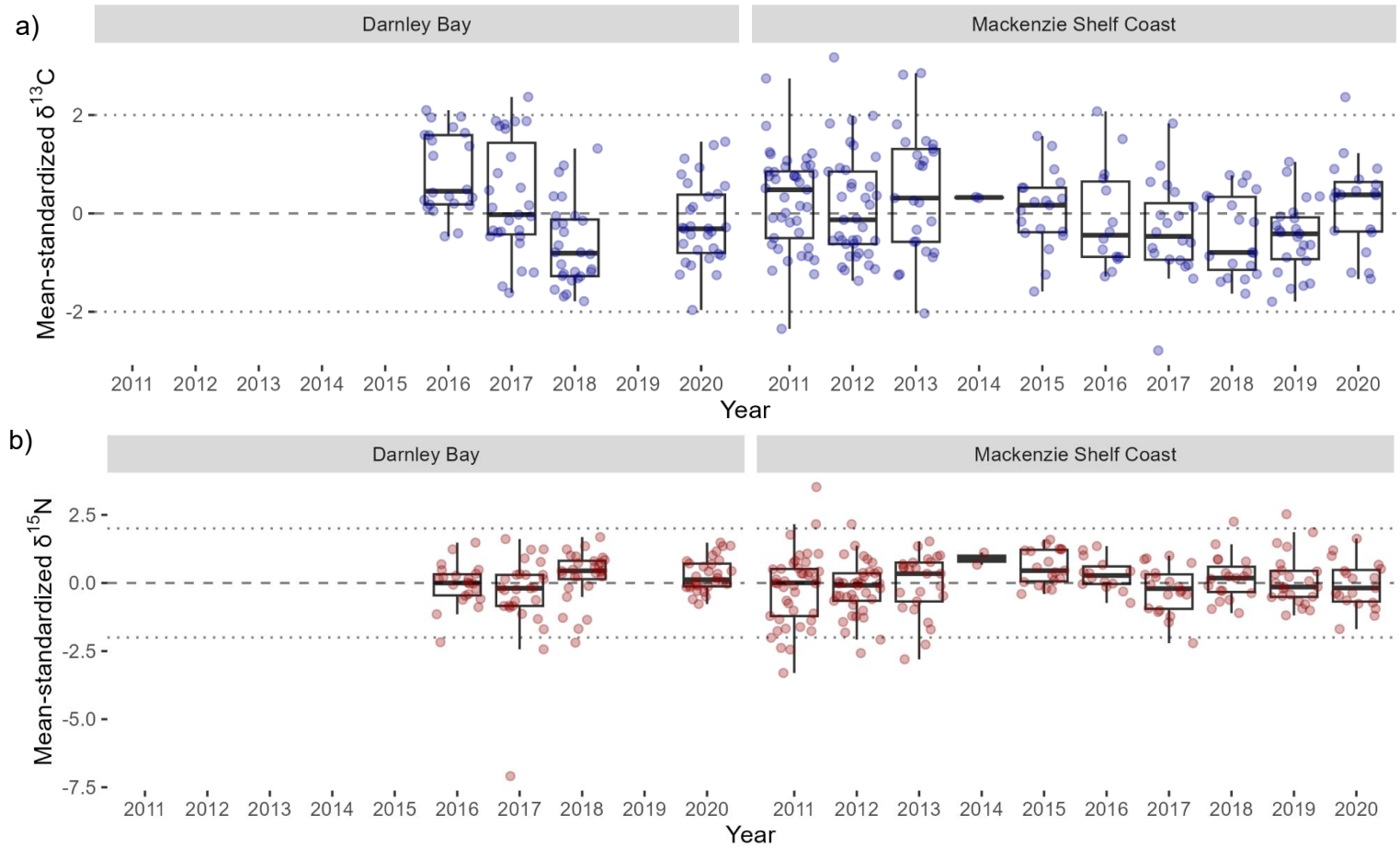

Figure 7 – Broad whitefish (*Coregonus nasus*) spatial and temporal variability in mean-standardized $\delta^{13}C$ (a) and $\delta^{15}N$ (b) isotope ratios from 2011 to 2020. Points represent individual samples, dashed lines indicate no difference from the mean isotope ratio across the entire study period for each area, and dotted lines indicate two standard deviations from the long-term mean

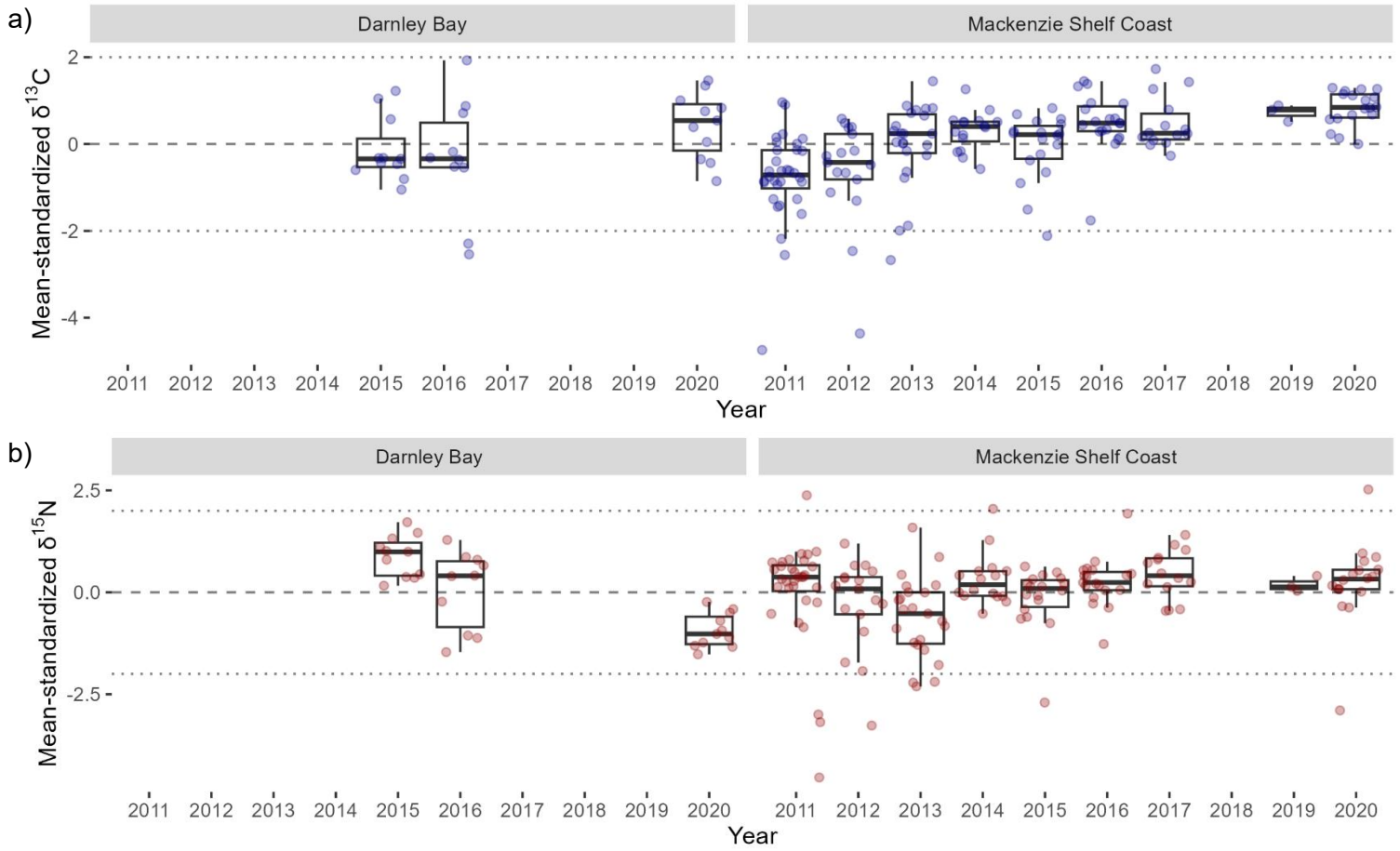

Figure 8 – Arctic cisco (*Coregonus autumnalis*) spatial and temporal variability in mean-standardized $\delta^{13}C$ (a) and $\delta^{15}N$ (b) isotope ratios from 2011 to 2020. Points represent individual samples, dashed lines indicate no difference from the mean isotope ratio across the entire study period for each area, and dotted lines indicate two standard deviations from the long-term mean

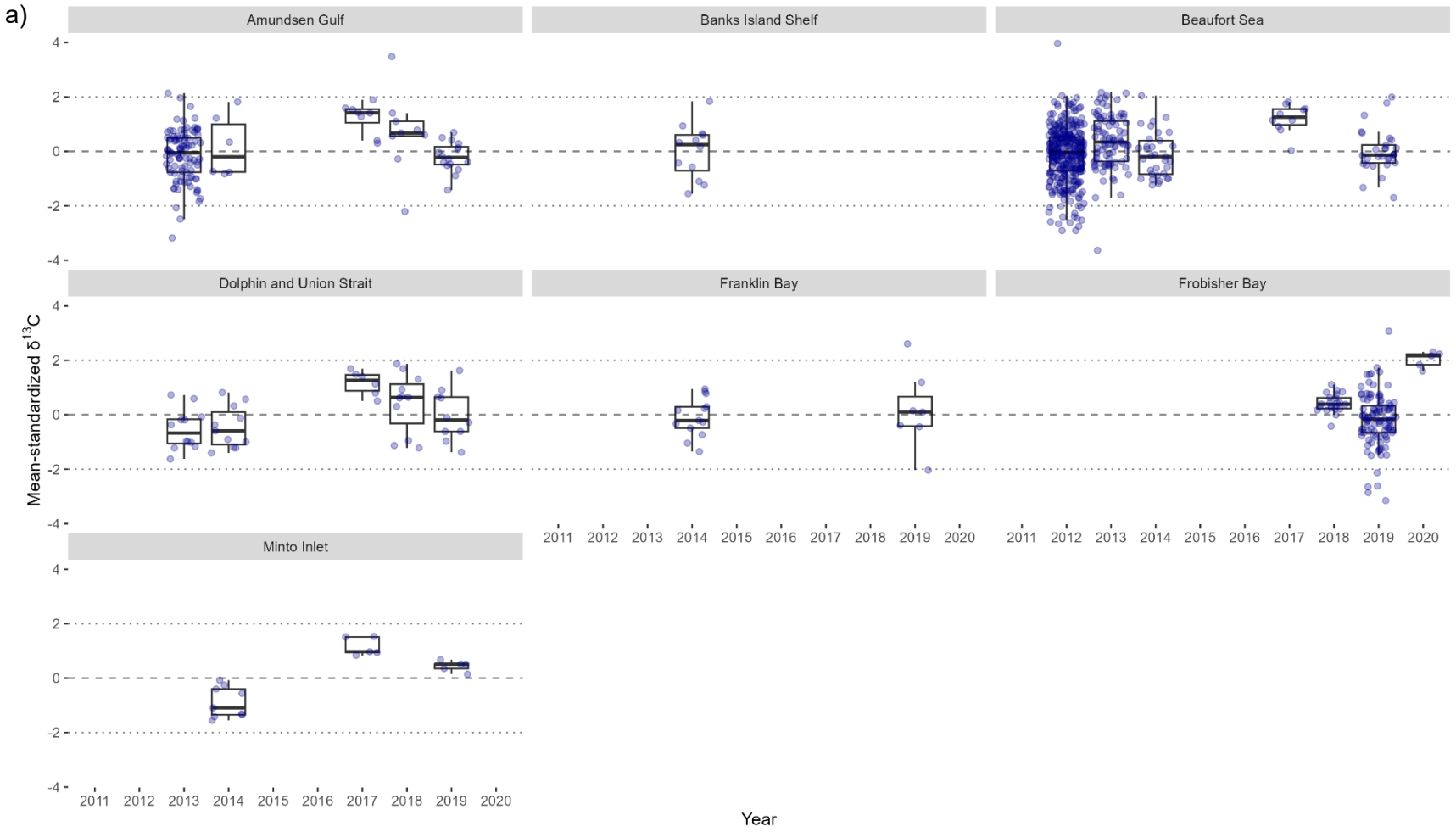

Figure 9 – Arctic cod (*Boreogadus saida*) spatial and temporal variability in mean-standardized $\delta^{13}C$ (a) and $\delta^{15}N$ (b) isotope ratios from 2011 to 2020. Points represent individual samples, dashed lines indicate no difference from the mean isotope ratio across the entire study period for each area, and dotted lines indicate two standard deviations from the long-term mean

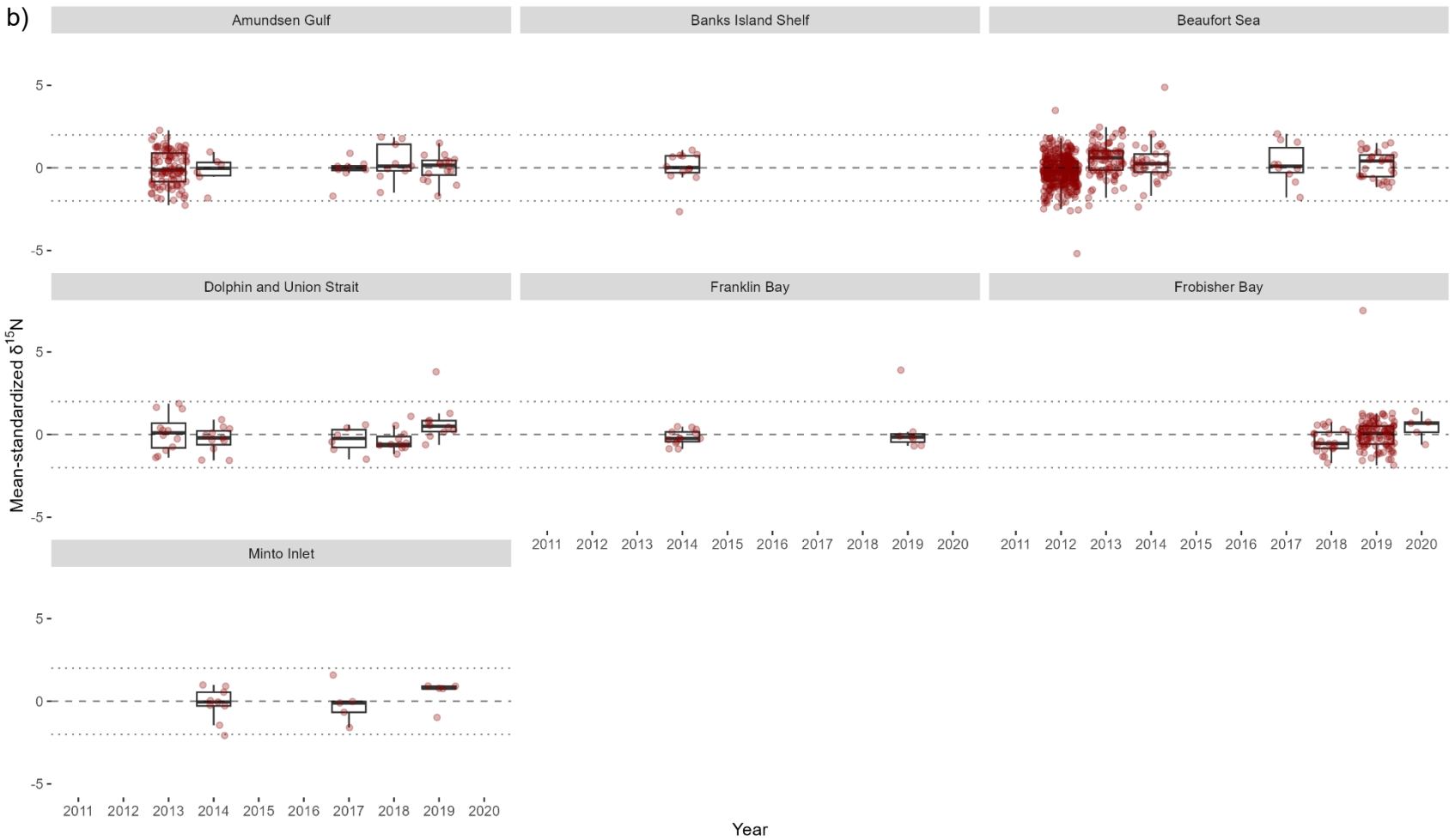

Figure 9 (cont'd) – Arctic cod (*Boreogadus saida*) spatial and temporal variability in mean-standardized $\delta^{13}C$ (a) and $\delta^{15}N$ (b) isotope ratios from 2011 to 2020. Points represent individual samples, dashed lines indicate no difference from the mean isotope ratio across the entire study period for each area, and dotted lines indicate two standard deviations from the long-term mean

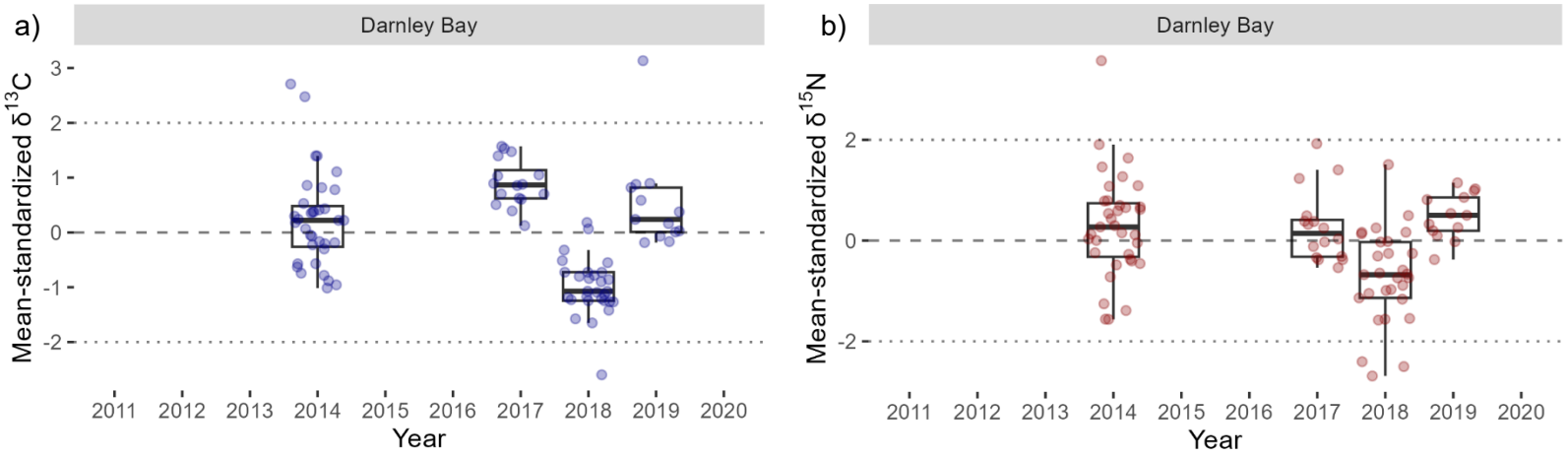

Figure 10 – Capelin (*Mallotus villosus*) temporal variability in mean-standardized $\delta^{13}C$ (a) and $\delta^{15}N$ (b) isotope ratios from 2011 to 2020. Points represent individual samples, dashed lines indicate no difference from the mean isotope ratio across the entire study period for each area, and dotted lines indicate two standard deviations from the long-term mean

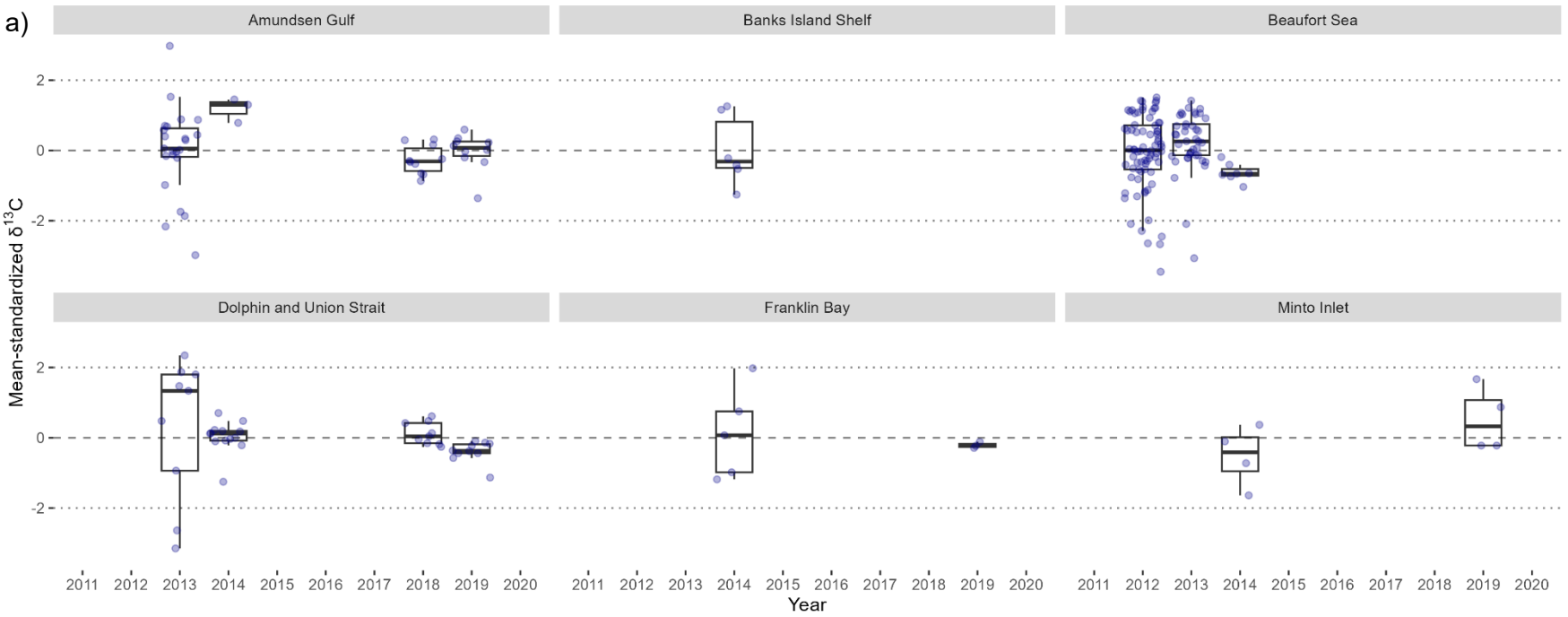

Figure 11 – Arctic alligatorfish (*Aspidophoroides olrikii*) spatial and temporal variability in mean-standardized $\delta^{13}C$ (a) and $\delta^{15}N$ (b) isotope ratios from 2011 to 2020. Points represent individual samples, dashed lines indicate no difference from the mean isotope ratio across the entire study period for each area, and dotted lines indicate two standard deviations from the long-term mean

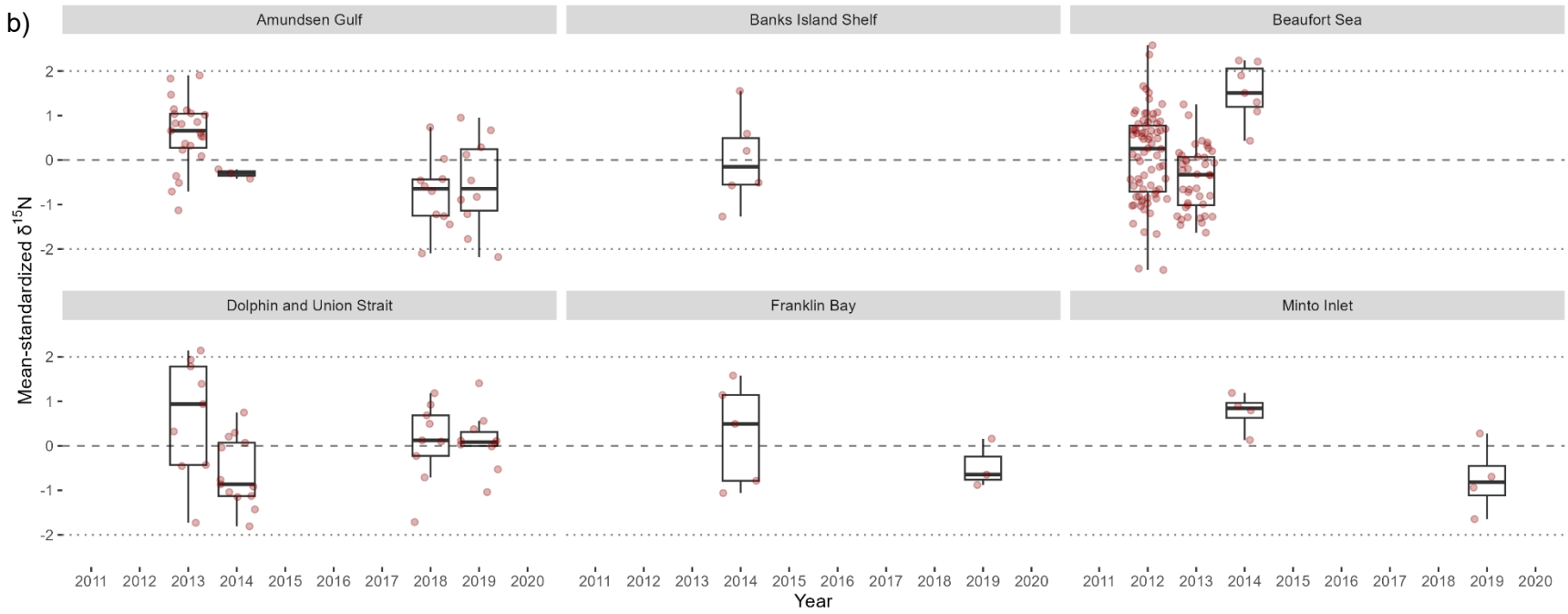

Figure 11 (cont'd) - Arctic alligatorfish (*Aspidophoroides olrikii*) spatial and temporal variability in mean-standardized $\delta^{13}C$ (a) and $\delta^{15}N$ (b) isotope ratios from 2011 to 2020. Points represent individual samples, dashed lines indicate no difference from the mean isotope ratio across the entire study period for each area, and dotted lines indicate two standard deviations from the long-term mean

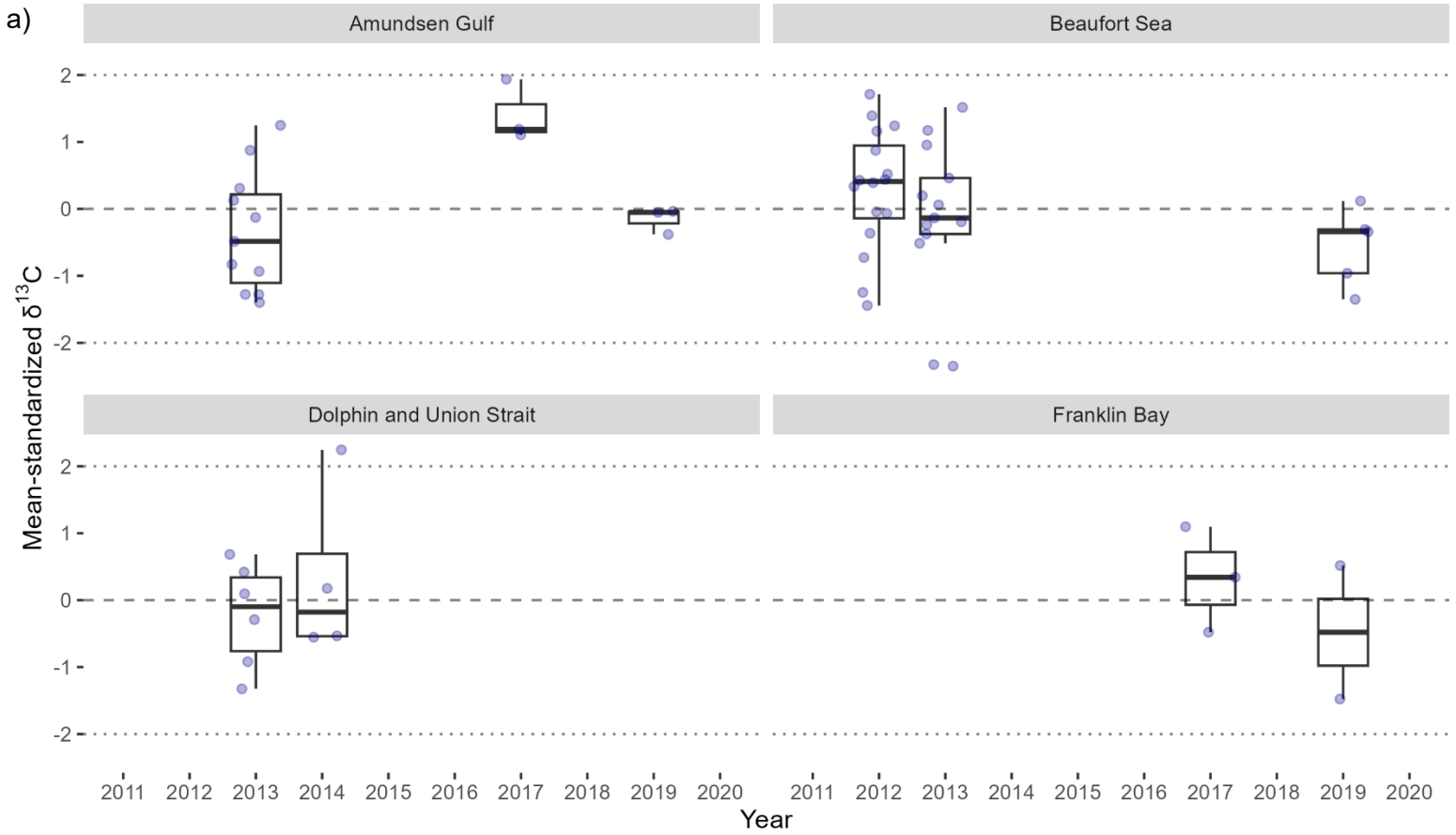

Figure 12 – Gelatinous seasnail (*Liparis fabricii*) spatial and temporal variability in mean-standardized $\delta^{13}C$ (a) and $\delta^{15}N$ (b) isotope ratios from 2011 to 2020. Points represent individual samples, dashed lines indicate no difference from the mean isotope ratio across the entire study period for each area, and dotted lines indicate two standard deviations from the long-term mean

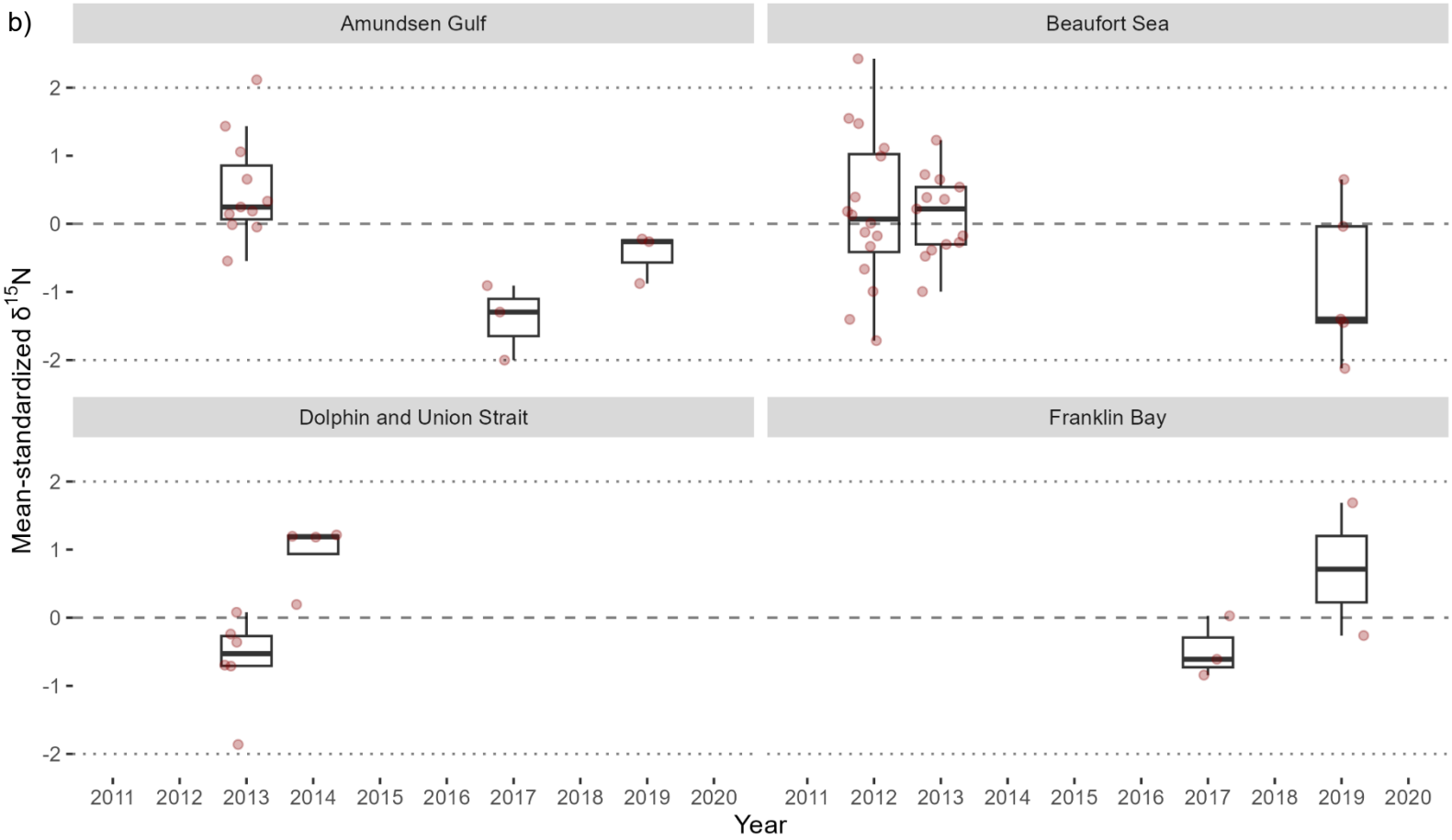

Figure 12 (cont'd) – Gelatinous seasnail (*Liparis fabricii*) spatial and temporal variability in mean-standardized $\delta^{13}C$ (a) and $\delta^{15}N$ (b) isotope ratios from 2011 to 2020. Points represent individual samples, dashed lines indicate no difference from the mean isotope ratio across the entire study period for each area, and dotted lines indicate two standard deviations from the long-term mean

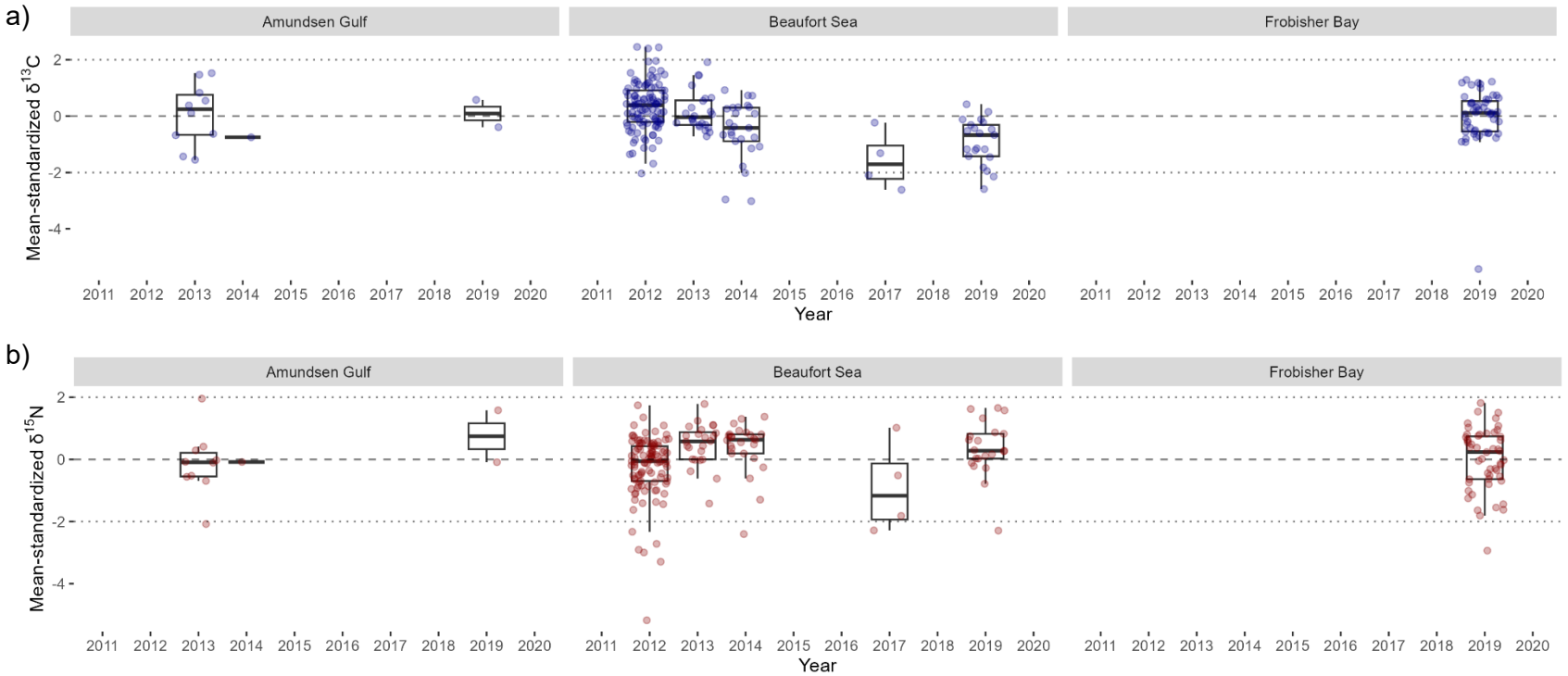

Figure 13 – Greenland halibut (*Reinhardtius hippoglossoides*) spatial and temporal variability in mean-standardized $\delta^{13}C$ (a) and $\delta^{15}N$ (b) isotope ratios from 2011 to 2020. Points represent individual samples, dashed lines indicate no difference from the mean isotope ratio across the entire study period for each area, and dotted lines indicate two standard deviations from the long-term mean

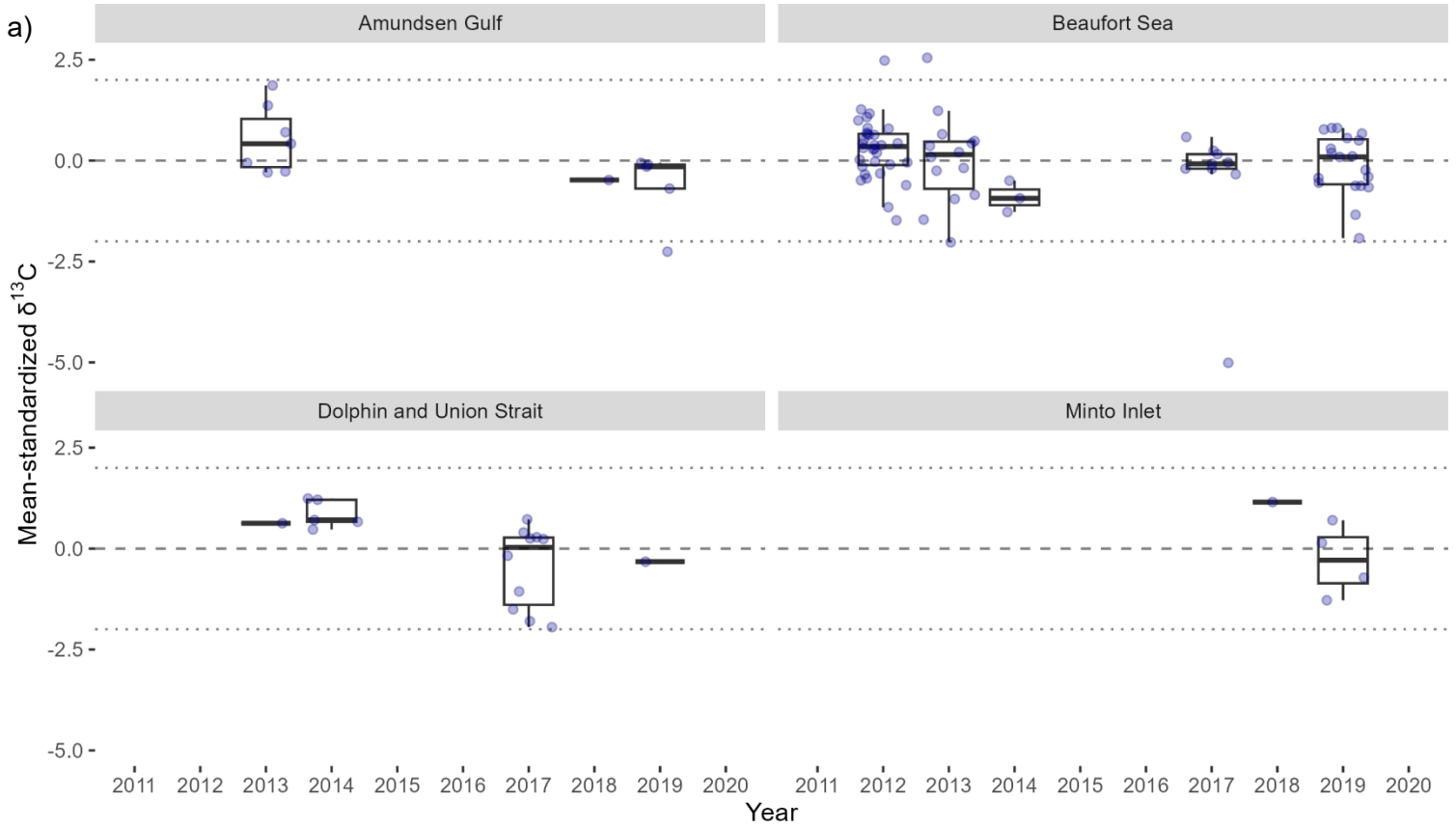

Figure 14 – Longeared eelpout (*Lycodes seminudus*) spatial and temporal variability in mean-standardized $\delta^{13}C$ (a) and $\delta^{15}N$ (b) isotope ratios from 2011 to 2020. Points represent individual samples, dashed lines indicate no difference from the mean isotope ratio across the entire study period for each area, and dotted lines indicate two standard deviations from the long-term mean

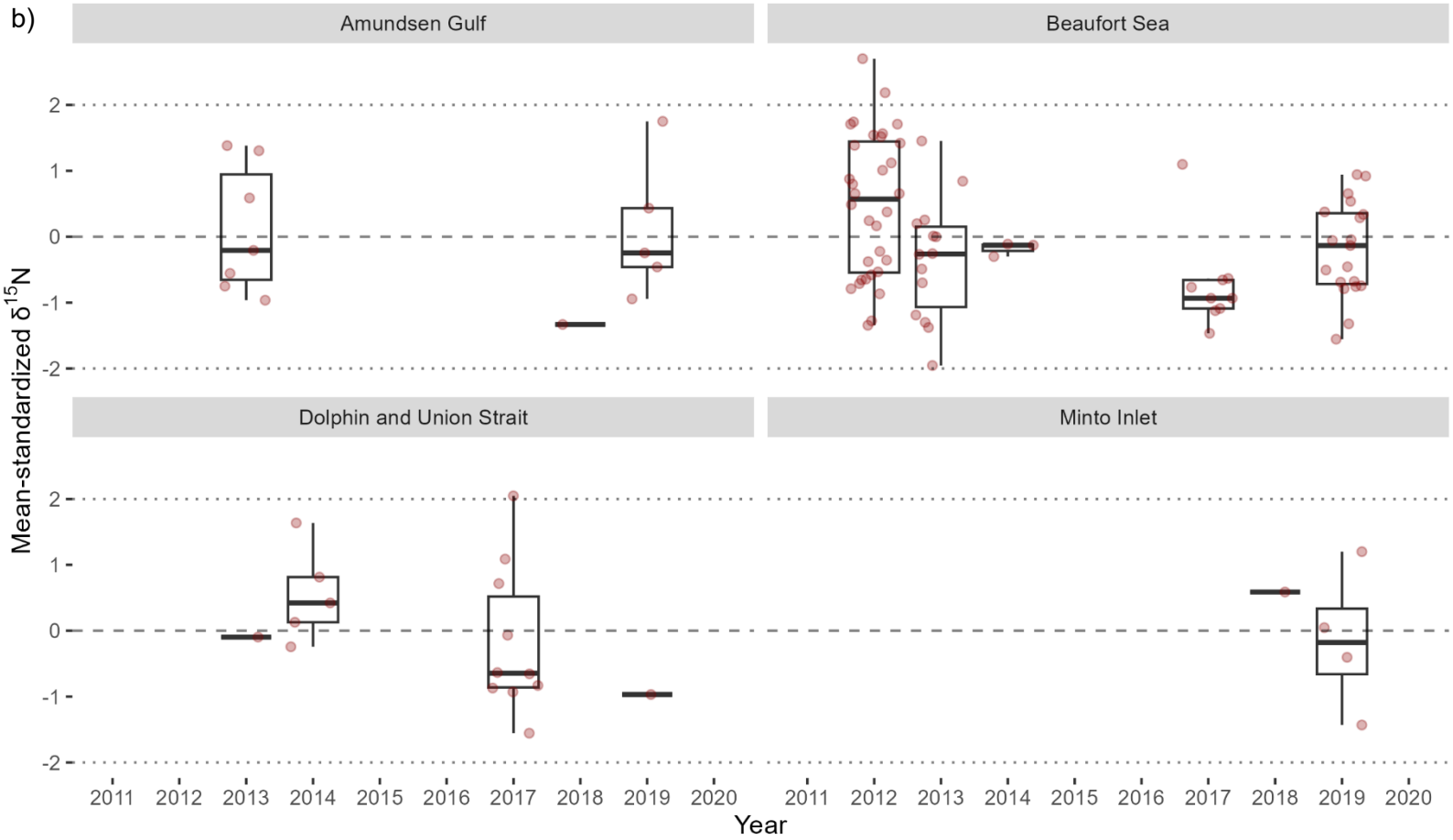

Figure 14 (cont'd) – Longeared eelpout (*Lycodes seminudus*) spatial and temporal variability in mean-standardized $\delta^{13}C$ (a) and $\delta^{15}N$ (b) isotope ratios from 2011 to 2020. Points represent individual samples, dashed lines indicate no difference from the mean isotope ratio across the entire study period for each area, and dotted lines indicate two standard deviations from the long-term mean

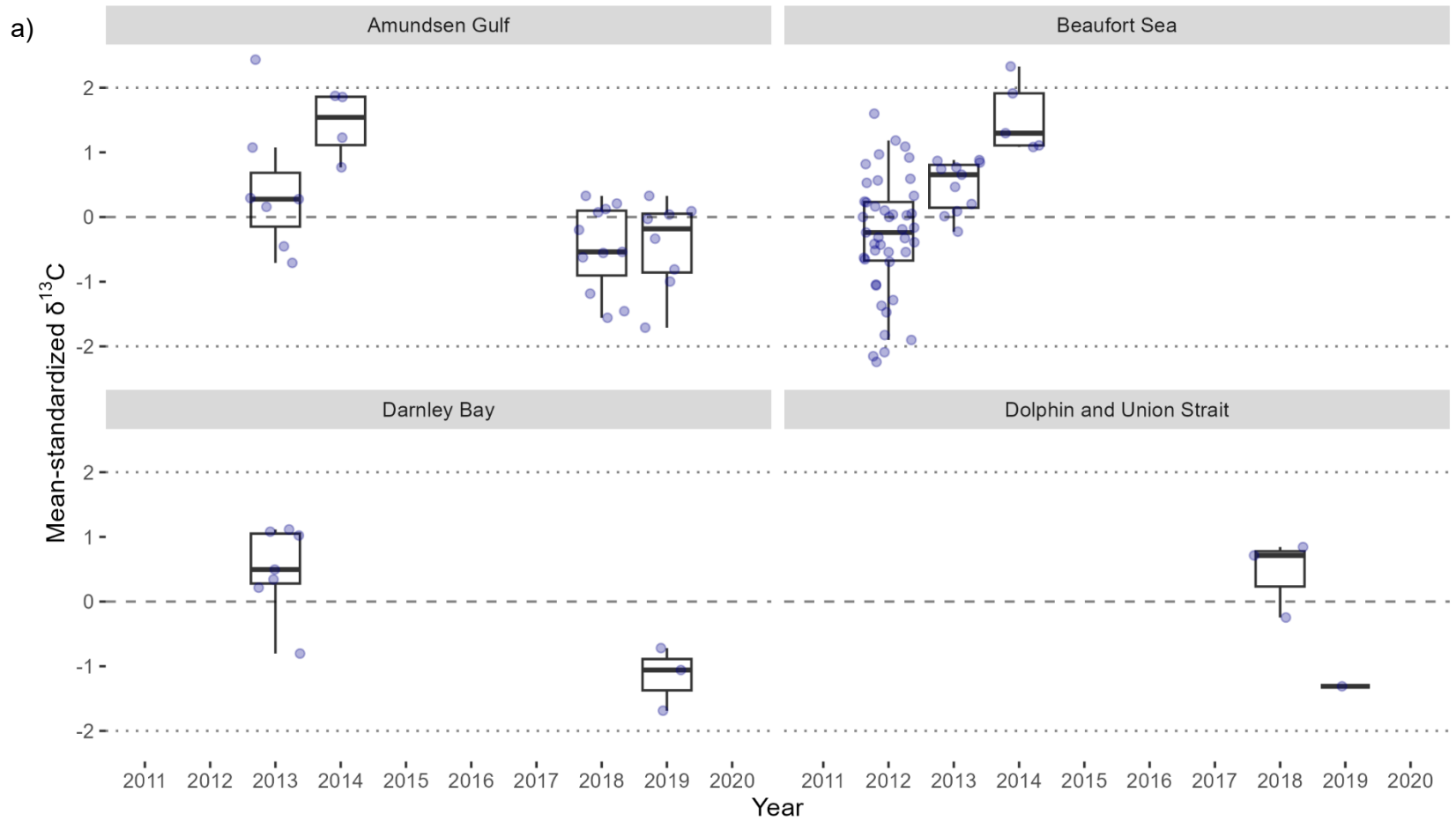

Figure 15 – Ribbed sculpin (*Triglops pingelii*) spatial and temporal variability in mean-standardized $\delta^{13}C$ (a) and $\delta^{15}N$ (b) isotope ratios from 2011 to 2020. Points represent individual samples, dashed lines indicate no difference from the mean isotope ratio across the entire study period for each area, and dotted lines indicate two standard deviations from the long-term mean

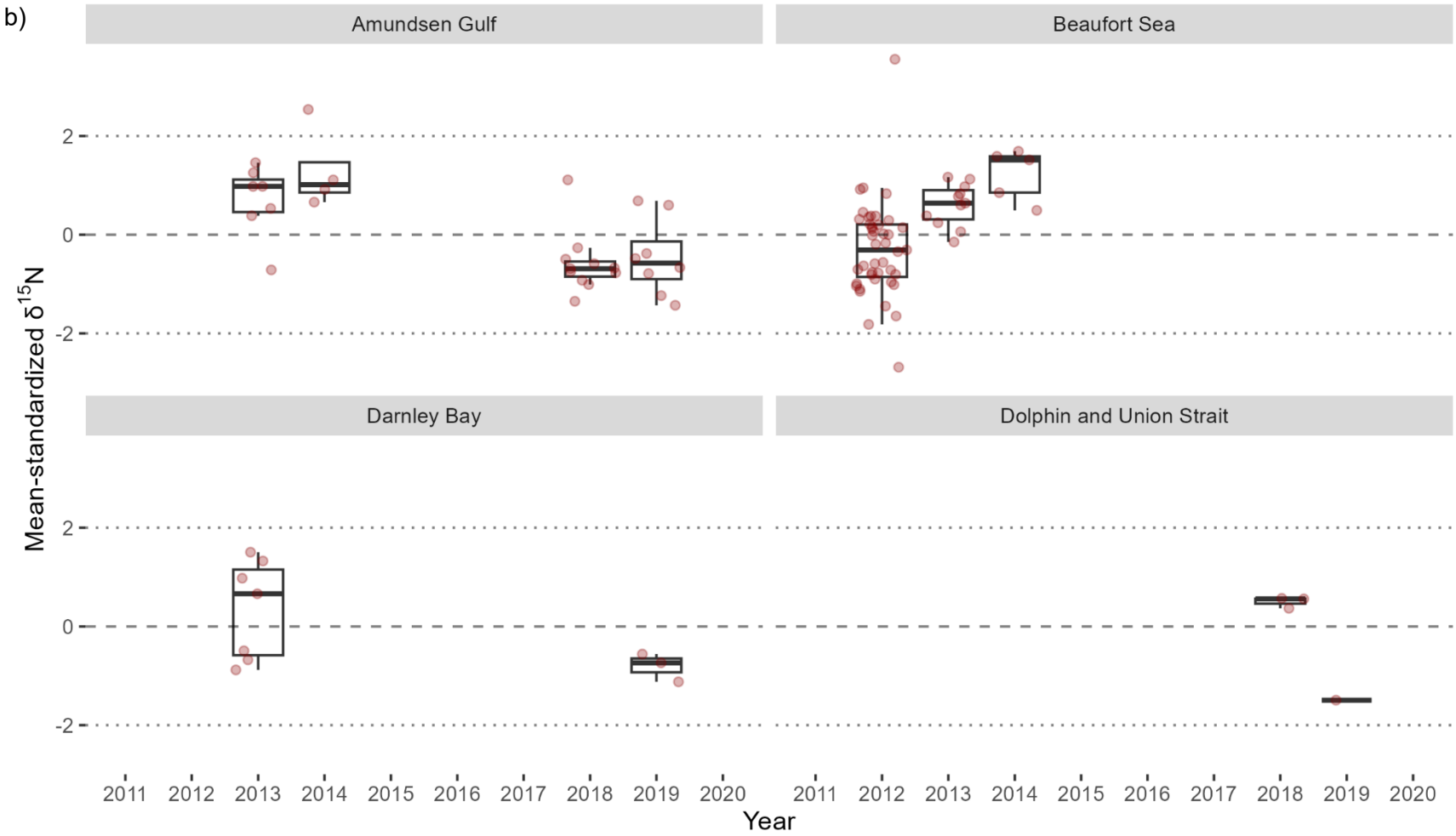

Figure 15 (cont'd) – Ribbed sculpin (*Triglops pingelii*) spatial and temporal variability in mean-standardized $\delta^{13}C$ (a) and $\delta^{15}N$ (b) isotope ratios from 2011 to 2020. Points represent individual samples, dashed lines indicate no difference from the mean isotope ratio across the entire study period for each area, and dotted lines indicate two standard deviations from the long-term mean

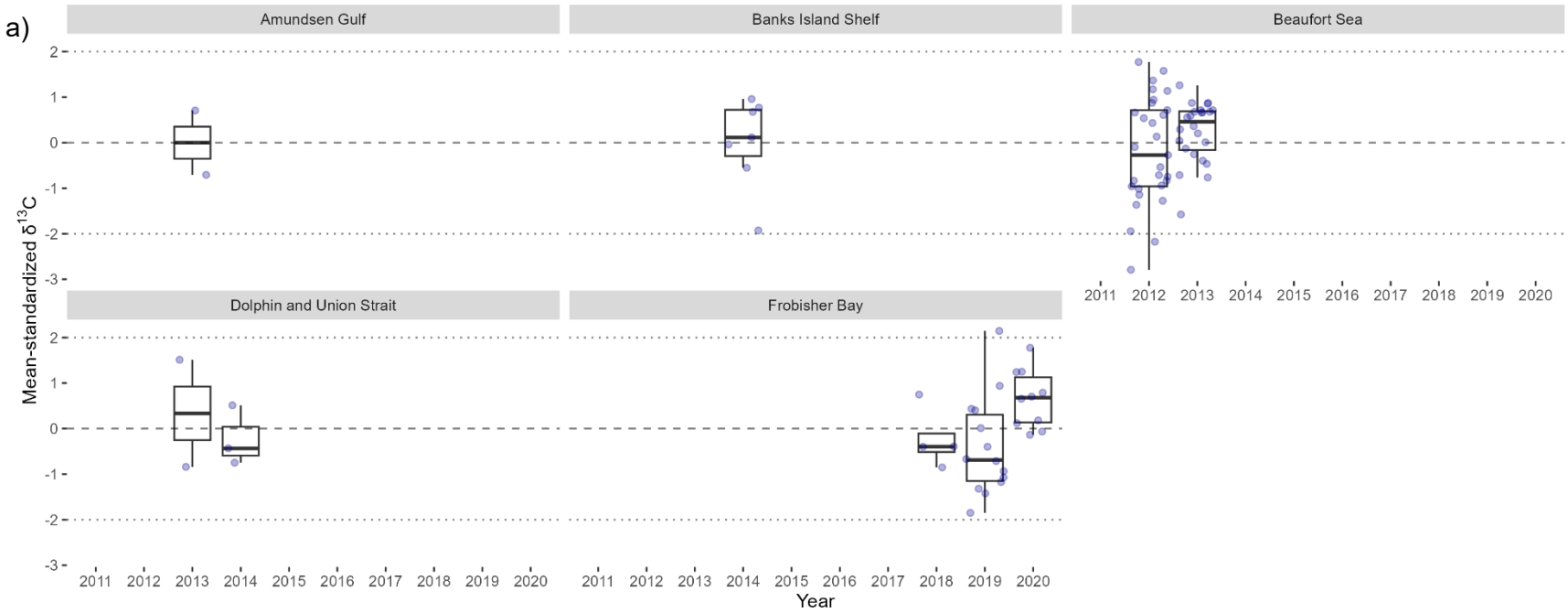

Figure 16 – Spatulate sculpin (*Icelus spatula*) spatial and temporal variability in mean-standardized $\delta^{13}C$ (a) and $\delta^{15}N$ (b) isotope ratios from 2011 to 2020. Points represent individual samples, dashed lines indicate no difference from the mean isotope ratio across the entire study period for each area, and dotted lines indicate two standard deviations from the long-term mean

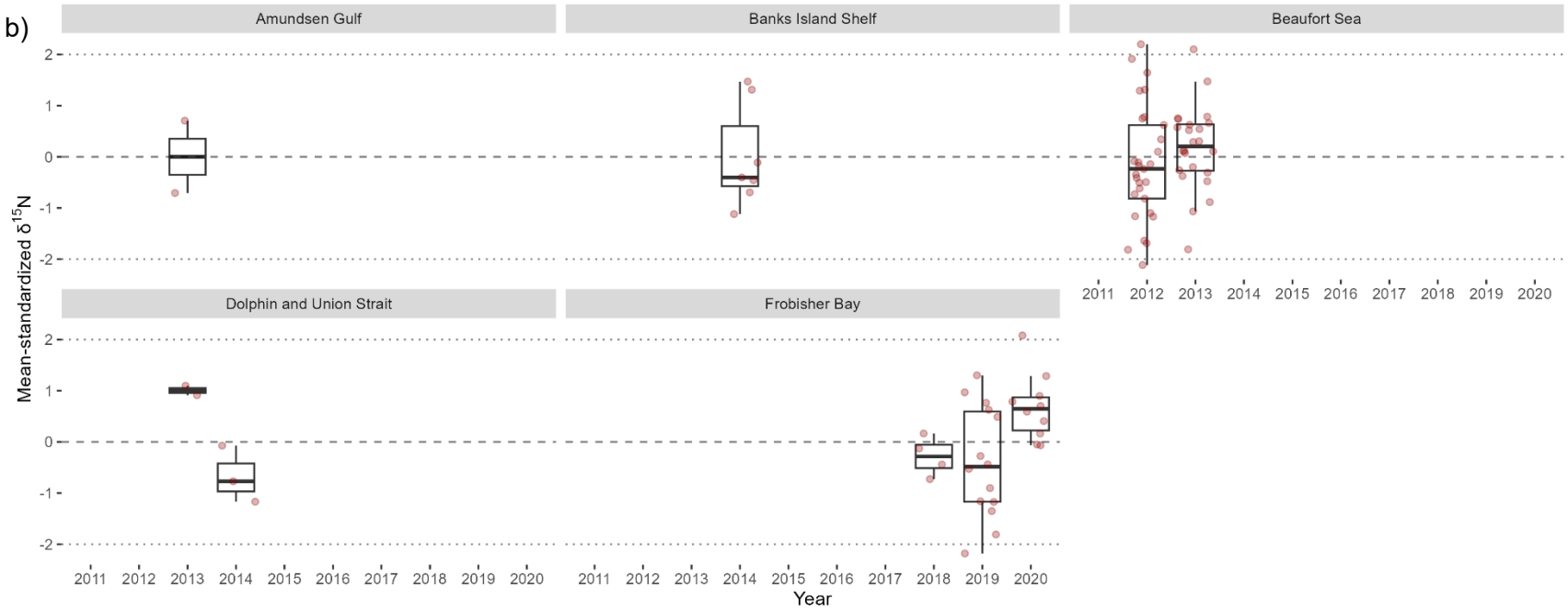

Figure 16 (cont'd) – Spatulate sculpin (*Icelus spatula*) spatial and temporal variability in mean-standardized $\delta^{13}C$ (a) and $\delta^{15}N$ (b) isotope ratios from 2011 to 2020. Points represent individual samples, dashed lines indicate no difference from the mean isotope ratio across the entire study period for each area, and dotted lines indicate two standard deviations from the long-term mean

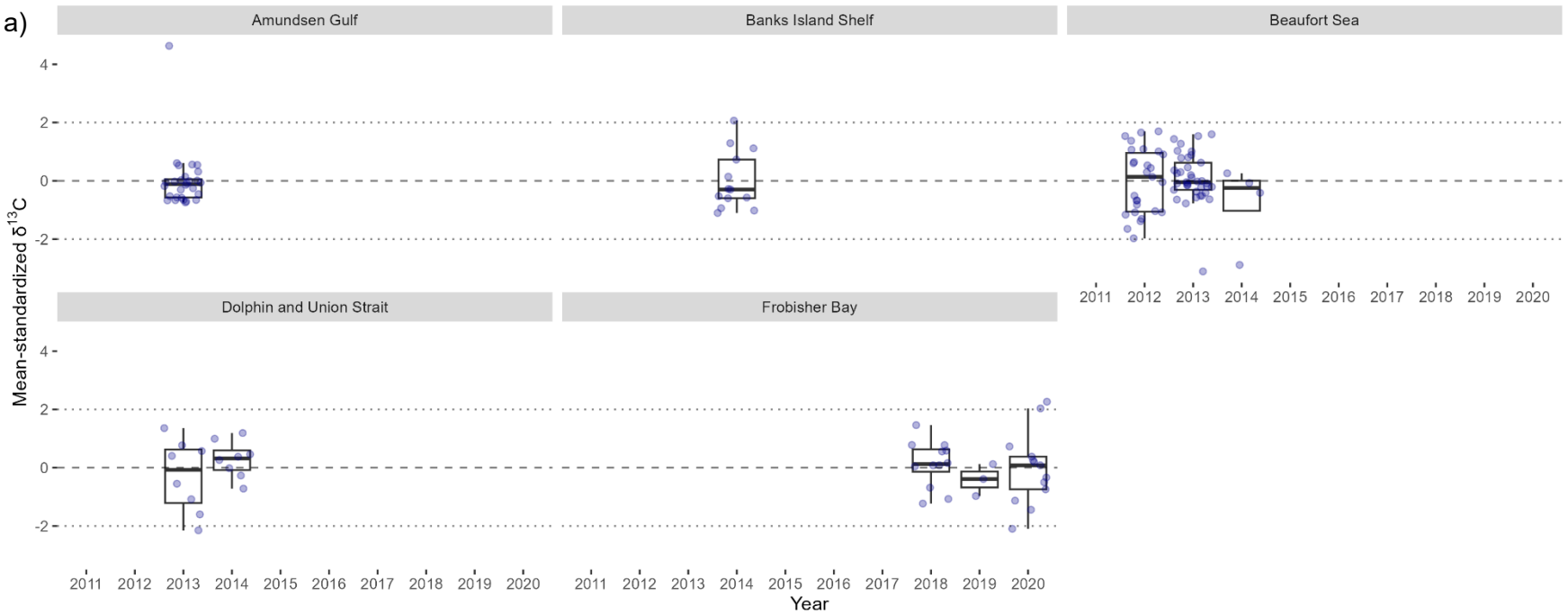

Figure 17 – Twohorn sculpin (*Icelus bicornis*) spatial and temporal variability in mean-standardized $\delta^{13}C$ (a) and $\delta^{15}N$ (b) isotope ratios from 2011 to 2020. Points represent individual samples, dashed lines indicate no difference from the mean isotope ratio across the entire study period for each area, and dotted lines indicate two standard deviations from the long-term mean

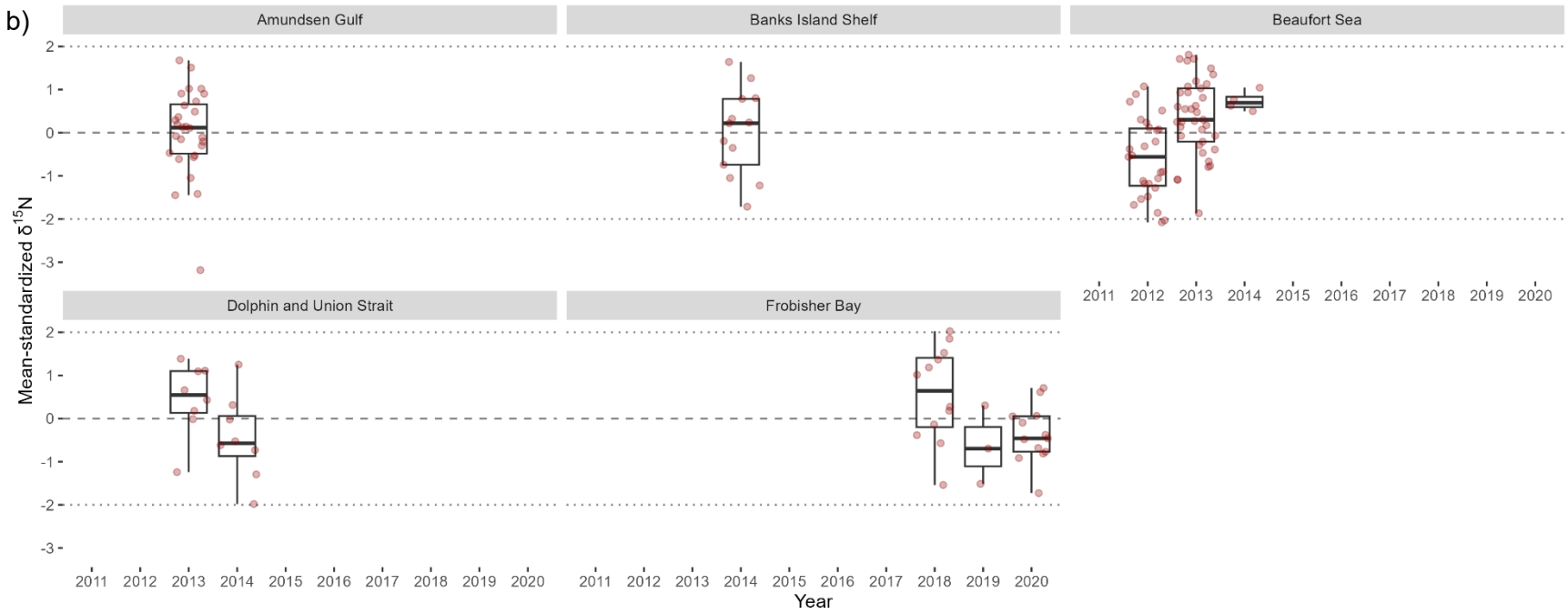

Figure 17 (cont'd) – Twohorn sculpin (*Icelus bicornis*) spatial and temporal variability in mean-standardized $\delta^{13}C$ (a) and $\delta^{15}N$ (b) isotope ratios from 2011 to 2020. Points represent individual samples, dashed lines indicate no difference from the mean isotope ratio across the entire study period for each area, and dotted lines indicate two standard deviations from the long-term mean

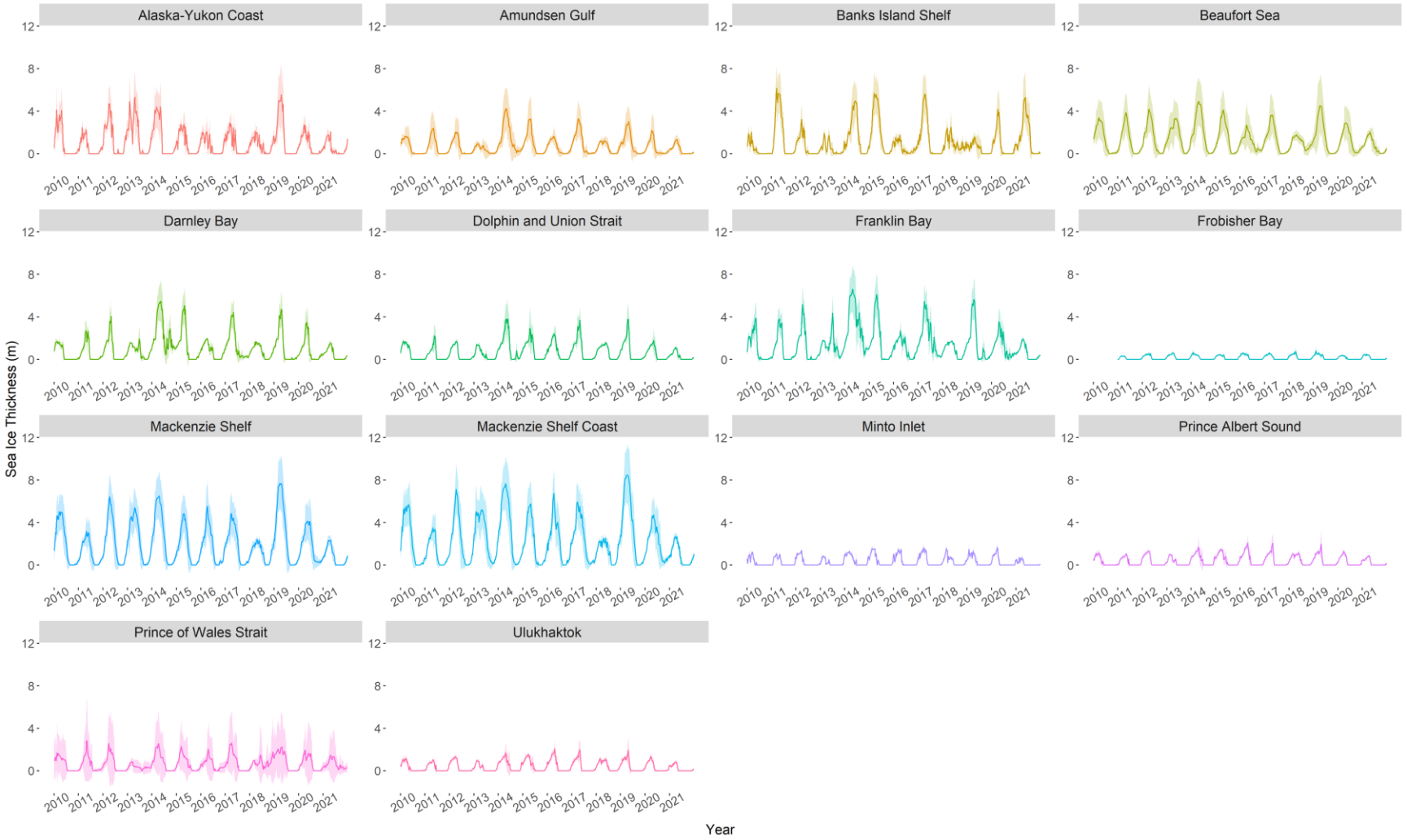

Figure 18 – Weekly mean sea ice thickness (m) by area in the western Canadian Arctic and Frobisher Bay from 2010-2021. Shaded areas around each line represent standard deviation of the mean weekly sea ice thickness (m) for each area.

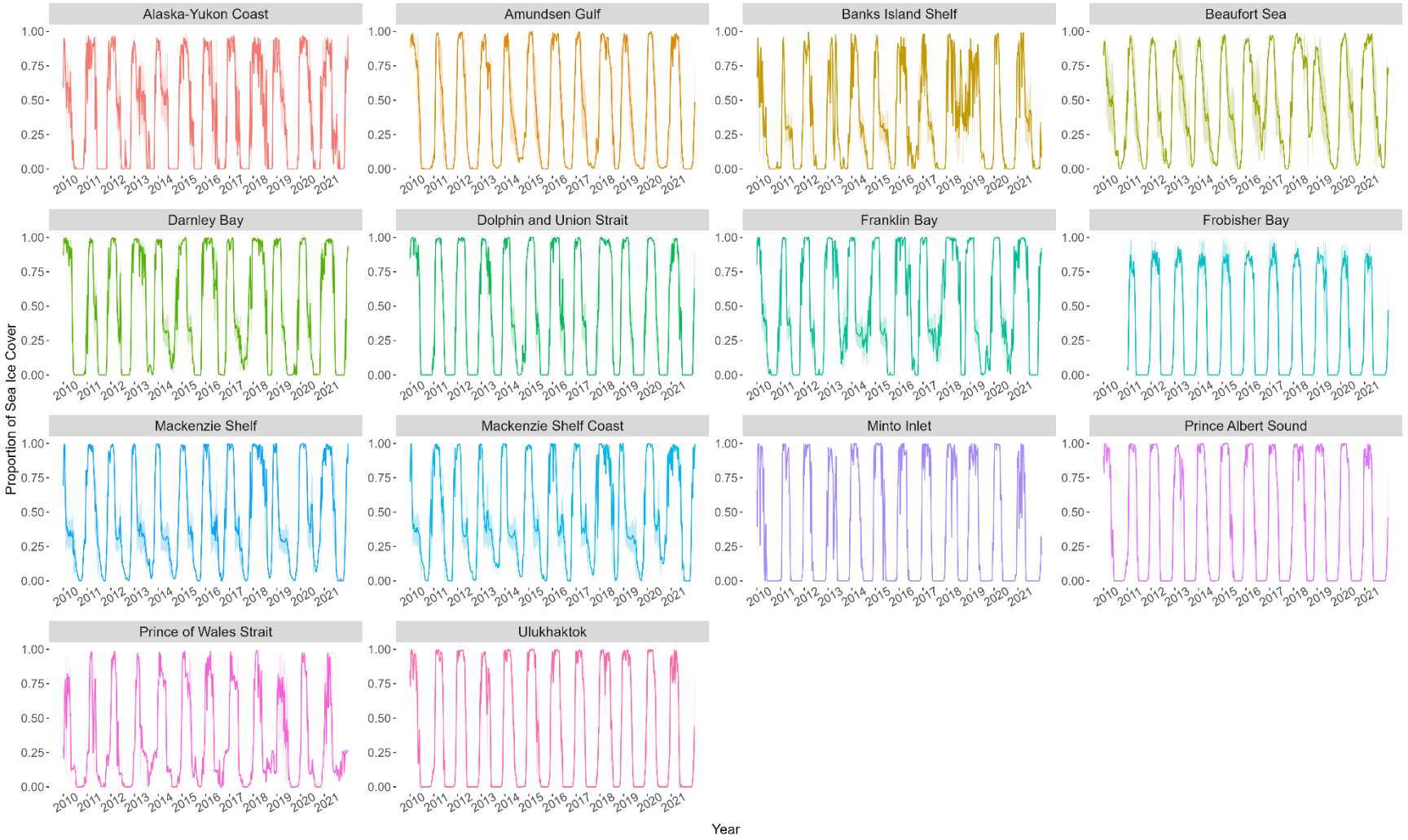

Figure 19 – Weekly mean sea ice concentration, expressed as proportion of sea ice cover by area in the western Canadian Arctic and Frobisher Bay from 2010-2021. Shaded areas around each line represent standard deviation of the mean weekly proportion of sea ice cover for each area.

Figure 20 - Weekly mean thickness of snow on sea ice (m) by area in the western Canadian Arctic and Frobisher Bay from 2010-2021. Shaded areas around each line represent standard deviation of the mean weekly snow thickness for each area.

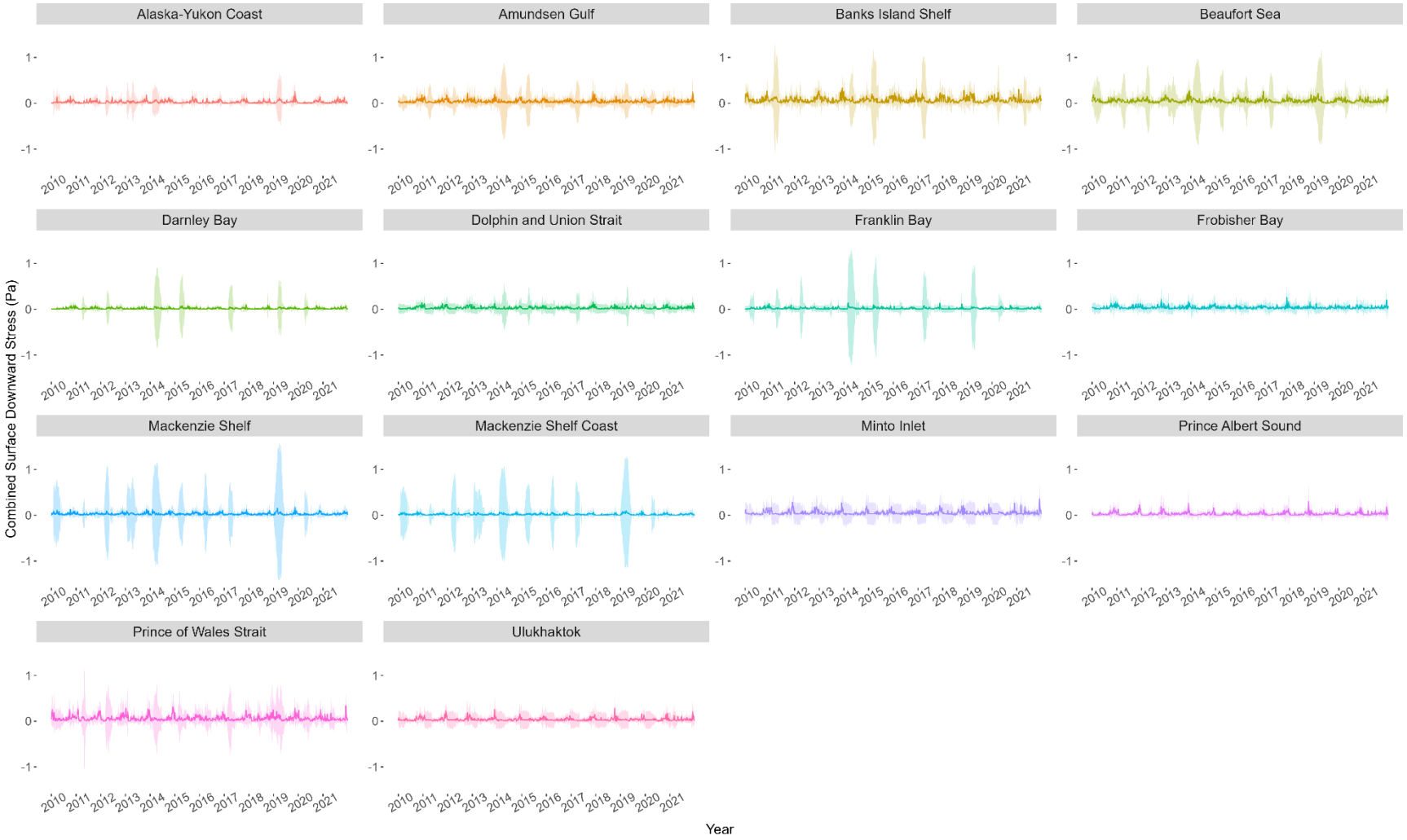

Figure 21 - Weekly mean combined surface downward stress (Pa) by area in the western Canadian Arctic and Frobisher Bay from 2010-2021. Surface downward stress represents wind stresses on the ocean's surface during the open water period, and stress due to ice movement during ice-covered periods. Shaded areas around each line represent standard deviation of the mean surface downward stress for each area.

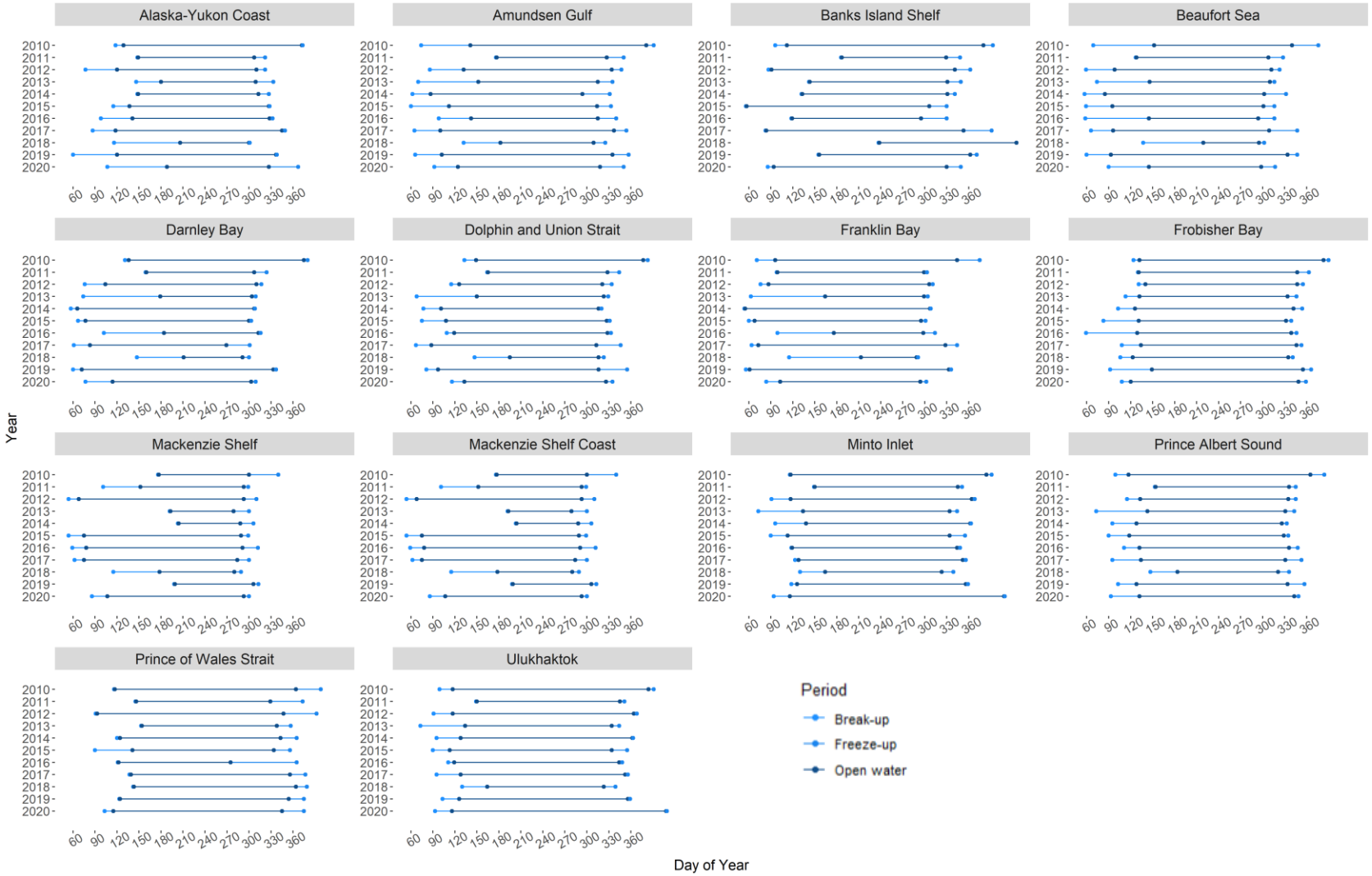

Figure 22 – Break-up period, open water period, and freeze-up periods for each study area from 2010-2020, calculated according to break-up and freeze-up date definitions described by Walsh et al. (2022). Points represent the day of the year in which each period started and ended, with coloured segments indicating the duration of each ice period. Points and segments extending beyond the 365th day of the year on the x axis indicated part of the period extended into the next calendar year.

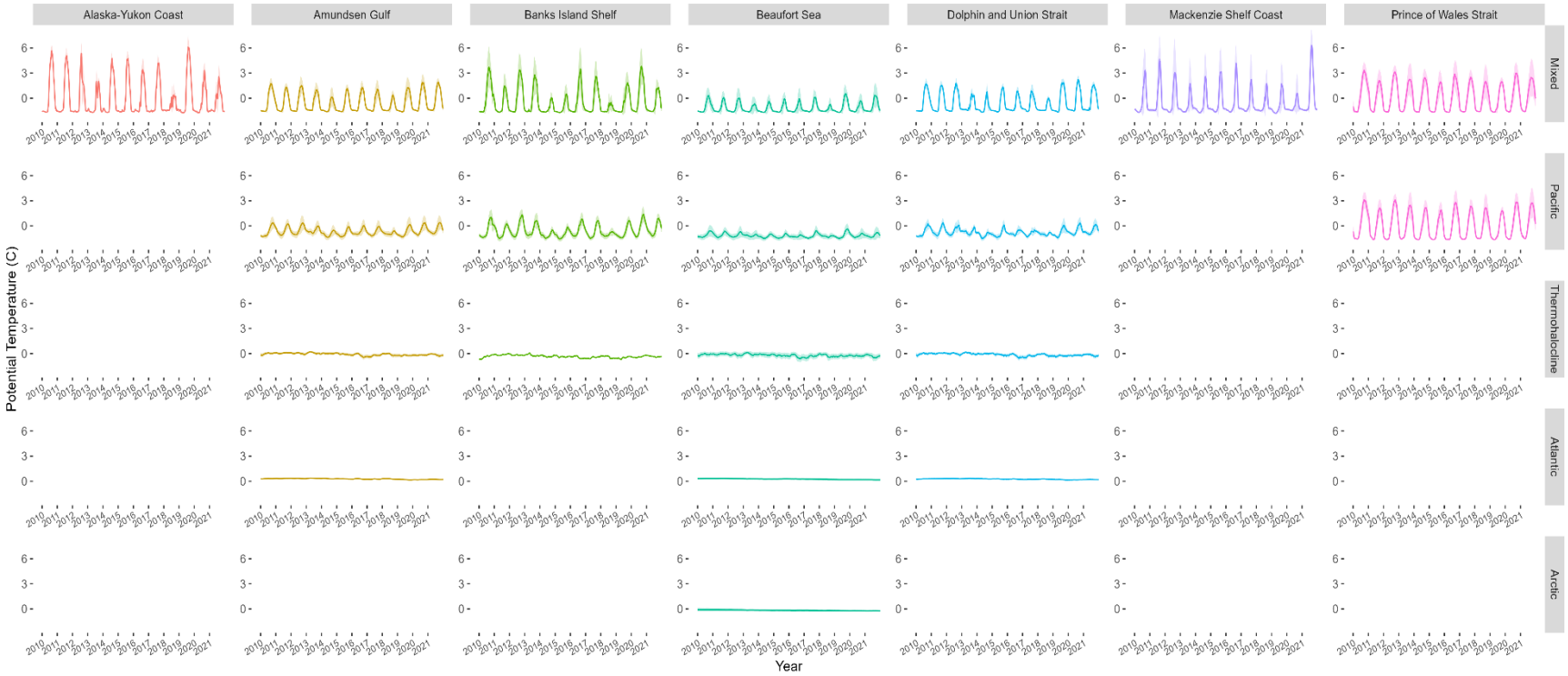

Figure 23 – Weekly mean potential temperature (°C) for water masses by area in the western Canadian Arctic and Frobisher Bay from 2010-2021. Shaded areas around each line represent standard deviation of the mean weekly potential temperature for each area. (N.B. – Panels were left blank where water depths within an area were shallower than the specified water mass depth range, except for Frobisher Bay which was only summarized for the surface mixed layer).

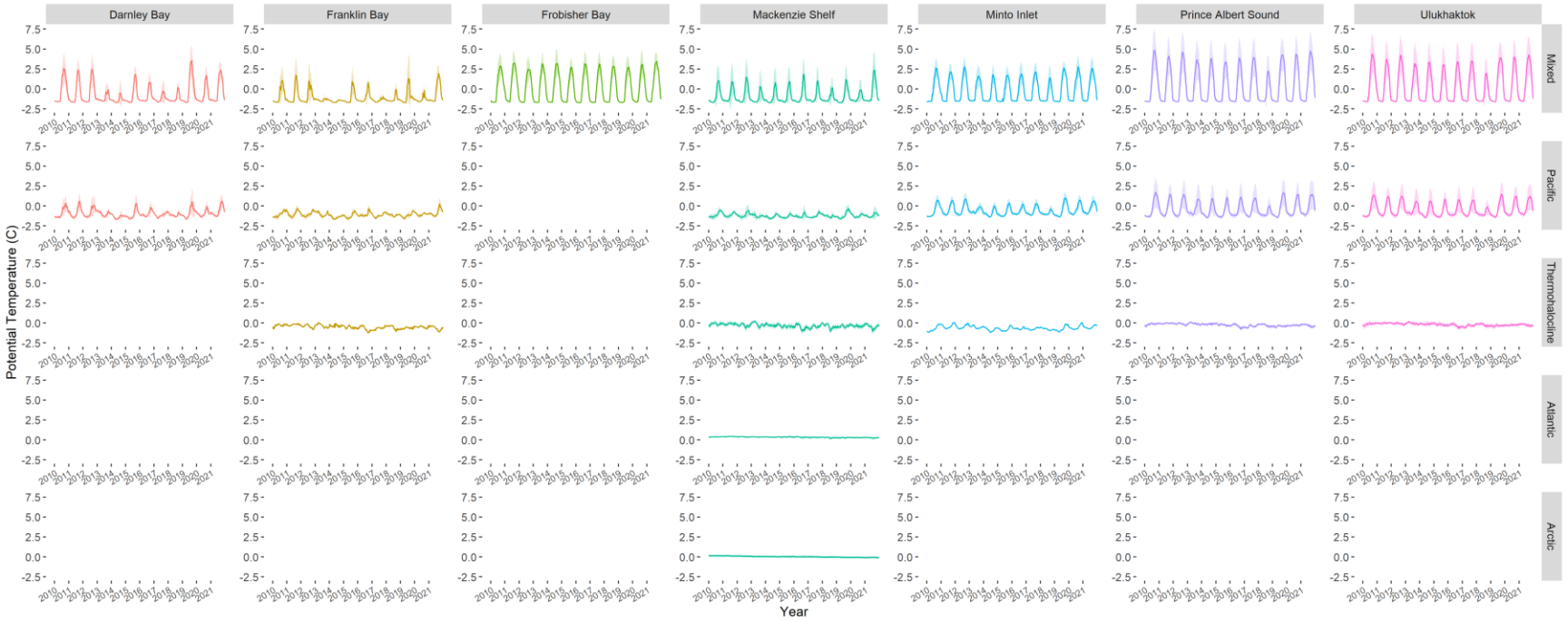

Figure 23 (cont'd) – Weekly mean potential temperature (°C) for water masses by area in the western Canadian Arctic and Frobisher Bay from 2010-2021. Shaded areas around each line represent standard deviation of the mean weekly potential temperature for each area (N.B. – Panels were left blank where water depths within an area were shallower than the specified water mass depth range, except for Frobisher Bay which was only summarized for the surface mixed layer).

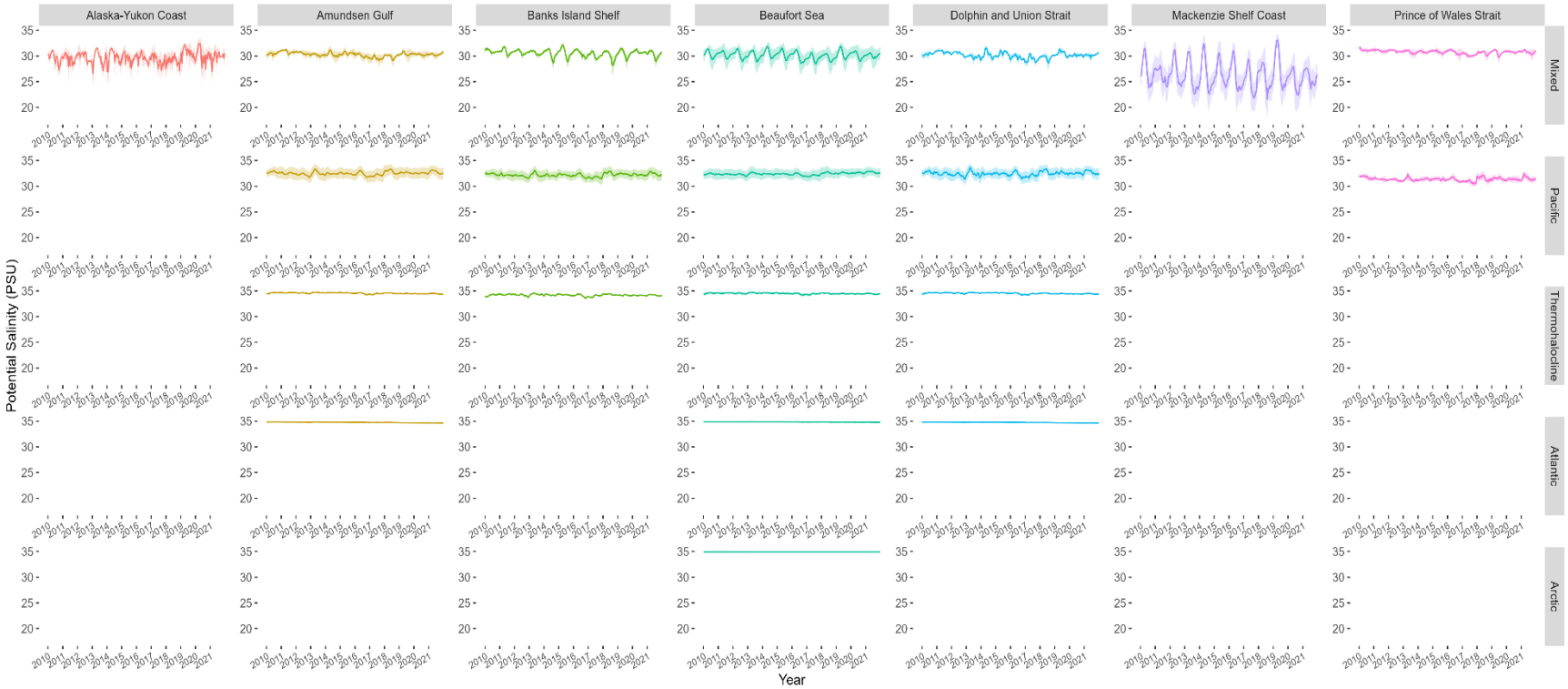

Figure 24 – Weekly mean potential salinity (PSU) for water masses by area in the western Canadian Arctic and Frobisher Bay from 2010-2021. Shaded areas around each line represent standard deviation of the mean weekly potential salinity for each area (N.B. – Panels were left blank where water depths within an area were shallower than the specified water mass depth range, except for Frobisher Bay which was only summarized for the surface mixed layer).

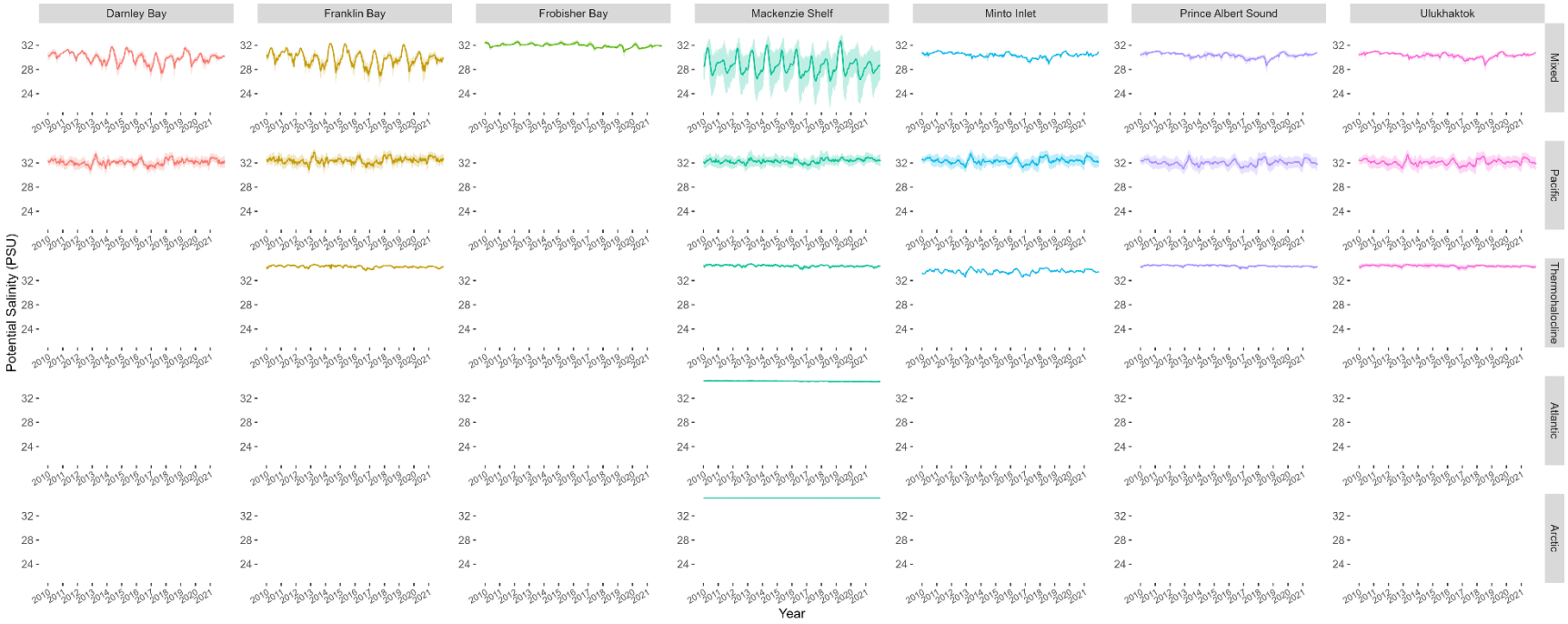

Figure 24 (cont'd) – Weekly mean potential salinity (PSU) for water masses by area in the western Canadian Arctic and Frobisher Bay from 2010-2021. Shaded areas around each line represent standard deviation of the mean weekly potential salinity for each area (N.B. – Panels were left blank where water depths within an area were shallower than the specified water mass depth range, except for Frobisher Bay which was only summarized for the surface mixed layer).

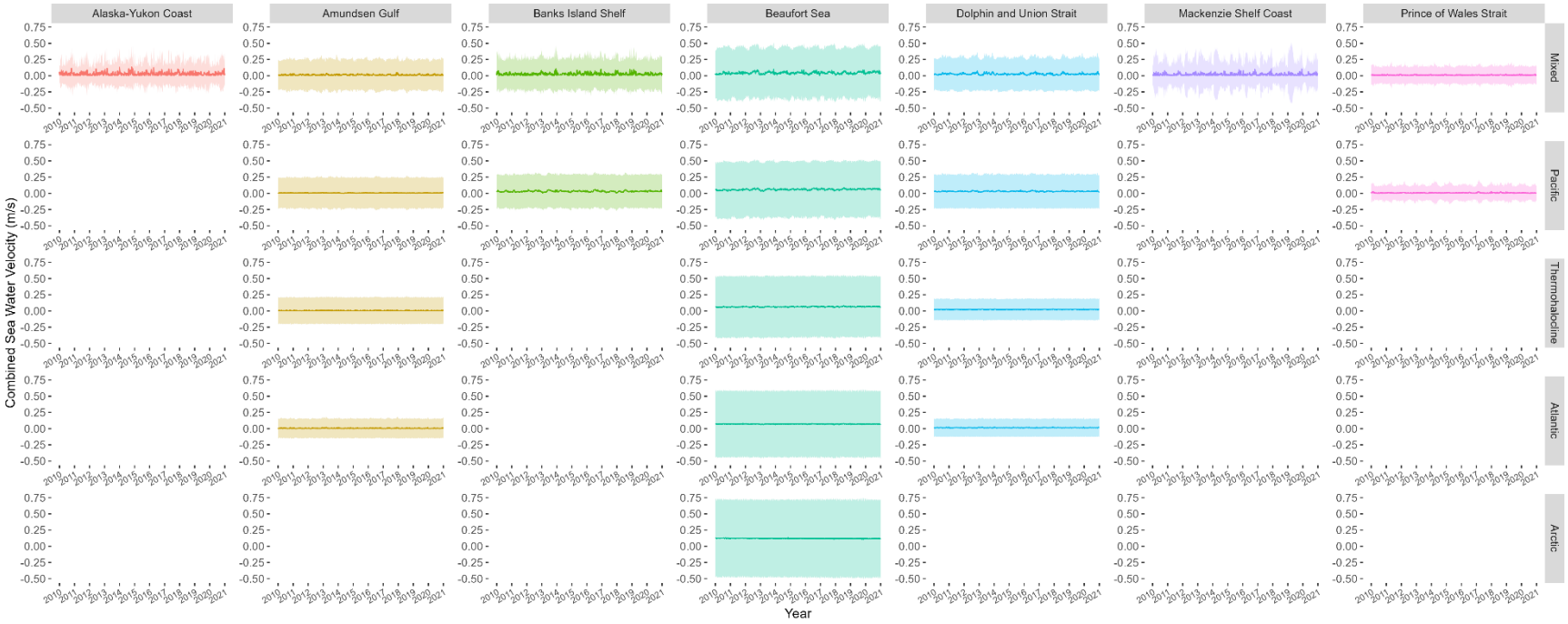

Figure 25 – Weekly mean sea water velocity (m/s) for water masses by area in the western Canadian Arctic and Frobisher Bay from 2010-2021. Shaded areas around each line represent standard deviation of the mean weekly sea water velocity (m/s) for each area (N.B. – Panels were left blank where water depths within an area were shallower than the specified water mass depth range, except for Frobisher Bay which was only summarized for the surface mixed layer).

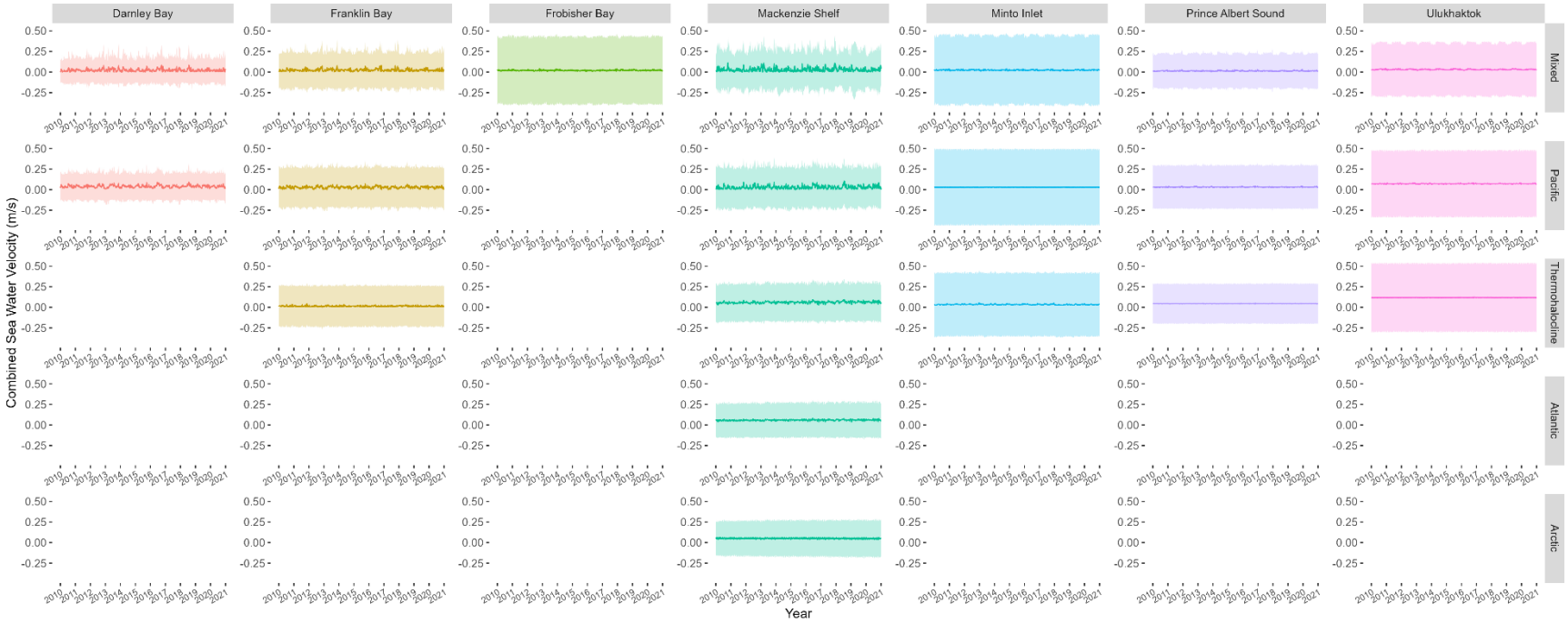

Figure 25 (cont'd) – Weekly mean sea water velocity (m/s) for water masses by area in the western Canadian Arctic and Frobisher Bay from 2010-2021. Shaded areas around each line represent standard deviation of the mean weekly sea water velocity (m/s) for each area (N.B. – Panels were left blank where water depths within an area were shallower than the specified water mass depth range, except for Frobisher Bay which was only summarized for the surface mixed layer).

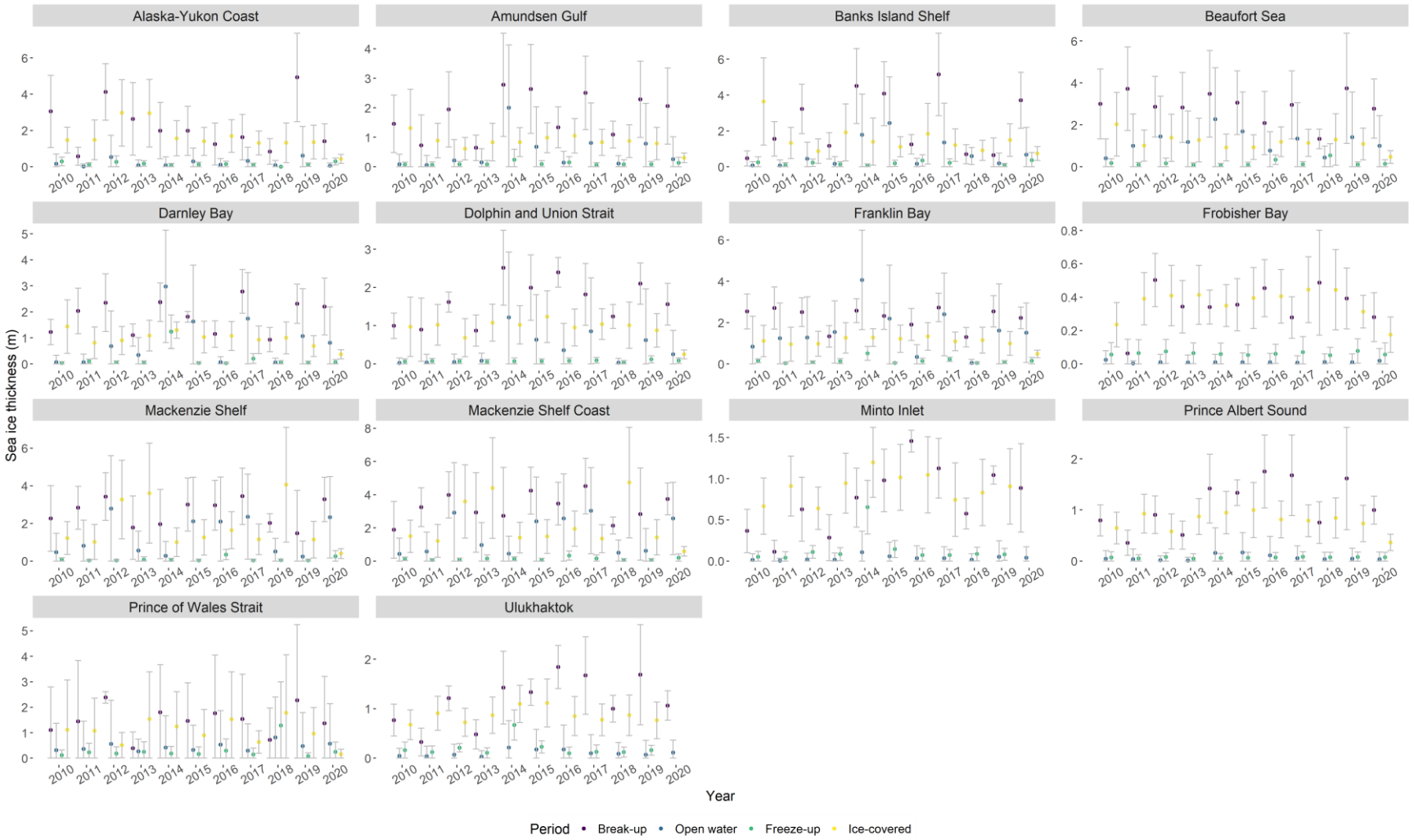

Figure 26 – Mean sea ice thickness (m) in ice break-up, open water, freeze-up, and ice-covered periods by area in the western Canadian Arctic and Frobisher Bay from 2010-2020 for each water mass. Error bars represent standard deviation of the mean sea ice thickness (m) for each area. (N.B. – Y-axis scales differ among panels).

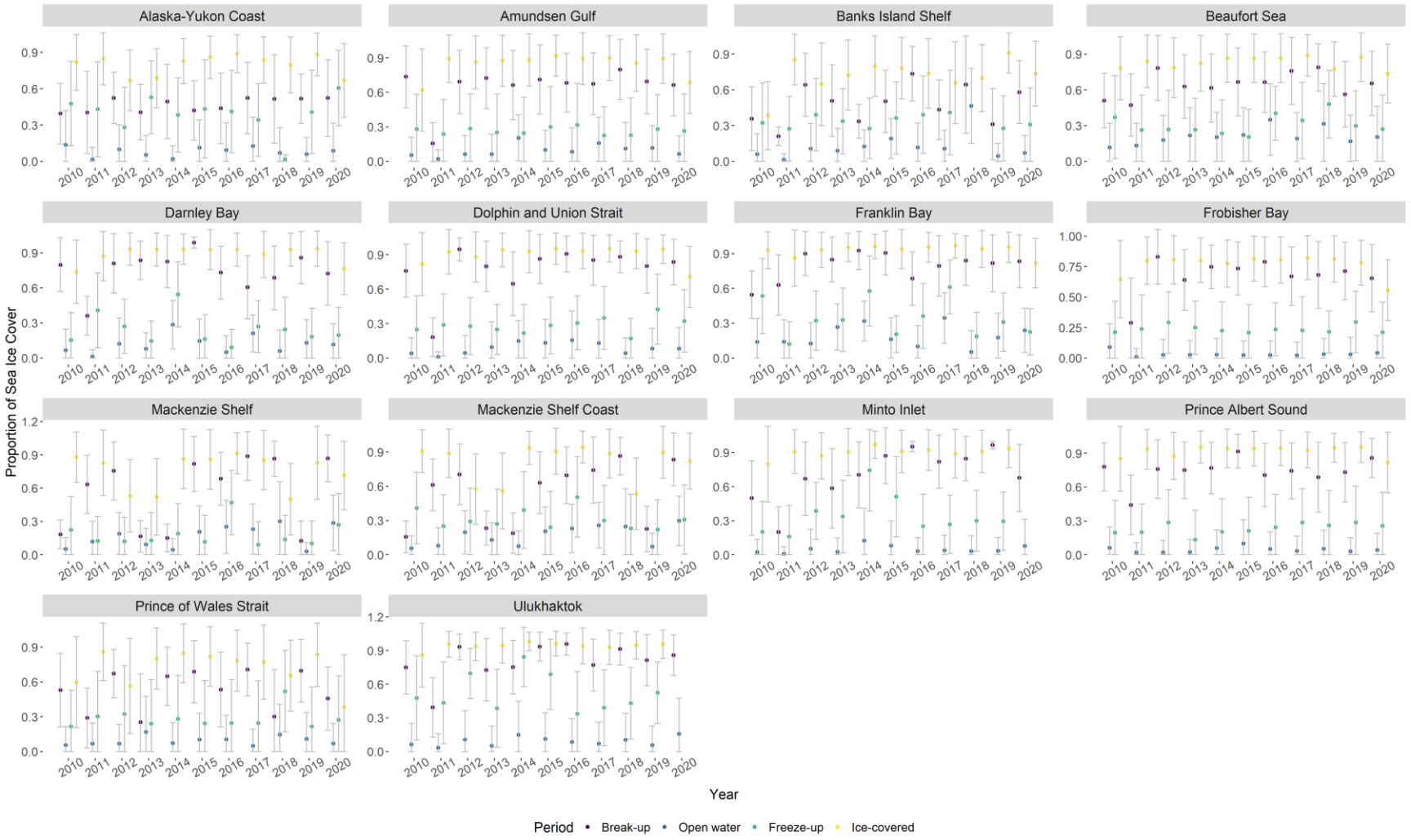

Figure 27 – Mean proportion of sea ice cover in ice break-up, open water, freeze-up, and ice-covered periods by area in the western Canadian Arctic and Frobisher Bay from 2010-2020 for each water mass. Error bars represent standard deviation of the mean proportion of sea ice cover for each area. (N.B. – Y-axis scales differ among panels).

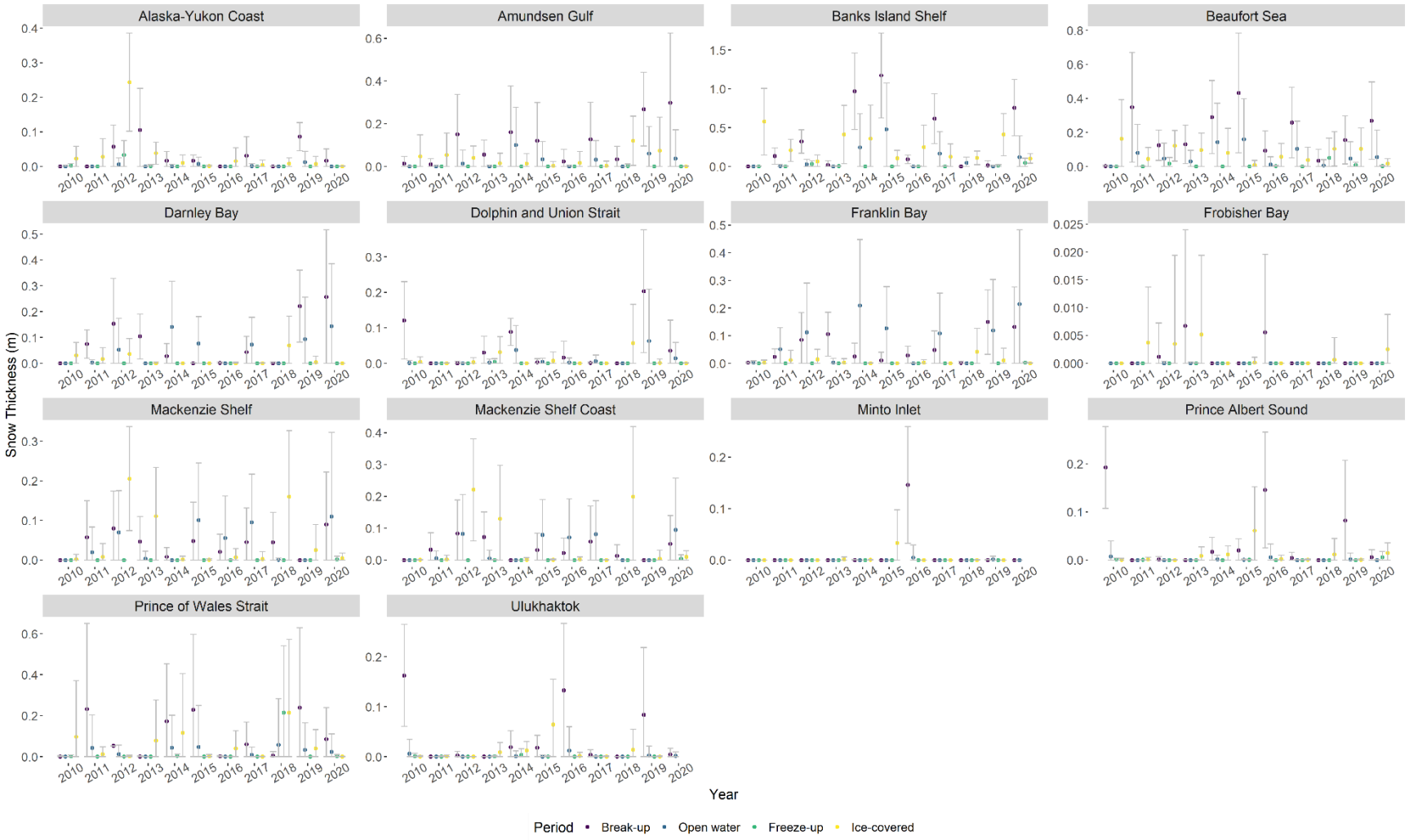

Figure 28 – Mean thickness of snow on ice (m) in ice break-up, open water, freeze-up, and ice-covered periods by area in the western Canadian Arctic and Frobisher Bay from 2010-2020 for each water mass. Error bars represent standard deviation of the mean thickness of snow on ice (m) for each area. (N.B. – Y-axis scales differ among panels).

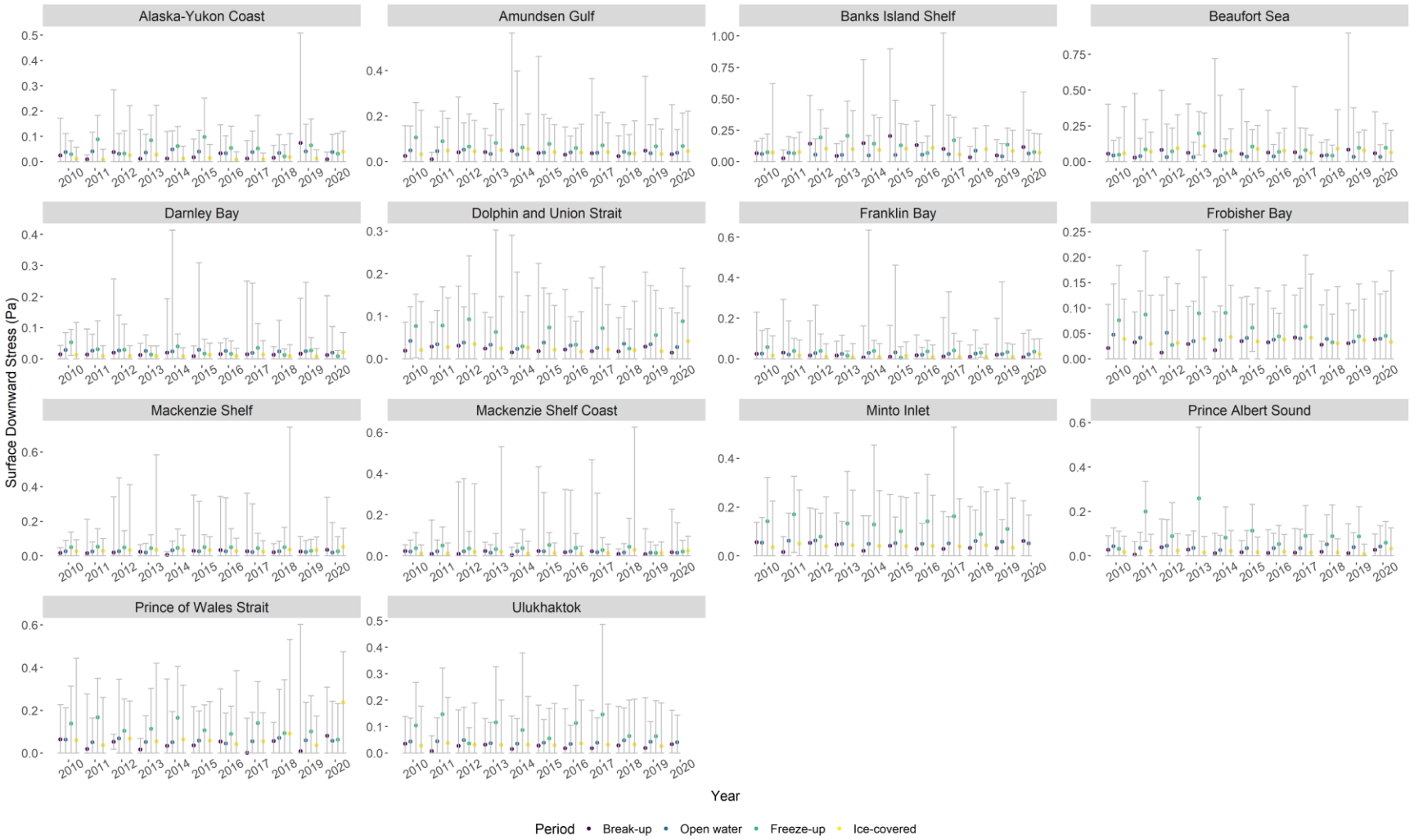

Figure 29 – Mean stress on the ocean surface (Pa) in ice break-up, open water, freeze-up, and ice-covered periods by area in the western Canadian Arctic and Frobisher Bay from 2010-2020 for each water mass. Error bars represent standard deviation of the mean stress on the ocean surface (Pa) for each area. (N.B. – Y-axis scales differ among panels).

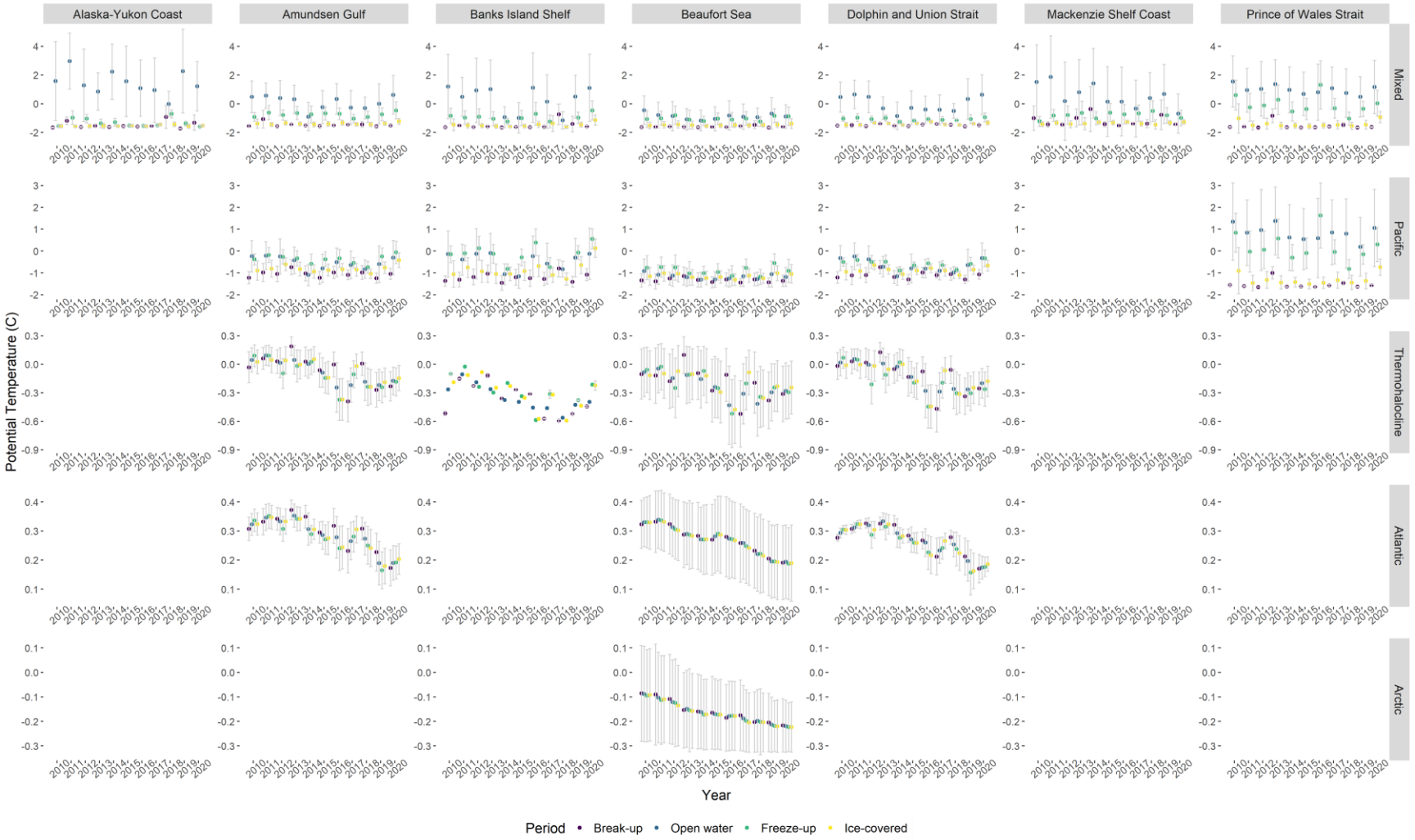

Figure 30 – Mean potential temperature (ºC) in ice break-up, open water, freeze-up, and ice-covered periods by area in the western Canadian Arctic and Frobisher Bay from 2010-2020 for each water mass. Error bars represent standard deviation of the mean potential temperature (ºC) for each area. (N.B. – Panels were left blank where water depths within an area were shallower than the specified water mass depth range, except for Frobisher Bay which was only summarized for the surface mixed layer. Y-axis scales differ among rows).

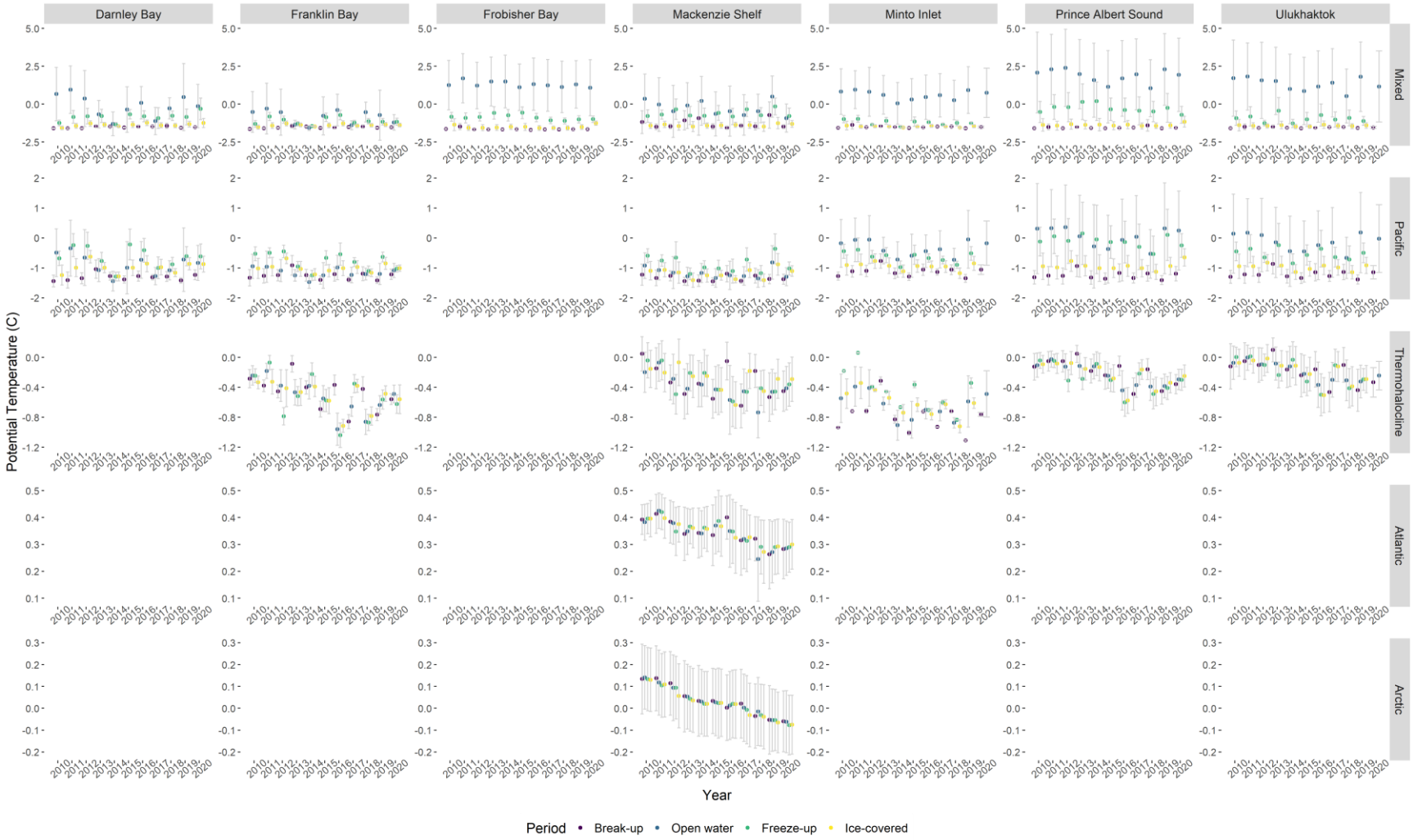

Figure 30 (cont'd) – Mean potential temperature (°C) in ice break-up, open water, freeze-up, and ice-covered periods by area in the western Canadian Arctic and Frobisher Bay from 2010-2020 for each water mass. Error bars represent standard deviation of the mean potential temperature (°C) for each area. (N.B. – Panels were left blank where water depths within an area were shallower than the specified water mass depth range, except for Frobisher Bay which was only summarized for the surface mixed layer. Y-axis scales differ among rows).

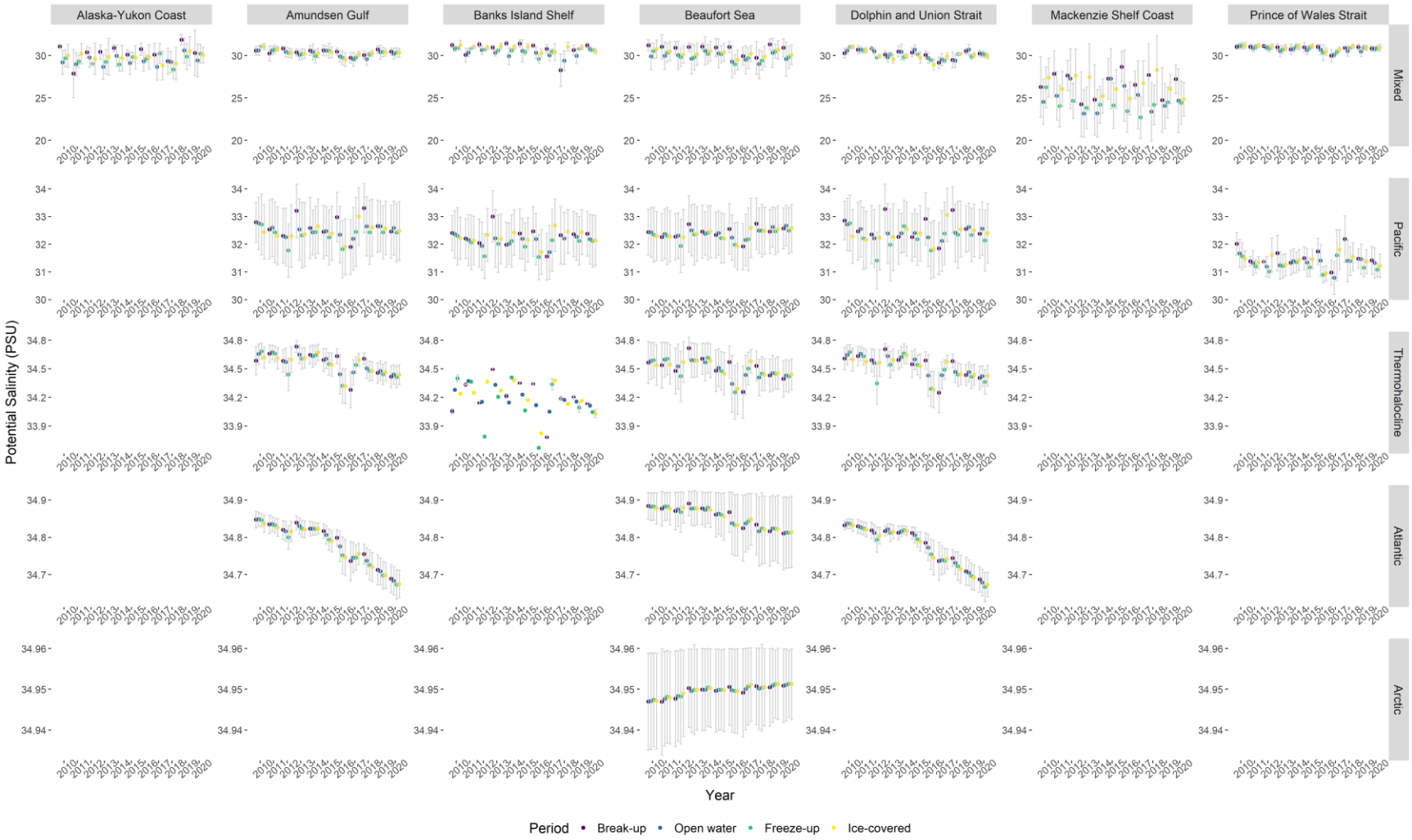

Figure 31 – Mean potential salinity (PSU) in ice break-up, open water, freeze-up, and ice-covered periods by area in the western Canadian Arctic and Frobisher Bay from 2010-2021 for each water mass. Error bars represent standard deviation of the mean potential salinity (PSU) for each area. (N.B. – Panels were left blank where water depths within an area were shallower than the specified water mass depth range, except for Frobisher Bay which was only summarized for the surface mixed layer. Y-axis scales differ among rows).

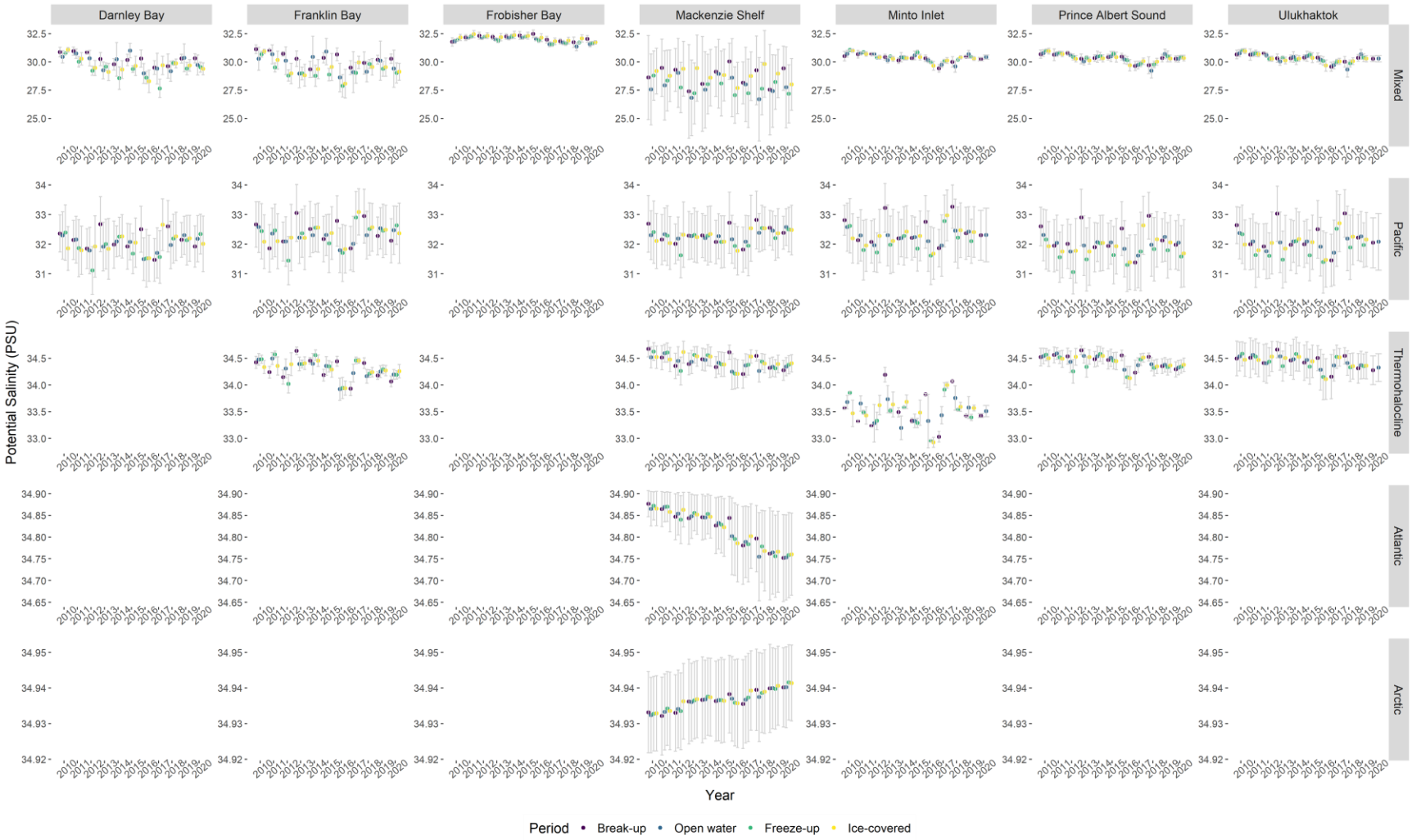

Figure 31 (cont'd) – Mean potential salinity (PSU) in ice break-up, open water, freeze-up, and ice-covered periods by area in the western Canadian Arctic and Frobisher Bay from 2010-2021 for each water mass. Error bars represent standard deviation of the mean potential salinity (PSU) for each area. (N.B. – Panels were left blank where water depths within an area were shallower than the specified water mass depth range, except for Frobisher Bay which was only summarized for the surface mixed layer. Y-axis scales differ among rows).

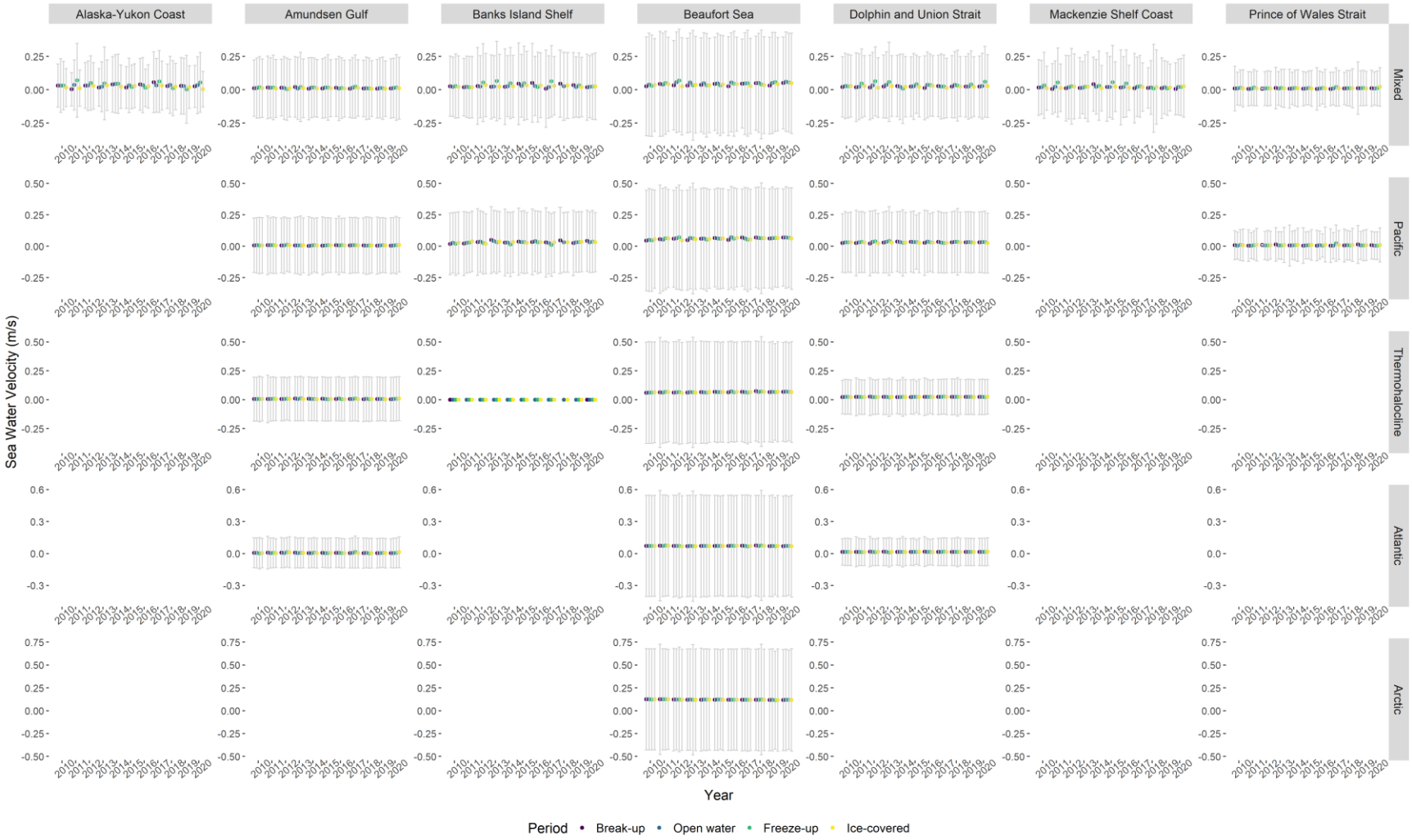

Figure 32 – Mean sea water velocity (m/s) in ice break-up, open water, freeze-up, and ice-covered periods by area in the western Canadian Arctic and Frobisher Bay from 2010-2021 for each water mass. Error bars represent standard deviation of the mean sea water velocity (m/s) for each area. (N.B. – Panels were left blank where water depths within an area were shallower than the specified water mass depth range, except for Frobisher Bay which was only summarized for the surface mixed layer. Y-axis scales differ among rows).

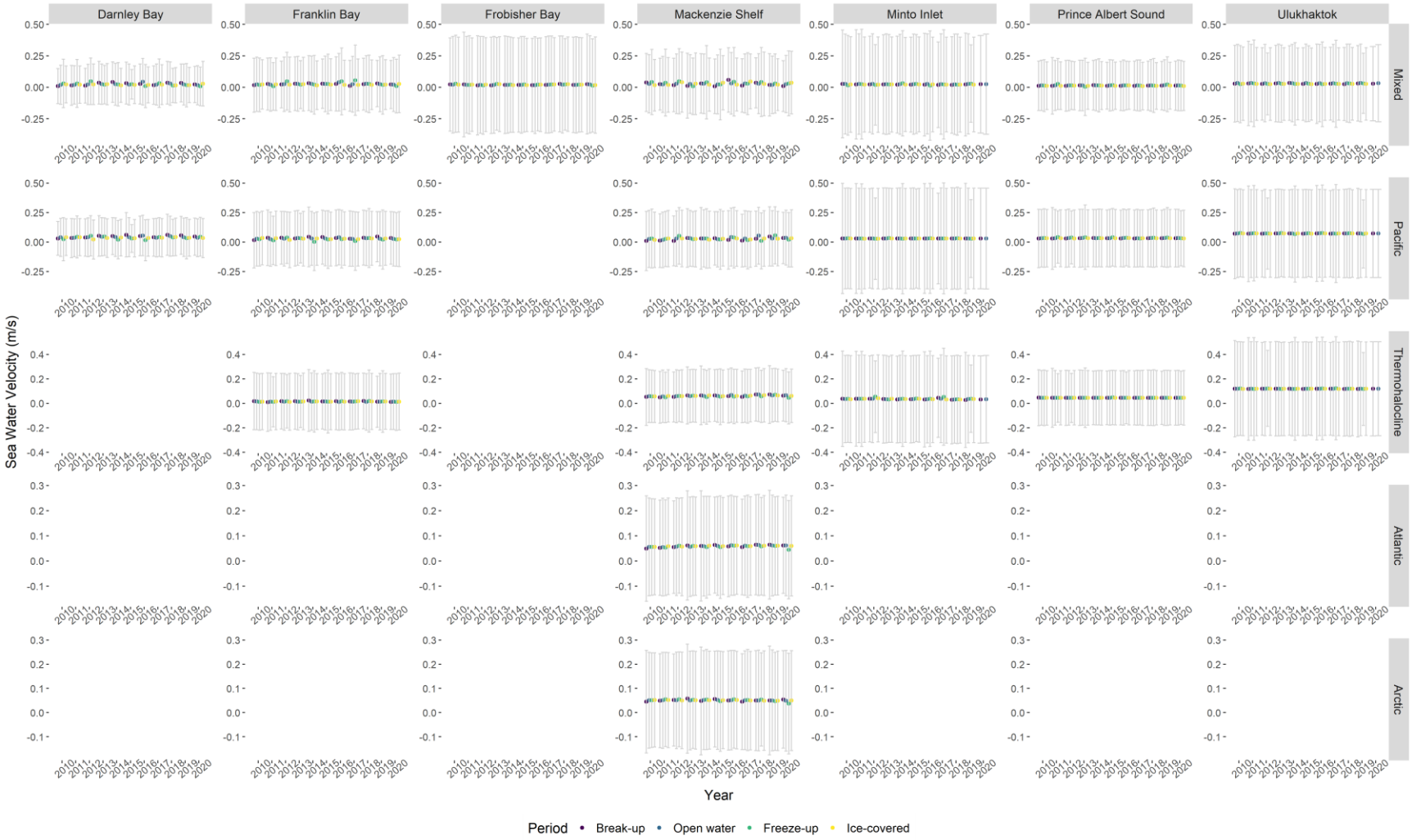

Figure 32 (cont'd) – Mean sea water velocity (m/s) in ice break-up, open water, freeze-up, and ice-covered periods by area in the western Canadian Arctic and Frobisher Bay from 2010-2021 for each water mass. Error bars represent standard deviation of the mean sea water velocity (m/s) for each area. (N.B. – Panels were left blank where water depths within an area were shallower than the specified water mass depth range, except for Frobisher Bay which was only summarized for the surface mixed layer. Y-axis scales differ among rows).

4.0 References

Benoit, D., Simard, Y., and Fortier, L. 2008. Hydroacoustic detection of large winter aggregations of Arctic cod (Boreogadus saida) at depth in ice-covered Franklin Bay (Beaufort Sea). Journal of Geophysical Research: Oceans **113**(C6). doi:https://doi.org/10.1029/2007JC004276.

Bouchard, C., Geoffroy, M., LeBlanc, M., Majewski, A., Gauthier, S., Walkusz, W., Reist, J.D., and Fortier, L. 2017. Climate warming enhances polar cod recruitment, at least transiently. Progress in Oceanography **156**: 121-129. doi:10.1016/j.pocean.2017.06.008.

Choy, E.S., Roth, J.D., and Loseto, L.L. 2016. Lipid removal and acidification affect nitrogen and carbon stable isotope ratios of beluga whales (Delphinapterus leucas) and their potential prey species in the Beaufort Sea ecosystem. Marine Biology **163**(10): 220. doi:10.1007/s00227-016-2992-x.

Christie, L.R., McNicholl, D.G., Illasiak, S., Green, I., Wolki, F., Wolki, B.J., and Dunmall, K.M. 2025. Community-led coastal ecosystem assessments in the Anguniaqvia Niqiqyuam Marine Protected Area (ANMPA) field projects in 2022, 2023, and 2024 through Arctic Coast. Canadian Data Report of Fisheries and Aquatic Sciences(1436): 1436: xii + 1489 p. doi:https://doi.org/10.60825/w389-me37.

De Niro, M.J., and Epstein, S. 1981. Influence of diet on the distriubution of nitrogen isotopes in animals. Geochimica et Cosmochimica Acta **45**(3): 341-351. doi:10.1016/0016-7037(81)90244-1.

Deering, R., Misiuk, B., Bell, T., Forbes, D., Edinger, E., Tremblay, T., Telka, A., Aitken, A., and Campbell, D. 2018. Characterization of the seabed and postglacial sediments of inner Frobisher Bay, Baffin Island, Nunavut.

Fischer, G. 1991. Stable carbon isotope ratios of plankton carbon and sinking organic matter from the Atlantic sector of the Southern Ocean. Marine Chemistry **34**(1-4): 581-596. doi:10.1016/S0304-4203(09)90044-5.

Gallagher, C.P., Howland, K.L., and Harwood, L.A. 2017. Harvest, catch-effort, and biological information of Arctic char (*Salvelinus alpinus*) collected from subsistence harvest monitoring programs at Hornaday River, Lasard Creek, and Tippitiuyak, Darnley Bay, Northwest Territories. DFO Canadian Science Advisory Secretariat Research Document **2016/108**: 81.

Gallagher, C.P., Courney, M.B., Seitz, A.C., Lea, E.V., and Howland, K.L. 2021. Ocean-entry timing and marine habitat-use of Canadian Dolly Varden: Dispersal among conservation, hydrocarbon exploration, and shipping areas in the Beaufort Sea. Estuarine, Coastal and Shelf Science **262**: 107609. doi:10.1016/j.ecss.2021.107609.

Gallagher, C.P., Howland, K.L., Harris, L.N., Bajno, R., Sandstrom, S., Loewen, T.N., and Reist, J.D. 2013. Dolly Varden (*Salvelinus malma malma*) from the Big Fish River: abundance estimates, effective population size, biological characteristics, and contribution to the mixed-stock fishery. DFO Canadian Science Advisory Secretariat Research Document **2013/059**: 46.

Galley, R.J., Niemi, A., Eert, J., Majewski, A., and Williams, W.J. 2023. Canadian Beaufort Sea - Marine Ecosystem Assessment (CBS-MEA) report on the physical system - 2019. Canadian Technical Report of Hydrography and Ocean Sciences **364**: ix + 115 p.

Galley, R.J., Babb, D., Ogi, M., Else, B.G.T., Geilfus, N.-X., Crabeck, O., Barber, D.G., and Rysgaard, S. 2016. Replacement of multiyear sea ice and changes in the open water season duration in the Beaufort Sea since 2004. Journal of Geophysical Research: Oceans **121**(3): 1806-1823. doi:https://doi.org/10.1002/2015JC011583.

Geoffroy, M., Majewski, A., LeBlanc, M., Gauthier, S., Walkusz, W., Reist, J.D., and Fortier, L. 2016. Vertical segregation of age-0 and age-1+ polar cod (Boreogadus saida) over the annual cycle in the Canadian Beaufort Sea. Polar Biology **39**(6): 1023-1037. doi:10.1007/s00300-015-1811-z.

Grebmeier, J.M., Overland, J.E., Moore, S.E., Farley, E.V., Carmack, E.C., Cooper, L.W., Frey, K.E., Helle, J.H., McLaughlin, F.A., and McNutt, S.L. 2006. A Major Ecosystem Shift in the Northern Bering Sea. Science **311**(5766): 1461-1464. doi:doi:10.1126/science.1121365.

Harwood, L.A., and Babaluk, J.A. 2014. Spawning, Overwintering and Summer Feeding Habitats Used by Anadromous Arctic Char (*Salvelinus alpinus*) of the Hornaday River, Northwest Territories, Canada. Arctic **67**(4): 449-461. doi:10.14430/arctic4422.

Herbig, J., Fisher, J., Bouchard, C., Niemi, A., LeBlanc, M., Majewski, A., Gauthier, S., and Geoffroy, M. 2023. Climate and juvenile recruitment as drivers of Arctic Cod (*Boreogadus saida*) dynamics in two Canadian Arctic seas. Elementa: Science of the Anthropocene **11**: 1. doi:10.1525/elementa.2023.00033.

Hollins, J., Pettitt-Wade, H., Gallagher, C.P., Lea, E.V., Loseto, L.L., and Hussey, N.E. 2022. Distinct freshwater migratory pathways in Arctic char (*Salvelinus alpinus*) coincide with separate patterns of marine spatial habitat-use across a large coastal landscale. Canadian Journal of Fisheries and Aquatic Sciences **79**: 1447-1464. doi:10.1139/cjfas-2021-0291.

Lansard, B., Mucci, A., Miller, L.A., Macdonald, R.W., and Gratton, Y. 2012. Seasonal variability of water mass distribution in the southeastern Beaufort Sea determined by total alkalinity and δ18O. Journal of Geophysical Research: Oceans **117**(C3).

Layman, C.A., Arrington, D.A., Montana, C.G., and Post, D.M. 2007. Can stable isotope ratios provide for community-wide measures of trophic structure? Ecology **88**(1): 42-48.

Lea, E.V., Gallagher, C.P., Carder, G.M., Matari, K.G.A., and Harwood, L.A. 2022. Ulukhaktok, Northwest Territories coastal Arctic Char (*Salvelinus alpinus*) subsistence (1993-1997 and 2011-2015) and commercial (2010-2015) fisheries: Catch-per-unit-effort and biological sampling. Canadian Data Report of Fisheries and Aquatic Sciences: iv + 41 pp.

Logan, J.M., Jardine, T.D., Miller, T.J., Bunn, S.E., Cunjak, R.A., and Lutcavage, M.E. 2008. Lipid Corrections in Carbon and Nitrogen Stable Isotope Analyses: Comparison of Chemical Extraction and Modelling Methods. Journal of Animal Ecology **77**(4): 838-846. Available from http://www.jstor.org/stable/20143256 [accessed 2025/04/22/].

Long, Z., Perrie, W., Zhang, M., and Liu, Y. 2024. Responses of Atlantic Water Inflow Through Fram Strait to Arctic Storms. Geophysical Research Letters **51**(6): e2023GL107777. doi:https://doi.org/10.1029/2023GL107777.

Lovrity, J.E. 1984. Oceanographic Data from Frobisher Bay in the Eastern Canadian Arctic for the Years 1982 and 1983. Canadian Data Report of Fisheries and Aquatic Sciences **432**: 57 pp.

Madec, G., Bourdallé-Badie, R., Bouttier, P.-A., Bricaud, C., Bruciaferri, D., Calvert, D., Chanut, J., Clementi, E., Coward, A., Delrosso, D., Ethé, C., Flavoni, S., Graham, T., Harle, J., Iovino, D., Lea, D., Lévy, C., Lovato, T., Martin, N., Masson, S., Mocavero, S., Paul, J., Rousset, C., Storkey, D., Storto, A., and Vancoppenolle, M. 2017. NEMO ocean engine.

Maechler, M., Rousseeuw, P., Croux, C., Todorov, V., Ruckstuhl, A., Salibian-Barrera, M., Verbeke, T., Koller, M., Conceicao, E.L.T., and di Palma, A. 2022. robustbase: Basic Robust Statistics R package.

Majewski, A.R., Walkusz, W., Lynn, B.R., Atchison, S., Eert, J., and Reist, J.D. 2016. Distribution and diet of demersal Arctic Cod, Boreogadus saida, in relation to habitat characteristics in the Canadian Beaufort Sea. Polar Biology **39**(6): 1087-1098. doi:10.1007/s00300-015-1857-y.

McLaughlin, F.A., Carmack, E.C., Macdonald, R.W., and Bishop, J.K.B. 1996. Physical and geochemical properties across the Atlantic/Pacific water mass front in the southern Canadian Basin. Journal of Geophysical Research: Oceans **101**(C1): 1183-1197. doi:https://doi.org/10.1029/95JC02634.

McNicholl, D.G., Dunmall, K.M., Majewski, A.R., Niemi, A., Gallagher, C.P., Sawatzky, C., and Reist, J.D. 2020. Distribution of Marine and Anadromous Fishes of Darnley Bay and the Anguniaqvia Niqiqiyuam Marine Protected Area, NT. Canadian Technical Report of Fisheries and Aquatic Sciences **3394**: x + 90 p.

McNicholl, D.G., Christie, L.R., Dunmall, K.M., Illasiak, S., Ruben, N., Illasiak, D., Green, B., Green, T., Green, N., Ruben, R., Jody, I., Ruben, B.S., Ruben, R., and Committee, T.P.H.a.T. 2024. Anguniaqvia Niqiqyuam Marine Protected Area Coastal Monitoring: Synthesis of 2017-2021 Summer and Winter Field Programs. Canadian Technical Report of Fisheries and Aquatic Sciences **3595**: xiv + 103 p.

Moore, J.-S., Harris, L.N., Kessel, S.T., Bernatchez, L., Tallman, R.F., and Fisk, A.T. 2016. Preference for nearshore and estuarine habitats in anadromous Arctic char (*Salvelinus alpinus*) from the Canadian high Arctic (Victoria Island, Nunavut) revealed by acoustic telemetry. Canadian Journal of Fisheries and Aquatic Sciences **73**: 1434-1445. doi:10.1139/cjfas-2015-0436.

Peterson, B.J., and Fry, B. 1987. Stable isotopes in ecosystem studies. Annual Review of Ecology and Systematics **18**: 293-320.

Post, D.M. 2002. Using stable isotopes to estimate trophic position: Models, methods, and assumptions. Ecology **83**(3): 703-718. doi:10.1890/0012-9658(2002)083[0703:USITET]2.0.CO;2.

Rosenberg, B., Neumann, D., and Loseto, L.L. 2015. Stable Isotope Laboratory QA/QC and Inter-lab Comparison Report. Canadian Data Report of Fisheries and Aquatic Sciences **1260**: vi + 7p.

Service, C.H. 2024. Tides, currents, and water levels - Iqaluit 04140. Available from https://www.tides.gc.ca/en/stations/04140 [accessed Oct 7, 2024.

Skinner, M.M., Martin, A.A., and Moore, B.C. 2016. Is lipid correction necessary in the stable isotope analysis of fish tissues? Rapid Communications in Mass Spectrometry **30**(7): 881-889. doi:https://doi.org/10.1002/rcm.7480.

Stammerjohn, S., Massom, R., Rind, D., and Martinson, D. 2012. Regions of rapid sea ice change: An inter-hemispheric seasonal comparison. Geophysical Research Letters **39**(6). doi:https://doi.org/10.1029/2012GL050874.

Steele, M., Dickinson, S., Zhang, J., and W. Lindsay, R. 2015. Seasonal ice loss in the Beaufort Sea: Toward synchrony and prediction. Journal of Geophysical Research: Oceans **120**(2): 1118-1132. doi:https://doi.org/10.1002/2014JC010247.

Steiner, N., Azetsu-Scott, K., Hamilton, J., Hedges, K., Hu, X., Janjua, M.Y., Lavoie, D., Loder, J., Melling, H., Merzouk, A., Perrie, W., Peterson, I., Scarratt, M., Sou, T., and Tallmann, R. 2015. Observed trends and climate projections affecting marine ecosystems in the Canadian Arctic. Environmental Reviews **23**(2): 191-239. doi:10.1139/er-2014-0066.

Trischenko, A.P., Kostylev, V.E., Luo, Y., Ungureanu, C., Whalen, D., and Li, J. 2022. Landfast ice properties over the Beaufort Sea region in 2000-2019 from MODIS and Canadian Ice Service data. Canadian Journal of Earth Sciences **59**(11): 847-865. doi:10.1139/cjes-2021-0011.

Walsh, J.E., Eicken, H., Redilla, K., and Johnson, M. 2022. Sea ice breakup and freeze-up indicators for users of the Arctic coastal environment. The Cryosphere **16**: 4617-4635. doi:10.5194/tc-16-4617-2022.

Welch, H.E., Bergmann, M.A., Siferd, T.D., Martin, K.A., Curtis, M.F., Crawford, R.E., Conover, R.J., and Hop, H. 1992. Energy flow through the marine ecosystem of the Lancaster Sound Region, Arctic Canada. Arctic **45**(4): 343-357. doi:10.14430/arctic1413.

Appendix 1

Table A1 – Comparison of mean carbon ($\delta^{13}C$) and nitrogen ($\delta^{15}N$) stable isotope ratios (± s.d.) in untreated and lipid-extracted samples. Isotope values were compared using a paired t-test and Holm-Bonferroni test for multiple comparisons.

			$\delta^{13}C$ (‰)			$\delta^{15}N$ (‰)		
Common Name	**Species Name**	**N**	**Untreated**	**Lipid Extracted**	**Difference**	**Untreated**	**Lipid Extracted**	**Difference**
Arctic alligatorfish	*Aspidophoroides olrikii*	10	-21.32 ± 0.49	-20.94 ± 0.53	0.37 ± 0.27*	15.31 ± 0.73	15.54 ± 0.77	0.23 ± 0.33
Arctic char	*Salvelinus alpinus*	30	-24.74 ± 1.70	-22.21 ± 0.90	2.45 ± 1.74*	15.26 ± 0.61	15.43 ± 0.67	0.12 ± 0.58
Dolly Varden	*Salvelinus malma*	28	-25.55 ± 1.68	-22.93 ± 0.86	2.34 ± 1.64*	14.50 ± 0.79	14.94 ± 0.61	0.50 ± 0.61*
Greenland halibut	*Reinhardtius hippoglossoides*	12	-24.32 ± 0.84	-21.03 ± 0.38	3.29 ± 0.93*	16.83 ± 0.91	18.41 ± 0.85	1.58 ± 0.40*
Ribbed sculpin	*Triglops pingelii*	9	-23.09 ± 0.72	-22.28 ± 0.93	0.81 ± 0.30*	14.53 ± 1.30	14.82 ± 1.34	0.29 ± 0.25

*$p < 0.05$ for paired t-test comparing lipid-extracted and untreated samples for $\delta^{13}C$ and $\delta^{15}N$

Appendix 2

Table A2 – Results of significant (f-test $p < 0.05$) robust regression models relating $\delta^{15}N$ to fish mass (g) and depth (m).

			Mass				Depth			
Common Name	**Species Name**	**Region**	**Slope**	**Intercept**	**Median (g)**	**R^2**	**Slope**	**Intercept**	**Median (m)**	**R^2**
Arctic char	*Salvelinus alpinus*	WCA	0.0005	13.1658	2300	0.25				
Dolly Varden	*Salvelinus malma*	WCA	1.1606*	10.8272*	1500	0.05*				
Arctic cisco	*Coregonus autumnalis*	WCA	1.1483*	10.0602*	465.5	0.21				
Saffron cod	*Eleginus gracilis*	WCA	0.0041	12.7346	597	0.65				
Starry flounder	*Platychthys stellatus*	WCA	0.0033	11.8899	240	0.22				
Capelin	*Mallotus villosus*	WCA	-1.1640*	15.9624*	22.3	0.17*				
Arctic cod	*Boreogadus saida*	WCA & ECA	1.8564*	12.2916*	9.026	0.25*	0.0010	14.0568	202	0.06
Greenland halibut	*Reinhardtius hippoglossoides*	WCA	0.0004	15.8771	1024.5	0.10				
		ECA	0.5408*	10.5500*	36.889	0.15*				
Arctic alligatorfish	*Aspidophoroides olrikii*	WCA	2.2526*	15.2529*	1.058	0.23	0.0047	14.9192	75	0.07
Gelatinous seasnail	*Liparis fabricii*	WCA	1.3664*	13.6735*	11.951	0.23				
Ribbed sculpin	*Triglops pingelii*	WCA	1.4308*	13.4219*	2.253	0.31				
Spatulate sculpin	*Icelus spatula*	WCA & ECA	1.6645*	15.0364*	2.1965	0.15	0.0067	15.2605	45	0.18
Twohorn sculpin	*Icelus bicornis*	WCA & ECA					0.0089	14.7938	75	0.42

* - Dependent variable was $\log_{10}$-transformed prior to robust regression

Appendix 3

Table A3 – Mean and standard deviation of $\delta^{13}C$ and $\delta^{15}N$ ratios and mean-standardized $\delta^{13}C$ and $\delta^{15}N$ for each fish species by year and area. Mean-standardized values were calculated by subtracting the annual mean for each area from the total mean for the entire study period (2011-2020) for that area, and dividing by the standard deviation of the area total mean.

Habitat Domain	Common Name	Scientific Name	Code	Year	Area	*n*	$\delta^{13}C$ (mean ± s.d.)	Mean-standardized $\delta^{13}C$ (mean ± s.d.)	$\delta^{15}N$ (mean ± s.d.)	Mean-standardized $\delta^{15}N$ (mean ± s.d.)
Anadromous	Arctic char	*Salvelinus alpinus*	ARCH	2011	Darnley Bay	20	-22.24 ± 0.52	-0.21 ± 0.68	15.05 ± 0.5	-0.16 ± 0.49
				2014	Darnley Bay	4	-22.99 ± 0.65	-1.19 ± 0.84	14.99 ± 1.04	-0.22 ± 1.02
					Ulukhaktok	23	-22.74 ± 0.59	-0.07 ± 0.67	14.67 ± 0.59	0.27 ± 0.8
				2015	Darnley Bay	27	-21.95 ± 0.66	0.17 ± 0.86	15.2 ± 0.81	-0.02 ± 0.8
					Ulukhaktok	20	-22.03 ± 0.86	0.73 ± 0.97	14.36 ± 0.68	-0.15 ± 0.93
				2016	Darnley Bay	5	-21.37 ± 0.35	0.92 ± 0.45	14.81 ± 0.49	-0.4 ± 0.48
					Ulukhaktok	20	-22.9 ± 0.85	-0.26 ± 0.97	14.16 ± 0.87	-0.42 ± 1.18
				2017	Darnley Bay	26	-21.94 ± 0.92	0.18 ± 1.2	14.51 ± 1.02	-0.69 ± 1
					Ulukhaktok	7	-21.68 ± 1.69	1.12 ± 1.92	14.51 ± 1.19	0.06 ± 1.62
				2018	Darnley Bay	48	-22.09 ± 0.91	-0.01 ± 1.19	15.15 ± 1.13	-0.06 ± 1.11
					Ulukhaktok	18	-22.85 ± 0.71	-0.2 ± 0.81	14.73 ± 0.66	0.36 ± 0.9
				2019	Darnley Bay	16	-21.77 ± 0.58	0.4 ± 0.76	15.86 ± 0.82	0.63 ± 0.8
					Ulukhaktok	18	-22.98 ± 0.46	-0.34 ± 0.52	14.5 ± 0.62	0.05 ± 0.84
				2020	Darnley Bay	10	-21.68 ± 0.88	0.52 ± 1.14	16.03 ± 1.23	0.8 ± 1.2
					Ulukhaktok	14	-23.04 ± 0.75	-0.42 ± 0.85	14.32 ± 0.7	-0.2 ± 0.95
	Dolly Varden	*Salvelinus malma*	DVCH	2011	Mackenzie Shelf	40	-23.64 ± 0.53	-0.51 ± 0.59	14.65 ± 0.64	0.24 ± 0.93
				2012	Mackenzie Shelf	40	-24.2 ± 0.79	-1.14 ± 0.89	14.42 ± 0.6	-0.08 ± 0.86
				2013	Mackenzie Shelf	40	-23.95 ± 0.52	-0.86 ± 0.58	14.99 ± 0.57	0.74 ± 0.82
				2014	Mackenzie Shelf	40	-23.44 ± 0.36	-0.29 ± 0.4	14.84 ± 0.62	0.53 ± 0.9
				2015	Mackenzie Shelf	38	-22.94 ± 0.81	0.27 ± 0.91	14.04 ± 0.73	-0.64 ± 1.05
				2016	Mackenzie Shelf	40	-22.06 ± 0.46	1.25 ± 0.52	13.8 ± 0.38	-0.98 ± 0.55
				2017	Mackenzie Shelf	11	-23.14 ± 0.64	0.04 ± 0.72	14.22 ± 0.35	-0.37 ± 0.51
				2018	Mackenzie Shelf	36	-23.02 ± 0.78	0.18 ± 0.87	14.27 ± 0.59	-0.29 ± 0.85
				2019	Mackenzie Shelf	43	-22.54 ± 0.59	0.71 ± 0.66	14.47 ± 0.6	-0.01 ± 0.87

Habitat Domain	Common Name	Scientific Name	Code	Year	Area	*n*	$\delta^{13}C$ (mean ± s.d.)	Mean-standardized $\delta^{13}C$ (mean ± s.d.)	$\delta^{15}N$ (mean ± s.d.)	Mean-standardized $\delta^{15}N$ (mean ± s.d.)
				2020	Mackenzie Shelf	30	-22.75 ± 0.58	0.48 ± 0.65	14.96 ± 0.49	0.71 ± 0.71
Coastal	Arctic cisco	*Coregonus autumnalis*	ARCS	2011	Mackenzie Shelf Coast	32	-25.08 ± 1.72	-0.78 ± 1.05	13.09 ± 1.43	0.03 ± 1.33
				2012	Mackenzie Shelf Coast	17	-24.86 ± 2	-0.64 ± 1.23	12.74 ± 1.21	-0.29 ± 1.13
				2013	Mackenzie Shelf Coast	23	-23.87 ± 1.63	-0.03 ± 1	12.38 ± 1.07	-0.63 ± 0.99
				2014	Mackenzie Shelf Coast	16	-23.33 ± 0.74	0.3 ± 0.45	13.4 ± 0.68	0.32 ± 0.63
				2015	Darnley Bay	11	-22.15 ± 0.69	-0.14 ± 0.75	13.72 ± 0.69	0.89 ± 0.51
					Mackenzie Shelf Coast	18	-23.94 ± 1.27	-0.08 ± 0.78	12.91 ± 0.82	-0.14 ± 0.76
				2016	Darnley Bay	10	-22.33 ± 1.26	-0.32 ± 1.35	12.58 ± 1.32	0.05 ± 0.96
					Mackenzie Shelf Coast	19	-23.02 ± 1.13	0.49 ± 0.69	13.33 ± 0.66	0.26 ± 0.61
				2017	Mackenzie Shelf Coast	14	-23.04 ± 0.98	0.48 ± 0.6	13.53 ± 0.65	0.43 ± 0.6
				2019	Mackenzie Shelf Coast	3	-22.63 ± 0.31	0.73 ± 0.19	13.26 ± 0.21	0.19 ± 0.19
				2020	Darnley Bay	11	-21.62 ± 0.7	0.43 ± 0.75	11.22 ± 0.58	-0.94 ± 0.42
					Mackenzie Shelf Coast	18	-22.48 ± 0.65	0.82 ± 0.4	13.33 ± 1.09	0.25 ± 1.01
	Arctic flounder	*Liopsetta glacialis*	ARFL	2012	Mackenzie Shelf Coast	37	-24.05 ± 1.09	-0.03 ± 0.86	11.41 ± 0.74	-0.09 ± 1.05
				2013	Mackenzie Shelf Coast	40	-23.84 ± 1.58	0.13 ± 1.26	11.31 ± 0.71	-0.23 ± 1.01
				2014	Mackenzie Shelf Coast	6	-23.47 ± 0.83	0.43 ± 0.66	11.57 ± 0.39	0.14 ± 0.56
				2015	Mackenzie Shelf Coast	20	-24.37 ± 1.32	-0.29 ± 1.05	11.4 ± 0.59	-0.1 ± 0.84
				2016	Darnley Bay	31	-15.93 ± 1.13	-0.04 ± 1.03	11.42 ± 0.99	0.23 ± 0.9
					Mackenzie Shelf Coast	12	-24.26 ± 0.52	-0.2 ± 0.42	11.83 ± 0.46	0.51 ± 0.64
				2017	Darnley Bay	25	-16.32 ± 1.12	-0.4 ± 1.03	10.92 ± 1.16	-0.22 ± 1.06
				2018	Darnley Bay	33	-15.4 ± 0.9	0.44 ± 0.82	10.68 ± 1.16	-0.44 ± 1.06
				2019	Mackenzie Shelf Coast	4	-23.74 ± 0.73	0.22 ± 0.58	12.78 ± 0.26	1.85 ± 0.37
				2020	Darnley Bay	34	-16.17 ± 0.98	-0.27 ± 0.89	11.43 ± 0.97	0.25 ± 0.89
					Mackenzie Shelf Coast	1	-23.49	0.42	11.44	-0.04
	Broad whitefish	*Coregonus nasus*	BDWF	2011	Mackenzie Shelf Coast	41	-27.26 ± 2.4	0.24 ± 0.97	9.06 ± 1.76	-0.21 ± 1.34
				2012	Mackenzie Shelf Coast	37	-27.57 ± 2.67	0.11 ± 1.08	9.02 ± 1.27	-0.24 ± 0.96
				2013	Mackenzie Shelf Coast	25	-26.79 ± 3.16	0.43 ± 1.27	9.27 ± 1.48	-0.05 ± 1.13
				2014	Mackenzie Shelf Coast	2	-27.06 ± 0.04	0.32 ± 0.01	10.51 ± 0.42	0.89 ± 0.32

Habitat Domain	Common Name	Scientific Name	Code	Year	Area	*n*	$\delta^{13}C$ (mean ± s.d.)	Mean-standardized $\delta^{13}C$ (mean ± s.d.)	$\delta^{15}N$ (mean ± s.d.)	Mean-standardized $\delta^{15}N$ (mean ± s.d.)
				2015	Mackenzie Shelf Coast	19	-27.69 ± 1.98	0.07 ± 0.8	10.09 ± 0.84	0.57 ± 0.64
				2016	Darnley Bay	22	-21.43 ± 1.9	0.83 ± 0.83	8.54 ± 0.54	-0.05 ± 0.78
					Mackenzie Shelf Coast	14	-28.1 ± 2.59	-0.1 ± 1.05	9.75 ± 0.78	0.31 ± 0.59
				2017	Darnley Bay	27	-22.67 ± 2.66	0.29 ± 1.16	8.26 ± 1.12	-0.45 ± 1.62
					Mackenzie Shelf Coast	20	-28.71 ± 2.44	-0.34 ± 0.99	8.99 ± 1.13	-0.26 ± 0.86
				2018	Darnley Bay	28	-24.82 ± 1.95	-0.64 ± 0.85	8.76 ± 0.64	0.27 ± 0.92
					Mackenzie Shelf Coast	19	-28.93 ± 2.05	-0.43 ± 0.83	9.57 ± 1.09	0.18 ± 0.83
				2019	Mackenzie Shelf Coast	23	-29.05 ± 1.82	-0.48 ± 0.74	9.47 ± 1.25	0.1 ± 0.95
				2020	Darnley Bay	30	-23.81 ± 1.92	-0.2 ± 0.84	8.77 ± 0.42	0.28 ± 0.61
					Mackenzie Shelf Coast	19	-27.41 ± 2.31	0.18 ± 0.93	9.25 ± 1.13	-0.06 ± 0.86
	Saffron cod	*Eleginus gracilis*	SFCD	2012	Mackenzie Shelf Coast	40	-22.92 ± 0.32	-0.26 ± 0.69	15.06 ± 0.57	-0.2 ± 0.92
				2013	Mackenzie Shelf Coast	46	-22.75 ± 0.42	0.12 ± 0.91	15.35 ± 0.56	0.28 ± 0.91
				2014	Mackenzie Shelf Coast	20	-22.7 ± 0.37	0.23 ± 0.8	15.62 ± 0.46	0.71 ± 0.75
				2015	Mackenzie Shelf Coast	20	-22.72 ± 0.43	0.19 ± 0.92	15.61 ± 0.46	0.7 ± 0.75
				2016	Darnley Bay	78	-18.48 ± 1.09	-0.25 ± 0.94	14.89 ± 0.6	-0.26 ± 0.92
					Mackenzie Shelf Coast	19	-23.31 ± 0.3	-1.09 ± 0.64	14.92 ± 0.7	-0.43 ± 1.15
				2017	Darnley Bay	14	-17.5 ± 0.85	0.6 ± 0.74	15.24 ± 0.39	0.26 ± 0.59
					Mackenzie Shelf Coast	20	-22.69 ± 0.28	0.25 ± 0.61	14.53 ± 0.55	-1.06 ± 0.9
				2018	Mackenzie Shelf Coast	20	-22.92 ± 0.35	-0.25 ± 0.75	15.02 ± 0.47	-0.26 ± 0.76
				2019	Mackenzie Shelf Coast	25	-22.59 ± 0.47	0.46 ± 1.02	15.12 ± 0.57	-0.1 ± 0.93
				2020	Mackenzie Shelf Coast	19	-22.7 ± 0.86	0.23 ± 1.86	15.3 ± 0.6	0.19 ± 0.98
	Starry flounder	*Platichthys stellatus*	STFL	2012	Mackenzie Shelf Coast	15	-25.37 ± 1.02	-0.37 ± 0.8	12.49 ± 0.73	-0.09 ± 0.94
				2013	Mackenzie Shelf Coast	27	-24.65 ± 1.19	0.19 ± 0.93	12.25 ± 1.14	-0.4 ± 1.47
				2014	Darnley Bay	10	-18.74 ± 0.95	0.57 ± 0.72	12.6 ± 0.75	-0.16 ± 0.79
					Mackenzie Shelf Coast	7	-24.9 ± 1.21	0 ± 0.94	12.62 ± 1.09	0.07 ± 1.41
				2015	Mackenzie Shelf Coast	20	-24.85 ± 0.89	0.03 ± 0.69	12.38 ± 0.47	-0.23 ± 0.61
				2016	Darnley Bay	29	-19.73 ± 1.2	-0.18 ± 0.91	12.84 ± 0.72	0.08 ± 0.76
					Mackenzie Shelf Coast	5	-24.95 ± 1.12	-0.04 ± 0.88	12.69 ± 0.5	0.17 ± 0.65

Habitat Domain	Common Name	Scientific Name	Code	Year	Area	*n*	$\delta^{13}C$ (mean ± s.d.)	Mean-standardized $\delta^{13}C$ (mean ± s.d.)	$\delta^{15}N$ (mean ± s.d.)	Mean-standardized $\delta^{15}N$ (mean ± s.d.)
				2017	Darnley Bay	10	-19.44 ± 1.35	0.05 ± 1.01	11.66 ± 1.63	-1.16 ± 1.72
					Mackenzie Shelf Coast	20	-24.13 ± 1.68	0.6 ± 1.31	12.79 ± 0.58	0.3 ± 0.75
				2018	Darnley Bay	31	-19.83 ± 1.28	-0.25 ± 0.96	12.83 ± 0.65	0.07 ± 0.68
					Mackenzie Shelf Coast	5	-25.36 ± 0.93	-0.36 ± 0.72	11.92 ± 0.52	-0.83 ± 0.67
				2019	Mackenzie Shelf Coast	14	-25 ± 1.25	-0.08 ± 0.98	13.05 ± 0.56	0.63 ± 0.73
				2020	Darnley Bay	29	-19.29 ± 1.48	0.16 ± 1.11	12.8 ± 1.05	0.05 ± 1.1
				2020	Mackenzie Shelf Coast	19	-24.77 ± 1.22	0.1 ± 0.95	12.87 ± 0.65	0.39 ± 0.84
Offshore	Arctic alligatorfish	*Aspidophoroides olrikii*	ARAF	2012	Beaufort Sea	76	-21.71 ± 0.84	-0.07 ± 1.09	15.5 ± 0.63	0.09 ± 1.01
				2013	Amundsen Gulf	23	-21.22 ± 1.19	-0.02 ± 1.27	15.52 ± 0.52	0.59 ± 0.76
					Darnley Bay	8	-20.96 ± 1.41	-0.14 ± 1.23	15.41 ± 0.44	-0.13 ± 1.15
					Dolphin and Union Strait	9	-20.61 ± 1.36	0.29 ± 2.04	15.06 ± 0.65	0.66 ± 1.32
					Beaufort Sea	41	-21.48 ± 0.66	0.23 ± 0.85	15.17 ± 0.45	-0.43 ± 0.71
				2014	Amundsen Gulf	3	-20.1 ± 0.33	1.18 ± 0.35	14.9 ± 0.07	-0.31 ± 0.11
					Banks Island Shelf	6	-18.92 ± 0.52	0 ± 1	15.38 ± 0.28	0 ± 1
					Dolphin and Union Strait	13	-20.78 ± 0.3	0.03 ± 0.46	14.44 ± 0.38	-0.6 ± 0.77
					Franklin Bay	5	-21.49 ± 0.9	0.13 ± 1.3	15.66 ± 0.5	0.27 ± 1.16
					Beaufort Sea	7	-22.15 ± 0.21	-0.63 ± 0.27	16.4 ± 0.41	1.53 ± 0.65
					Minto Inlet	4	-21.96 ± 0.29	-0.52 ± 0.87	16.29 ± 0.39	0.75 ± 0.45
				2018	Amundsen Gulf	10	-21.45 ± 0.39	-0.27 ± 0.41	14.59 ± 0.56	-0.74 ± 0.8
					Dolphin and Union Strait	9	-20.72 ± 0.21	0.12 ± 0.32	14.78 ± 0.44	0.09 ± 0.89
				2019	Amundsen Gulf	10	-21.24 ± 0.5	-0.03 ± 0.54	14.74 ± 0.72	-0.53 ± 1.04
					Darnley Bay	5	-20.55 ± 0.58	0.22 ± 0.5	15.54 ± 0.29	0.2 ± 0.77
					Dolphin and Union Strait	10	-21.06 ± 0.2	-0.4 ± 0.3	14.79 ± 0.32	0.11 ± 0.64
					Franklin Bay	3	-21.73 ± 0.06	-0.21 ± 0.09	15.34 ± 0.24	-0.46 ± 0.55
					Minto Inlet	4	-21.61 ± 0.31	0.52 ± 0.92	14.98 ± 0.69	-0.75 ± 0.8
	Arctic cod	*Boreogadus saida*	ARCD	2012	Beaufort Sea	330	-23.71 ± 0.84	-0.12 ± 1	14.09 ± 0.62	-0.2 ± 0.93
				2013	Amundsen Gulf	95	-23.56 ± 0.5	-0.15 ± 0.94	14.28 ± 0.72	-0.01 ± 1.05
					Darnley Bay	6	-23.5 ± 0.35	0 ± 1	14.57 ± 0.64	0 ± 1

Habitat Domain	Common Name	Scientific Name	Code	Year	Area	*n*	$\delta^{13}C$ (mean ± s.d.)	Mean-standardized $\delta^{13}C$ (mean ± s.d.)	$\delta^{15}N$ (mean ± s.d.)	Mean-standardized $\delta^{15}N$ (mean ± s.d.)
					Dolphin and Union Strait	12	-23.43 ± 0.33	-0.54 ± 0.74	14.46 ± 0.7	0.1 ± 1.13
					Beaufort Sea	90	-23.3 ± 0.82	0.36 ± 0.98	14.57 ± 0.64	0.51 ± 0.96
				2014	Amundsen Gulf	6	-23.39 ± 0.61	0.17 ± 1.14	14.17 ± 0.66	-0.18 ± 0.96
					Banks Island Shelf	12	-24.04 ± 0.38	0 ± 1	14.85 ± 0.44	0 ± 1
					Dolphin and Union Strait	11	-23.39 ± 0.34	-0.46 ± 0.77	14.22 ± 0.48	-0.28 ± 0.78
					Franklin Bay	13	-23.36 ± 0.44	-0.09 ± 0.72	14.07 ± 0.41	-0.17 ± 0.45
					Beaufort Sea	33	-23.71 ± 0.69	-0.13 ± 0.82	14.44 ± 0.81	0.33 ± 1.21
					Minto Inlet	9	-24.1 ± 0.38	-0.89 ± 0.57	14.69 ± 0.49	-0.18 ± 1.02
				2017	Amundsen Gulf	8	-22.82 ± 0.31	1.23 ± 0.57	14.21 ± 0.5	-0.12 ± 0.73
					Dolphin and Union Strait	6	-22.66 ± 0.2	1.17 ± 0.45	14.2 ± 0.49	-0.31 ± 0.8
					Beaufort Sea	10	-22.6 ± 0.45	1.2 ± 0.53	14.4 ± 0.8	0.27 ± 1.2
					Minto Inlet	5	-22.71 ± 0.23	1.16 ± 0.34	14.7 ± 0.56	-0.16 ± 1.16
				2018	Amundsen Gulf	9	-23.12 ± 0.8	0.68 ± 1.49	14.53 ± 0.77	0.35 ± 1.12
					Dolphin and Union Strait	11	-22.99 ± 0.49	0.43 ± 1.09	14.19 ± 0.41	-0.34 ± 0.66
					Frobisher Bay	22	-20.45 ± 0.22	0.42 ± 0.34	12.15 ± 0.45	-0.38 ± 0.7
				2019	Amundsen Gulf	16	-23.59 ± 0.3	-0.2 ± 0.55	14.29 ± 0.55	0 ± 0.8
					Dolphin and Union Strait	10	-23.19 ± 0.42	-0.02 ± 0.94	14.85 ± 0.74	0.74 ± 1.2
					Franklin Bay	7	-23.2 ± 0.89	0.17 ± 1.44	14.52 ± 1.48	0.32 ± 1.61
					Frobisher Bay	102	-20.85 ± 0.65	-0.19 ± 0.98	12.43 ± 0.67	0.06 ± 1.05
					Beaufort Sea	29	-23.61 ± 0.66	0 ± 0.79	14.35 ± 0.56	0.18 ± 0.84
					Minto Inlet	5	-23.2 ± 0.14	0.44 ± 0.2	15 ± 0.39	0.48 ± 0.82
				2020	Frobisher Bay	5	-19.38 ± 0.2	2.03 ± 0.3	12.7 ± 0.49	0.48 ± 0.76
	Capelin	*Mallotus villosus*	CPLN	2014	Darnley Bay	35	-22.96 ± 0.45	0.23 ± 0.86	14.51 ± 0.42	0.29 ± 1.03
				2017	Darnley Bay	16	-22.61 ± 0.22	0.9 ± 0.43	14.5 ± 0.29	0.27 ± 0.71
				2018	Darnley Bay	29	-23.59 ± 0.27	-1 ± 0.53	14.1 ± 0.38	-0.71 ± 0.92
				2019	Darnley Bay	13	-22.81 ± 0.45	0.52 ± 0.88	14.59 ± 0.19	0.49 ± 0.46
	Greenland halibut	*Reinhardtius hippoglossoides*	GLHB	2012	Beaufort Sea	104	-20.34 ± 0.43	0.33 ± 0.86	15.98 ± 0.92	-0.24 ± 1.02
				2013	Amundsen Gulf	10	-21.03 ± 0.23	0.06 ± 1.1	16.51 ± 0.71	-0.14 ± 1.02

Habitat Domain	Common Name	Scientific Name	Code	Year	Area	*n*	$\delta^{13}C$ (mean ± s.d.)	Mean-standardized $\delta^{13}C$ (mean ± s.d.)	$\delta^{15}N$ (mean ± s.d.)	Mean-standardized $\delta^{15}N$ (mean ± s.d.)
					Beaufort Sea	24	-20.42 ± 0.35	0.17 ± 0.7	16.62 ± 0.61	0.47 ± 0.68
				2014	Amundsen Gulf	1	-21.21	-0.75	16.55	-0.08
					Dolphin and Union Strait	1	-20.99	NA	16.21	NA
					Beaufort Sea	25	-20.77 ± 0.53	-0.53 ± 1.05	16.55 ± 0.74	0.39 ± 0.82
				2017	Beaufort Sea	4	-21.29 ± 0.52	-1.57 ± 1.04	15.38 ± 1.34	-0.9 ± 1.48
				2019	Amundsen Gulf	2	-21.03 ± 0.15	0.09 ± 0.69	17.13 ± 0.83	0.75 ± 1.18
					Frobisher Bay	51	-19.56 ± 0.45	0 ± 1	12.43 ± 0.56	0 ± 1
					Beaufort Sea	21	-20.96 ± 0.4	-0.9 ± 0.8	16.51 ± 0.81	0.35 ± 0.9
	Gelatinous seasnail	*Liparis fabricii*	GLSS	2012	Beaufort Sea	16	-23.27 ± 0.79	0.29 ± 0.91	15.51 ± 1.16	0.18 ± 1.12
				2013	Amundsen Gulf	11	-23.6 ± 0.6	-0.34 ± 0.9	15.46 ± 0.59	0.51 ± 0.76
					Dolphin and Union Strait	6	-23.48 ± 0.38	-0.22 ± 0.78	14.46 ± 0.44	-0.63 ± 0.67
					Beaufort Sea	13	-23.64 ± 1.01	-0.14 ± 1.16	15.45 ± 0.63	0.12 ± 0.61
				2014	Dolphin and Union Strait	4	-23.2 ± 0.65	0.33 ± 1.32	15.49 ± 0.33	0.95 ± 0.5
				2017	Amundsen Gulf	3	-22.43 ± 0.31	1.41 ± 0.46	13.97 ± 0.43	-1.4 ± 0.55
					Franklin Bay	3	-21.57 ± 0.49	0.32 ± 0.79	14.63 ± 0.26	-0.48 ± 0.45
				2019	Amundsen Gulf	3	-23.48 ± 0.13	-0.16 ± 0.19	14.71 ± 0.29	-0.45 ± 0.37
					Franklin Bay	2	-22.07 ± 0.88	-0.48 ± 1.41	15.33 ± 0.8	0.71 ± 1.38
					Beaufort Sea	5	-24.02 ± 0.51	-0.57 ± 0.58	14.43 ± 1.18	-0.87 ± 1.14
	Longeared eelpout	*Lycodes seminudus*	LEEP	2012	Beaufort Sea	32	-21.03 ± 0.44	0.29 ± 0.75	17.93 ± 0.98	0.48 ± 1.09
				2013	Amundsen Gulf	7	-21.39 ± 0.35	0.53 ± 0.83	17.42 ± 0.5	0.11 ± 0.98
					Dolphin and Union Strait	1	-21.32	0.63	17.3	-0.1
					Beaufort Sea	14	-21.19 ± 0.67	0.02 ± 1.14	17.18 ± 0.83	-0.34 ± 0.92
				2014	Dolphin and Union Strait	5	-21.16 ± 0.23	0.86 ± 0.35	17.64 ± 0.37	0.55 ± 0.72
					Franklin Bay	1	-20.85	NA	18.25	NA
					Beaufort Sea	3	-21.73 ± 0.23	-0.9 ± 0.39	17.33 ± 0.09	-0.18 ± 0.1
				2017	Dolphin and Union Strait	10	-22.05 ± 0.69	-0.46 ± 1.01	17.27 ± 0.57	-0.17 ± 1.11
					Beaufort Sea	9	-21.52 ± 1	-0.54 ± 1.7	16.84 ± 0.66	-0.72 ± 0.73
				2018	Amundsen Gulf	1	-21.82	-0.48	16.67	-1.33

Habitat Domain	Common Name	Scientific Name	Code	Year	Area	*n*	$\delta^{13}C$ (mean ± s.d.)	Mean-standardized $\delta^{13}C$ (mean ± s.d.)	$\delta^{15}N$ (mean ± s.d.)	Mean-standardized $\delta^{15}N$ (mean ± s.d.)
					Minto Inlet	1	-21.83	1.15	16.33	0.59
				2019	Amundsen Gulf	5	-21.89 ± 0.39	-0.65 ± 0.93	17.41 ± 0.54	0.11 ± 1.04
					Dolphin and Union Strait	1	-21.96	-0.32	16.86	-0.97
					Beaufort Sea	19	-21.26 ± 0.44	-0.1 ± 0.76	17.32 ± 0.65	-0.19 ± 0.72
					Minto Inlet	4	-22.22 ± 0.24	-0.29 ± 0.88	16.13 ± 0.3	-0.15 ± 1.09
	Ribbed sculpin	*Triglops pingelii*	RBSC	2012	Beaufort Sea	43	-23.65 ± 0.74	-0.3 ± 0.94	13.58 ± 0.68	-0.3 ± 0.97
				2013	Amundsen Gulf	7	-22.55 ± 0.62	0.44 ± 1.05	14.28 ± 0.44	0.7 ± 0.73
					Darnley Bay	7	-21.67 ± 0.8	0.5 ± 0.68	14.99 ± 0.73	0.35 ± 1
					Beaufort Sea	11	-23.03 ± 0.32	0.48 ± 0.4	14.21 ± 0.3	0.6 ± 0.43
				2014	Amundsen Gulf	4	-21.97 ± 0.31	1.43 ± 0.53	14.64 ± 0.51	1.31 ± 0.84
					Banks Island Shelf	1	-23.61	NA	14.85	NA
					Franklin Bay	1	-22.47	NA	14.55	NA
					Beaufort Sea	5	-22.18 ± 0.44	1.55 ± 0.55	14.64 ± 0.37	1.23 ± 0.53
				2018	Amundsen Gulf	11	-23.1 ± 0.4	-0.49 ± 0.67	13.5 ± 0.38	-0.58 ± 0.63
					Dolphin and Union Strait	3	-22.27 ± 0.69	0.44 ± 0.6	14.85 ± 0.08	0.5 ± 0.11
				2019	Amundsen Gulf	8	-23.07 ± 0.41	-0.43 ± 0.69	13.58 ± 0.46	-0.46 ± 0.77
					Darnley Bay	3	-23.61 ± 0.58	-1.16 ± 0.49	14.15 ± 0.21	-0.81 ± 0.29
					Dolphin and Union Strait	1	-24.29	-1.31	13.35	-1.49
	Spatulate sculpin	*Icelus spatula*	SPSC	2012	Beaufort Sea	29	-21.95 ± 0.67	-0.2 ± 1.18	15.48 ± 0.75	-0.15 ± 1.12
				2013	Amundsen Gulf	2	-22.04 ± 0.04	0 ± 1	15.25 ± 0.78	0 ± 1
					Darnley Bay	1	-20.41	NA	16.18	NA
					Dolphin and Union Strait	2	-20.86 ± 0.45	0.34 ± 1.66	16.29 ± 0.06	1.01 ± 0.13
					Beaufort Sea	24	-21.7 ± 0.38	0.24 ± 0.67	15.71 ± 0.54	0.18 ± 0.81
				2014	Banks Island Shelf	7	-21.28 ± 1.87	0 ± 1	15.61 ± 0.2	0 ± 1
					Dolphin and Union Strait	3	-21.01 ± 0.18	-0.22 ± 0.66	15.47 ± 0.27	-0.67 ± 0.55
				2018	Frobisher Bay	4	-18.6 ± 0.41	-0.22 ± 0.68	15.05 ± 0.24	-0.28 ± 0.39
				2019	Frobisher Bay	14	-18.71 ± 0.66	-0.4 ± 1.08	14.97 ± 0.69	-0.4 ± 1.09
				2020	Frobisher Bay	10	-18.07 ± 0.39	0.65 ± 0.63	15.66 ± 0.41	0.68 ± 0.65

Habitat Domain	Common Name	Scientific Name	Code	Year	Area	*n*	$\delta^{13}C$ (mean ± s.d.)	Mean-standardized $\delta^{13}C$ (mean ± s.d.)	$\delta^{15}N$ (mean ± s.d.)	Mean-standardized $\delta^{15}N$ (mean ± s.d.)
	Twohorn sculpin	*Icelus bicornis*	THSC	2012	Beaufort Sea	27	-22.03 ± 0.55	-0.02 ± 1.11	15.02 ± 0.46	-0.6 ± 0.91
				2013	Amundsen Gulf	28	-21.16 ± 1.44	0 ± 1	15.79 ± 0.61	0 ± 1
					Darnley Bay	10	-20.34 ± 0.52	0 ± 1	15.99 ± 0.59	0 ± 1
					Dolphin and Union Strait	8	-21.37 ± 0.45	-0.28 ± 1.25	15.84 ± 0.7	0.45 ± 0.84
					Beaufort Sea	37	-21.98 ± 0.42	0.1 ± 0.85	15.5 ± 0.44	0.36 ± 0.89
				2014	Banks Island Shelf	13	-21.74 ± 0.85	0 ± 1	15.37 ± 0.46	0 ± 1
					Dolphin and Union Strait	8	-21.16 ± 0.22	0.28 ± 0.63	15.09 ± 0.82	-0.45 ± 0.99
					Franklin Bay	5	-21.2 ± 0.37	0 ± 1	15.48 ± 0.48	0 ± 1
					Beaufort Sea	4	-22.41 ± 0.71	-0.78 ± 1.43	15.69 ± 0.12	0.73 ± 0.23
					Minto Inlet	5	-21.94 ± 0.37	0 ± 1	15.52 ± 0.92	0 ± 1
				2018	Frobisher Bay	12	-18.47 ± 0.43	0.13 ± 0.8	15.09 ± 0.79	0.57 ± 1.1
				2019	Frobisher Bay	3	-18.76 ± 0.3	-0.41 ± 0.55	14.23 ± 0.65	-0.64 ± 0.91
				2020	Frobisher Bay	13	-18.55 ± 0.67	-0.02 ± 1.25	14.42 ± 0.47	-0.38 ± 0.66

Appendix 4

Table A4 – Contact information for field programs that contributed fish isotope data to this data report.

Program	Area	Domain	Name	Email
Arctic Coastal Ecosystem Study (ACES)	TNMPA	Coastal	Jasmine Brewster	jasmine.brewster@dfo-mpo.gc.ca
Arctic Coast Monitoring Program	ANMPA	Coastal	Karen Dunmall Darcy McNicholl Laurissa Christie	karen.dunmall@dfo-mpo.gc.ca darcy.mcnicholl@dfo-mpo.gc.ca laurissa.christie@dfo-mpo.gc.ca
Arctic Char and Dolly Varden Monitoring		Anadromous	Colin Gallagher Ellen Lea Kimberley Howland	colin.gallagher@dfo-mpo.gc.ca ellen.lea@dfo-mpo.gc.ca kimberly.howland@dfo-mpo.gc.ca
Beaufort Regional Ecosystem Assessment Marine Fishes Project (BREA-MFP)/ Canadian Beaufort Sea Ecosystem Assessment (CBS-MEA)	Beaufort Sea/ Amundsen Gulf	Offshore	Andrea Niemi Andrew Majewski	andrea.niemi@dfo-mpo.gc.ca andrew.majewski@dfo-mpo.gc.ca
Iqaluit Coastal Ecosystem Baseline Program	Frobisher Bay	Coastal	Chris Lewis Andrea Niemi	christopher.lewis@dfo-mpo.gc.ca andrea.niemi@dfo-mpo.gc.ca
		Offshore	Kevin Hedges Tracey Loewen	kevin.hedges@dfo-mpo.gc.ca tracey.loewen@dfo-mpo.gc.ca